Print ISSN 0554-5587
On line eISSN 2406-1123
UDK 631 (059)

ПОЉОПРИВРЕДНА ТЕХНИКА

AGRICULTURAL ENGINEERING

НАУЧНИ ЧАСОПИС
SCIENTIFIC JOURNAL

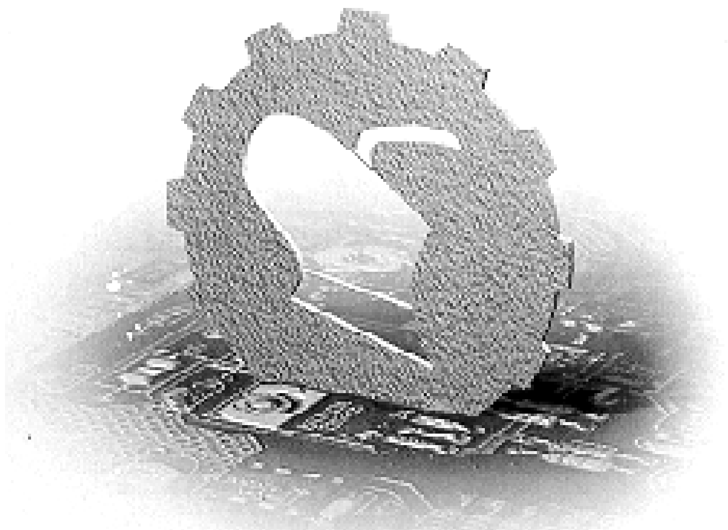

УНИВЕРЗИТЕТ У БЕОГРАДУ, ПОЉОПРИВРЕДНИ ФАКУЛТЕТ,
ИНСТИТУТ ЗА ПОЉОПРИВРЕДНУ ТЕХНИКУ
UNIVERSITY OF BELGRADE, FACULTY OF AGRICULTURE,
INSTITUTE OF AGRICULTURAL ENGINEERING

Година XLVII, Број 4., 2022.
Year XLVII, No.4., 2022.

ПОЉОПРИВРЕДНА ТЕХНИКА

НАУЧНИ ЧАСОПИС

AGRICULTURAL ENGINEERING

SCIENTIFIC JOURNAL

УНИВЕРЗИТЕТ У БЕОГРАДУ, ПОЉОПРИВРЕДНИ ФАКУЛТЕТ,
ИНСТИТУТ ЗА ПОЉОПРИВРЕДНУ ТЕХНИКУ

UNIVERSITY OF BELGRADE, FACULTY OF AGRICULTURE,
INSTITUTE OF AGRICULTURAL ENGINEERING

WEB адреса *(WEB Address)*
www.jageng.agrif.bg.ac.rs

Штампа *(Printed by)*
Пољопривредни факултет , 11080 Земун-Београд, Р.Србија
Часопис излази четири пута годишње

Тираж *(Circulation)*
200 примерака
Дистрибуција примерака часописа Пољопривредна техника за заинтересоване је бесплатна .

Радови објављени у часопису индексирани су у базама *(Abstracting and Indexing)*:
AGRIS (International Information System for the Agricultural Science and Technology)
SCIndeks (Serbian Citation Index)
NAAS (National Academy of Agricultural Sciences - India)
ScienceMediaCentre
ArgosBiotech
CiteFactor (International Academic Scientific Journals)
J4F (Journals for Free).
AgroSpace, Faculty of Agriculture, University of Belgrade, Republic of Serbia

Издавање часописа помогло *(Publication supported by)*
Министарство просвете, науке и технолошког развоја Републике Србије
Према одлукама Министра просвете, науке и технолошког развоја: 451-03-684/2020-14 и 451-03-1210/2020-14/2 .

На основу мишљења Министарства за науку и технологију Републике Србије према решењу бр. 413-00-606/96-01 од 24. 12. 1996. године, научни часопис Пољопривредна техника је ослобођен плаћања пореза на промет робе на мало.

S A D R Ž A J

C O N T E N T S

Univerzitet u Beogradu
Poljoprivredni fakultet
Institut za poljoprivrednu tehniku
Naučničasopis
POLJOPRIVREDNA TEHNIKA
Godina XLVII
Broj 4, 2022.
Strane: 1 – 14

University of Belgrade
Faculty of Agriculture
Institute of Agricultural Engineering
Scientific Journal
AGRICULTURAL ENGINEERING
Year XLVII
No 4, 2022.
pp. 1 – 14

UDK:621.1:631:1
Original Scientific paper
Originalni naučni rad
DOI:10.5937/PoljTeh2204001G

THE USE OF ARTIFICIAL INTELLIGENCE IN TRACTOR FIELD OPERATIONS: A REVIEW

Ikrang Elijah George[1], Udoumoh Unwana Iniobong[*2], Ehiomogue Precious Okhionkpamwunyi[3].

[1-2]Department of Agricultural and Food Engineering, University of Uyo, Uyo, Nigeria.
[3]Department of Agricultural and Bio-Resources Engineering, Michael Okpara University of Agriculture, Umudike, Nigeria

Abstract: According to UN Food and Agriculture Organization [1], the population of the world will increase by 2 billion by 2050. However, only 4% additional land will come under cultivation by then. It could be inferred that, with the global population expected to reach 9.1 billion in 2050, 70 percent more food needs to be produced, otherwise about 370 million people would be in hunger in 2050. In this light, the use of latest technological solutions to make farming more efficient remains one of the greatest imperatives. While Artificial Intelligence (AI) sees a lot of direct application across sectors, it can also bring a paradigm shift in how we see farming today. AI-powered solutions will not only enable farmers to do more with less, it will also improve quality and ensure faster go-to-market for crops. This paper presents a review of the applications of AI in tractor field operations.

The paper discusses elaborately, the use of robotics as a form of artificial intelligence which is very useful in tractor field operations such as tillage, weeding, seeding, herbicide spraying, and harvesting. A typical focus is laid on the strength and limitations of the applications and the way in utilizing expert systems for higher productivity.

Key words*: Artificial Intelligence, Agriculture, Tractor, Field Operations, Engineering*

INTRODUCTION

The term "Artificial Intelligence" was first introduced in the 1955 Dartmouth Conference, in which John McCarthy proposed a study to be carried out grounded on the

[*]Corresponding Author. E-mail: unwanaobong12@gmail.com

hypothesis that “every aspect of learning or any other feature of intelligence can in principle be so precisely described that a machine can be made to simulate it” [2]. Nowadays, AI, one of the essential areas in computer science, has penetrated a variety of domains, such as education, healthcare, finance and manufacturing, because of its nature to tackle problems that cannot be solved well by humans, [3].

AI is now one of the most important global issues of the 21st century. AI is the branch of computer science that deals with designing intelligent computer systems that mimic human intelligence (e.g. visual perception, speech recognition, decision-making, and language translation). The ability of machines to process natural language, to learn, to plan, makes it possible for new tasks to be performed by intelligent systems [3].

Today AI is integrated into our daily lives in several forms, such as personal assistants, automated mass transportation, aviation, computer gaming, facial recognition at passport control, voice recognition on virtual assistants, driverless cars, companion robots, etc. AI is not a single technology but a range of computational models and algorithms.

Artificial intelligence has endless potential to handle tasks commonly done by humans, including natural language processing, image recognition and data analytics, visual perception, decision-making, speech recognition, business process management, and even the diagnosis of disease, all of which normally require human intelligence. Artificial intelligence is now everywhere and has a great deal to offer the world of engineering. AI has had an impact on just about every field, including engineering [4]. Some of the most interesting applications of artificial intelligence are in the field of agriculture and engineering. For this reason, more and more people are becoming AI Engineers.

Agriculture, an essential consideration of any country, is still facing major challenges today. It is approximated that over 820 million people are in hunger today [1]. Furthermore, with the global population expected to reach 9.1 billion in 2050, 70 percent more food needs to be produced. In addition to the projected investments in agriculture, further investment will be needed, otherwise about 370 million people would be in hunger in 2050 [1]. The future of agriculture, would witness many innovations through AI suiting to the regional requirements and diverse climatic conditions.

AI enabled machines, going to be revolutionized the farm sector is by and large by the use of autonomous tractors for performing multiple tasks which not only saves time but also money in terms of labor. These self-driving or driverless tractors are enabled with computer programs to independently perform ploughing, harvesting and weed control operation and decide the speed without any interrupting obstacles such as inter-cultivation objects, humans and animals while performing various tasks.

Industries involved in improving the machine learning or AI-based products or services like training data for agriculture, drone and automated machine making are expected to get technological advancement in future and shall provide the more useful applications to agriculture sector [5]. Artificial Intelligence has given rise to autonomous platforms such as automatic steered tractor and research robot [6].

Focusing on crop production, a series of optimization models and software tools have been developed so far on field-operation level. This progress, in parallel with the technological advancements and equipment in field machinery, has provided radical solutions to several challenges that modern farmers face.

In crop production systems, one of the most significant issues is connected to human labour-intensive operations.

These are, mainly, field tasks (such as sensitive fruits harvesting and intra-row weed control) that are more difficult to be executed by traditional field machinery, and human workers are employed. This has brought the increased need for autonomous tractors and robotic platforms to be used in the crop field operations, currently developed at research stage [7].

Field operations in agriculture are quite complex, and various issues should be addressed to allow an effective transition towards the robotics era. To build a robotic solution, an overall system analysis of the field operation should be conducted, together with a cost–benefit analysis [3]. Such a system should comply with very specific requirements, such as lightweight, small size, autonomy, intelligence, communication, safety, and adaptability, to execute the potential task effectively [4]. The relatively smaller size of autonomous machines, compared to conventional tractors and implements, contributes to the reduction of the soil-related issues and in particular soil erosion and soil compaction, that was provoked by large and heavy modern farm machinery [1].

To automate these field operations, a decomposition of these tasks should be performed to transform them into discrete robotic functionalities. This can be achieved by classifying the agricultural tasks into deterministic (tasks that can be designed and optimized, in advance) and reactive (tasks that are associated with behaviors that should deal with unexpected conditions) [5].

The introduction of AI to agriculture will be enabled by other technological advances, including big data analytics, robotics, the internet of things, the availability of cheap sensors and cameras, drone technology, and even wide-scale internet coverage on geographically dispersed fields. By analyzing soil management data sources such as temperature, weather, soil analysis, moisture, and historic crop performance, AI systems will be able to provide predictive insights into which crop to plant in a given year and when the optimal dates to carry out specific field operations in a specific area, thus improving crop yields and decrease the use of water, fertilizers, and pesticides. In terms of tillage operations, via the application of AI technologies the impact on natural ecosystems can be reduced, and worker safety may increase, which in turn will keep food prices down and ensure that the food production will keep pace with the increasing population [8].

AI can influence greatly in terms of productivity where five key measures to improve agricultural productivity are smart water management (drip or sprinkler irrigation), varieties selection (heat/drought/ stress tolerant), conservation tillage (minimized loss of moisture and soil), precise nutrient supplement (save input cost) and farm management software to achieve a paradigm shift in production aspects.

AUTONOMOUS TRACTOR AND ITS USE IN THE FARM

The future success of agriculture is still heavily dependent on technology and how well farmers and other agricultural stakeholders are able to leverage the overall benefits of technology and tailor-make them to be used for the benefit of the agricultural sector. One such technology that is going to make a very big difference in the field of agriculture going into the future is the autonomous tractor.

A driverless tractor, otherwise known as autonomous tractor or self-driving tractor is an autonomous farm vehicle that uses a combination of sensors, cameras, radar and artificial intelligence (AI) to travel between destinations without a human operator inside it. It delivers a high effort (or torque) at slow speeds for the purposes of tillage and other agricultural tasks. It is considered driverless because it operates without the presence of a human inside the tractor itself. Like other unmanned ground vehicles, they are programmed to independently observe their position, decide speed, and avoid obstacles such as people, animals, or task [9]. The various driverless tractors are split into full autonomy and supervised autonomy. The idea of the driverless tractor appears as early as 1940, but the concept has significantly evolved in the last few years. The tractors use Global Positioning System (GPS) and other wireless technologies to farm land without requiring a driver. They operate simply with the aid of a supervisor monitoring the progress at a control station or with a manned tractor in lead.

The autonomous tractor employs high-tech systems and sensors to enable it move around without being manned by a driver. To enable it move around, the autonomous tractor will be remotely monitored and directed by a farmer or a technician who is not on site. The tractor will be directed remotely by directing it into areas of the farm that have already been mapped. To enable it avoid obstacle it is fitted with obstacle detection sensors that will enable it stop so as to enable the obstacles to clear before it continues with its journey. In extreme cases where the obstacle is permanent, the autonomous tractor stops and sends a signal to the farmer or the operator. After receiving the signal, the farmer or the operator will then direct the autonomous tractor around the obstacles with the help of high definition cameras fitted into the autonomous tractor. The driverless tractor is a part of a move to increase automation in farming. Other such autonomous technologies currently utilized in farming include automatic milking and automatic strawberry pickers [9].

(a) (b)

Figure 1. Driverless tractor on field operation, [10]

Other autonomous tractors in development include John Deere’s Autonomous Electric Tractor and the Case IH Autonomous Concept Vehicle, which debuted in 2016. Several tractors in Case IH’s Magnum AFS (Advanced Farming Systems) Connect Series now feature connectivity concept vehicle, including innovative display features, a new guidance system in 2020, and other Advanced Farming Systems Connect technologies, which allow operators to remotely monitor and manage field operations with the help of data collection.

A remotely-controlled tractor by Valtra and FlisaWalso launched in 2020. The connectivity products being used to enable autonomous tractors, including sensors, connectors, specialty cables, and LiDAR systems, are being borrowed from proven designs in automotive and transportation applications, and in smart farming technologies such as drones.

In agricultural applications, sensors can be used to evaluate moisture levels in the air, soil, and harvested crops; monitor fertilizer and water use; and track where and how much time each piece of machinery has been working. Farmer-driven tractors equipped with smart technologies are already working fields around the world, using sensor networks, AI-driven monitors, onboard controllers, and other advanced embedded technologies to drastically increase efficiency and productivity. These tractors can measure and place seeds, fertilizer, or pesticides with greater precision, evaluate crop health, and transmit information about fuel levels and required equipment maintenance to Smartphone apps or computers. Several of them also manage some driving functions without the farmer's direct intervention [10].

The two basic approaches to building and programming the tractors are:

I. Full Autonomy: currently, the majority of full autonomous tractors navigate using lasers that bounce signals off several mobile transponders located around the field. These lasers are accompanied with 150 MHz radios to deal with line-of-sight issues [9]. Instead of drivers, the tractors have controllers. Controllers are people that supervise the tractors without being inside them. These controllers can supervise multiple tractors on multiple fields from one location. Another fully autonomous tractor technology involves using the native electrical (or LAN bus) system of the tractor or farm equipment to send commands. Using GPS positioning and radio feedback, automation software manages the vehicles' path and controls farming implements. A retro-fit radio receiver and on-board computer are generally used to receive commands from the remote command station and translate it into vehicle commands such as steering, acceleration, braking, transmission, and implement control.

II. Sensor technologies such as lidar improve safety by detecting and reacting to unforeseen obstacles. However, the driverless tractor is considered controversial in terms of safety and public acceptance. A tractor operating without a driver makes people nervous [11]. Creating technology that stays safe in all scenarios where failure could possibly occur takes a lot of programming and time. In terms of motion detection, the tractors have sensors to stop them if they detect objects in their path such as people, animals, vehicles or other large objects [12].

III. Supervised Autonomy: Tractors that function with supervised autonomy (automated technology, but with a supervising operator present), use vehicle-to-vehicle (V2V) technology and communication. There is a wireless connection between the two tractors to exchange and share data. The leading tractor (with an operator) determines speed and direction which is then transmitted to the driverless tractor to imitate [13].

How the autonomous tractor as well as other self-driving cars works is that the developers of these self-driving vehicles use vast amounts of data from image recognition systems, along with machine learning and neural networks, to build systems that can drive autonomously.

The neural networks identify patterns in the data, which is fed to the machine learning algorithms. Such data as images from cameras from which the neural network learns to identify trees, farm houses, etc. Autonomous tractors work in the same principles as self-driving cars aside the fact that it delivers a high effort (or torque) at slow speeds for the purposes of tillage and other agricultural tasks. They identify objects, interpret situations, and make decisions based on object detection and object classification algorithms. They do this by detecting objects, classifying them, and interpreting what they see. The diversity and redundancy involved is that machine learning is accomplished through a fusion of many algorithms that overlap to minimize failure and ensure safety during field operations. These algorithms interpret road signs, identify lanes, trees, and so on, and recognize crossroads.

How they see is that the three major sensors used by these self-driving vehicles work together as the human eyes and brain. These sensors are cameras, radar, and lidar. Together, they give the vehicle a clear view of its environment. They help the vehicle to identify the location, speed, and 3D shapes of objects that are close to it. The cameras are stationed at every angle for a perfect view of their surroundings. The Radar detectors augment the efforts of camera sensors at night or whenever visibility is poor. They send pulses of radio waves to locate an object and send back signals about the speed and location of that object.

Lidar sensors calculate the distance through pulsed lasers, by empowering driverless vehicles with 3D visuals of their surroundings, adding richer information about shape and depth. LiDAR is one of the most important technologies used in the development of self-driving vehicles. Basically, it is a device that sends out pulses of light that bounce off an object and returns back to the LiDAR sensor which determines its distance. The LiDAR produces a 3D point cloud which is a digital representation of the way the vehicle sees the physical world [6].

To define the route and actions the tractor should carry out, a software is used. This software is a plug-in for AutoCAD that comprises of a number of scripts and tools to generate the final route plan. Thus, the software drive, controls the actions of the tractor.
The process starts by defining the tractor and equipment to be used and identifying the field boundary and existing structures in WGS84 or UTM coordinates. This can come from existing digital maps or can be obtained by driving the tractor around the field and logging the points. Next, the working direction is chosen, usually parallel to a long edge of the field. The software Navigation Plan then offers a set of suggested guidelines for the body of the field and the headlands (based on the working width and desired overlap of the implement) that the tractor could follow. These points can then be selected, one at a time by clicking the mouse, until the plan has been completed. If the user tried to define a route that cannot be achieved by the tractor, (e.g. defining a turning circle that is too tight) the software will alert the user Operations or treatments can also be defined in the route plan as the Software Drive also has control over the three point linkage as well as implement on and off and the PTO. See Figure 2. The final route plan (job file) is then stored as a text file that can be transferred to the tractor on a USB memory stick.

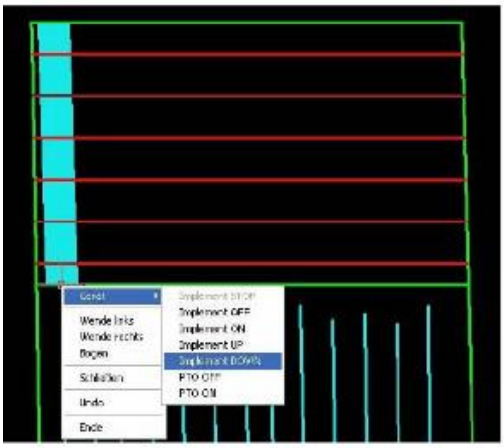

Figure 2. Screen shot from part of the Tractor route planning process, [6].

Figure 2 shows the screen shot from part of the route planning process showing the field boundary (green), headland guidelines (red), crop rows (thin blue lines), first part of the route (thick blue line) and defining the point where the implement should be lowered.

ARTIFICIAL INTELLIGENCE WITH ROBOTIC SYSTEMS IN AGRICULTURAL FIELD OPERATIONS

The existing literature of robotic systems in agricultural field operations was classified according to major field operations, as follows: (1) Tilling, (2) weeding, (3) seeding, (4) disease and insect detection, (5) crop scouting (plant monitoring and phenotyping), (6) spraying, (7) harvesting, (8) plant management robots, and (9) multi-purpose robotic systems [6]. This paper, however, intends to review a few of the most important literature on selected field operations, based on scientific and commercial resources, as presented below.

Tilling

Tilling operations consist of primary and secondary tilling. Primary tilling is deep agitation of the soil that produces a rough surface, while secondary tilling is the opposite of primary tilling. Plowing is an example of a primary tilling operation; harrowing, rototilling and cultivating are a few examples of secondary tilling. Primary tilling is followed by secondary tilling to produce a smooth surface. Tilling is a tedious and labor intensive process, making this task a clear target for automation [14]. Traditional tractors have sufficient power to pull up the soil because they are heavy and have high torque, but small robots cannot perform this task. Tractors also tend to damage soil through compaction.

One of the earliest studies on automatic plowing was conducted by [15] using a conventional tractor with a furrow following transducer and steering servo. This tractor used an optic-electronic sensing technique for turning around the corners; however, the system was not well suited for inclined slopes due to its large displacement errors. Trials conducted using the implemented guidance system and automatic turning control were monitored over 200 runs. The tractor returned to its target position within ± 30 cm over 50% of the time and within ± 60 cm over 75% of the time. In related research, an existing commercial tractor was modified into an autonomous robot, and additional equipment was attached to it in order to perform agricultural operations. [16] modified a commercial tractor (Yanmar EG65) by fixing a global navigation satellite system (GNSS) antenna for navigation and a DC motor for steering control. The GNSS of the tractor obtains the real-time reference position data from the global positioning systems (GPS) earth observation network system (GEONET) through the mobile phone network; the data then must be corrected for the inclination of the vehicle.

The inertial measurement unit (IMU) in the tractor provides information regarding roll, pitch and heading angle. The data from the azimuth sensor, GNSS and IMU are compared to estimate the control parameter that is converted into an actuator command. This control parameter corrects the error in following a particular trajectory. Path planning was performed manually by considering the coordinates of the four corners of a square field and was provided to the tractor as an input [17] modified a commercially available tractor into a robotic vehicle known as Robotra, as shown in Fig. 3. Robotra was able to perform unmanned tilling operations using its path-planning algorithm. This robot used the real-time kinematic-global navigation satellite system (RTK-GNSS) to provide position information for navigation. RTK is a technique that is used to improve the accuracy of satellite-based positioning systems, such as GNSS, by approximately a few centimeters. Three methods of navigation operation were analyzed: basic, diagonal and round operation methods. Each operation method used a two-step process consisting of path planning and vehicle guidance to follow the path.

Figure 3. Robotra performing a tilling operation, [18].

Weeding

Weeding robots have already been under development over the last years, and there are also a number of commercial robots on the market. Most of the major problems related to the existing weeding robots are being dealt with - mainly, the use of recent advancements in computer science (e.g., deep learning) and the integration of more accurate navigation systems (e.g., RTK GPS). At present, what remains to be done is to improve their performance, increase working area and working speed, and increase the accurate detection of weeds for selective spot spraying. There are a few key issues that should be taken into account; i.e., how the existing robotic systems could perform on crops with similar operational requirements, to expand their potential use and the overall development of weeding robots in crops with low competitiveness towards weeds, such as specific vegetables.

In most weeding robots, the vision sensors are currently used in combination with distance identification sensors. This, though, could be potentially enhanced by even higher resolution weed detection sensors for selective spot spraying. Generally, existing robots focus on above-ground weed detection. Possible solutions for future weeding robots may include the detection of weeds in their primary growth, when the weed sprouts are still below the ground. Such systems could be equipped with sensors measuring, for instance, the soil electric conductivity [19].

Similar to mechanical weeding robots, the effectiveness of the system for spotting weeds is among the most critical performance metrics for the chemical weeding robots. By using a Drop on Demand (DoD) system -a system that detects the weeds within the plant row and selectively shoots droplets of herbicide onto those weed leaves - 100% effectiveness was achieved, which is the highest among chemical robots [20]. In parallel, 98% and 89% detection accuracy were presented in a double experiment of a different vision-based weeding robot [21].

Finally, effectiveness (weed detection and destruction) of more than 85% under ideal conditions is underlined by the Eco Robotix weeding robot [22].

While a series of commercial chemical weeding robotic systems are available, almost no performance metrics exist [23, 24, 25]. The perception sensors used for weeding offer similar levels of performance. All robots make use of a camera, where RGB (Red–Green–Blue), infrared (IR) and web cameras are the most commonly used. There also exist sensors that allow the robot to identify it surroundings and its relative position to the weeds, using acoustic distance sensors, gyroscopes, laser range finders, Inertial Measurement Unit (IMU), etc., [18].

Figure 4. Field Robot Weedy, [26].

Seeding

The last years' seeding robots have been developed for seeding both at com0mercial and research level, but to a limited number due to the complexity of the operation. Even though the current advancements in sensors play a crucial role in facing the issues related to these robots, they should be optimized further by minimizing the errors and maximizing the accuracy rates.

Presently, there are a few key challenges identified for seeding robots, such as the working speed of the robot, as it is one of the main factors for precision seeding, making its calibration crucial for each robot. Moreover, the need to improve speed and accuracy, with better vision systems. Better image detection systems that use more advanced algorithms are already under development [27]. Before seeding, such vision systems should be able to identify the soil surface quality and structure, the existence of any weeds, and possible obstacles that may occur. After seeding, the seeding performance should be evaluated, especially in fields with an uneven surface.

There has been progress in commercial seeding robots made by Fendt [28, 29], which can be used as an intelligent fleet of seeding robots or individual units. The most important information for seeding is the depth and the position that the seed is going to be planted. As a result, force, pressure, angle and displacement sensors are used in combination with wheel encoders, compasses and displacement sensors [18].

Spraying

Besides weed management, where herbicide sprayers are used, spraying robots can be used for pests (diseases and insects) and also for liquid fertilizers (foliar). As a result, the farmer is exposed to large quantities of those toxic active ingredients no matter the protective measures that are taken. It is therefore, crucial to introduce spraying robots to prevent possible health hazards. Due to the rapid development of computer vision and artificial intelligence, robotic sprayers feature novel intelligence systems that enable selective spraying, compared to conventional uniform spraying across the crop.

Robots could make use of such technologies, reducing agriculture's environmental impact as well as consumer exposure to pesticides, and preventing the development of resistance to those substances by the targeted organisms [30].

Various approaches have been proposed when designing a spraying robot, mainly due to restrictions and possibilities of the operating environment. For instance, in greenhouses, two approaches have been identified, namely robots that move using the greenhouse piping system [30, 31], and robots that navigate between rows without being mounted on those pipes [32, 33, 34]. Finally, the spraying system (nozzles) could be mounted directly on the spraying platform [33, 18], or it could be mounted on a robotic manipulator with various degrees of freedom (DOF).

Harvesting

Harvesting/fruit-picking is one of the most common tasks in agriculture and also one of the most demanding and challenging areas for agricultural robotics. The research on harvesting and fruit-picking Agricultural Robotic Systems (ARS) started more than three decades ago, focusing mainly on open fields and orchard crops such as citrus, apple, cotton, industry tomato, melon and watermelon [35, 36].

A harvesting device was developed for lettuce heads using a 3-DOF manipulator, an end effector, a lettuce-feeding conveyor, an air blower, a machine-vision device, six photo-electric sensors and a fuzzy logic controller, which gave an ASR of 94% [37] developed an eggplant robot harvester based on a machine-vision algorithm combining a colour segment operator and a vertical division operator to detect fruits under different lighting conditions. A visual-size feedback fuzzy controller actuating a manipulator, and an end effector including a fruit-grasper, a judger and a peduncle-cutter were also integrated into the demonstrator.

CONCLUSIONS

The use of artificial intelligence in tractor field operations is the future of agriculture. Autonomous tractors and other forms of AI applications in the farm will enable farmers to fully automate their operations and therefore reduce all the disadvantages associated with human labour in agriculture. It will also herald a future for agriculture where the farmers will be able to optimize their output while using very limited and less resources with the overall aim of increasing agricultural productivity.

REFERENCES

[1] FAO. *Hunger and Food Insecurity*. 2020.Food and Agriculture Organization of the United Nations, Food and Agriculture Organization of the United Nations, 2020, www.fao.org/hunger/en/.

[2] McCarthy J, Minsky ML, Rochester N, Shannon CE. 1955.A Proposal for the Dartmouth Summer Research Project on Artificial Intelligence.

[3] Banerjee, G., Sarkar, U., Das, S., and Ghosh, I. 2018. Artificial Intelligence in Agriculture: A Literature Survey. *International Journal of Scientific Research in Computer Science Applications and Management Studies*, 3(1): pp.18-29.

[4] Johnson, R. 2020. *Jobs of the future: starting a career in artificial intelligence*, https://www.bestcolleges.com/blog/future-proof-industries-artificial -intelligence.
[5] Nawaz, A.S.N., Nadaf, H.A., Kareem, A.M. and Nagaraja, H.2020. Application of Artificial Intelligence in Agriculture-Pros and Cons. *VigyanVarta*1(8): pp. 22-25.
[6] Blackmore B.S., Fountas S., Gemtos T.A., Griepentrog H.W. 2009. A specification for an Autonomous Crop Production Mechanization System. *Proceedings of the International Symposium on Application of Precision Agriculture for Fruits and Vegetables*; Orlando, FL, USA. pp.201–216.
[7] Humm, B.G. 2016. *Applied Artificial Intelligence: An Engineering Approach*. Learn Publishing, 291 p.
[8] Ngozi, O., Clara, A, Eli-Chukwu, I. 2019. Applications of artificial intelligence in agriculture: a review. *Engineering, Technology and Applied Science Research*, 9(4): pp.4377 - 4383.
[9] Mark, B. 2011. Autonomous tractor is outstanding in its field. https://www.wired.com/2011/09/autonomous-tractor-is-outstanding-in-its-field/
[10] Connectorsupplier.com, https: //www.connectorsupplier.com/autonomous-tractors-take-the-farmer-out-of-the-field). [Accesses 13th January, 2020].
[11] Alistair Driver. 2013. OFC13: *Driverless tractors and robots to be the future of farming*. Farmers Guardian.
[12] Anthony, S. 2012. A system for semi-autonomous tractor operations. Autonomous Robots. The Robotic Institute, 13(1): 87-103.
[13] Lucas, C. 2011. Case IH Wins SIMA Innovation Awards. Tractor.com
[14] Micheal A.M., Ojha TP, 2008. Principles of agricultural engineering, vol. I. Jain, Brothers. 638 p.
[15] Harries GO, Ambler B, 1981. Automatic ploughing: A tractor guidance system using opto-electronic remote sensing techniques and a microprocessor based controller. *Journal of Agric. Eng. Res.*, 26: pp.33-53.
[16] Nagasaka Y., Tamaki K., Nishiwaki K., Saito M., Motobayashi K., Kikuchi Y., Hosokawa H., 2011. Autonomous rice field operation project in NARO. IEEE Int. Conf on Mechatronics and Automation; August. pp: 870-874.
[17] Matsuo Y., Yukumoto O., Noguchi N., 2012. Enhanced adaptability of tilling robot (initial report). JARQ 46: 295-303. https://doi.org/10.6090/jarq.46.295
[18] Krishnaswamy Rangarajan, Purushothaman Raja, Manuel Perez Ruiz, 2017. Task-based agricultural mobile robots in arable farming: A review. Spanish Journal of Ag. Research 15(1), pp. 1-16. https://doi.org/10.5424/sjar/2017151-9573.
[19] Spyros Fountas, Nikos Mylonas, LoannisMalounas, EfthymiosRodias, Christoph Hellmann Santos and Erik Pekkeriet. 2020. Agricultural Robotics for Field Operations. *Sensors* 20, 2672; doi; 10.3390/s20092672.
[20] Utstumo T., Urdal F., Brevik A., Dørum J., Netland J., Overskeid Ø., Berge T.W., Gravdahl J.T. 2018. Robotic in-row weed control in vegetables. *Computer Electronic in Agriculture* 154: 36–45.
[21] Van Evert F.K., Van Der Heijden G.W.A.M., Lotz L.A.P., Polder G., Lamaker A., De Jong A., Kuyper M.C., Groendijk E.J.K., Neeteson J.J., Van Der Zalm T. 2006. A mobile field robot with vision-based detection of volunteer potato plants in a corn crop. Weed Technology 20: pp.853–861.
[22] EcoRobotix. [(accessed on 6 May 2020)]; Available online: https://www.ecorobotix.com/en/
[23] Klose R., Thiel M., Ruckelshausen A., Marquering J. Weedy . 2008. A sensor fusion based autonomous field robot for selective weed control; Proceedings of the Conference: Agricultural Engineering—Land-Technik 2008: Landtechnik regional und International; Stuttgart-Hohenheim, Germany. 25–26. September 2008; pp.167–172.
[24] Ibex. [(accessed on 6 May 2020)]; Available online: http://www.ibexautomation.co.uk/
[25] Rippa&Vippa. [(accessed on 6 May 2020)]; Available online: https://confluence.acfr.usyd.edu.au/display/AGPub/Our+Robots.

[26] Ralph Klose, Johannes Marquering, Marius Thiel, Arno Ruckelshausen. 2020.Weedy – a sensor fusion based autonomous field robot for selective weed controlUniversity of Applied Sciences Osnabrück / Competence Center of Applied Agricultural Engineering – COALA, Osnabrück B. Strautmann&Söhne GmbH & Co. KG

[27] Rehman T.U., Mahmud M.S., Chang Y.K., Jin J., Shin J. 2019. Current and future applications of statistical machine learning algorithms for agricultural machine vision systems. *Computer Electronics in Agriculture* 156: pp.585–605.

[28] Xaver. [(accessed on 6 May 2020)]; Available online: https://www.fendt.com/int/xaver.

[29] Mars. [(accessed on 6 May 2020)]; Available online: https://www.fendt.com/int/fendt-mars.

[30] Sammons P.J., Furukawa T., Bulgin A. 2005. Autonomous pesticide spraying robot for use in a greenhouse; Proceedings of the Australasian Conference on Robotics and Automation; Sydney, Australia. 5–7 December 2005.

[31] Holland Green Machine. [(accessed on 6 May 2020)]; Available online: http://www.hollandgreenmachine.com/sprayrobot/product-information-spray-robot-s55/

[32] Sanchez-Hermosilla J., Rodriguez F., Gonzalez R., Luis J., Berenguel M. Mobile Robots Navigation. INTECH Open Access Publisher; London, UK: 2010. A mechatronic description of an autonomous mobile robot for agricultural tasks in greenhouses.

[33] Mahmud M.S.A., Abidin M.S.Z., Mohamed Z., Rahman M.K.I.A., Iida M. 2019. Multi-objective path planner for an agricultural mobile robot in a virtual greenhouse environment. *Computer Electronics in Agriculture*. 157: pp. 488–499.

[34] Singh S., Burks T.F., Lee W.S. 2005. Autonomous robotic vehicle development for greenhouse spraying. Trans. Am. Soc. Agric. Eng.;48: pp. 2355–2361.

[35] Underwood J.P., Calleija M., Taylor Z., Hung C., Nieto J., Fitch R., Sukkarieh S.2015. Real-time target detection and steerable spray for vegetable crops; Proceedings of the International Conference on Robotics and Automation: Robotics in Agriculture Workshop; Seattle, WA, USA. 26–30 May 2015.

[36] Umeda, M., Kubota, S., & Iida, M. 1999. Development of "STORK, a watermelon-harvesting robot. Artif. Life Robotics, 3, pp.143-147.

[37] Cho, S.I., Chang, S.J., Kim, Y.Y., & An, K.J. 2002. AE-automation and emerging Technologies: Developmentofa three-degrees-of-freedom robot for harvesting lettuce using machine vision and fuzzy logic control. Biosystems Engineering, 82(2), pp.143-149.

UPOTREBA VEŠTAČKE INTELIGENCIJE NA TRAKTORIMA U OPERACIJAMA NA NJIVAMA: PREGLED

[1-2]*Department of Agricultural and Food Engineering,*
University of Uyo, Uyo, Nigeria.
[3]*Department of Agricultural and Bio-Resources Engineering,*
Michael Okpara University of Agriculture, Umudike, Nigeria

Apstrakt: Prema organizaciji UN za hranu i poljoprivredu [1], svetska populacija će se povećati za 2 milijarde do 2050. Međutim, do tada, obrađivati će se samo 4% dodatne površine zemljišta. Može se zaključiti: obzirom da se očekuje da globalna populacija treba dostići 9,1 milijardu 2050. godine, potrebno je proizvesti 70 % više hrane, inače bi oko 370 miliona ljudi bilo gladno 2050 godine.

U tom svetlu, korišćenje najnovijih tehnoloških rešenja treba učiniti poljoprivredu efikasnijom, što ostaje kao jedan od najvećih imperativa.

Dok veštačka inteligencija (VI) ima mnoge direktne primene u različitim sektorima, ona takođe može doneti promenu paradigme u tome kako danas vidimo poljoprivredu. Rešenja zasnovana na primeni veštačke inteligencije (VI) neće samo omogućiti poljoprivrednicima da urade više sa manje rada, već će takođe poboljšati kvalitet i obezbediti brži izlazak prinosa useva na tržište.

Ovaj rad predstavlja pregled primene VI u radu traktora na terenu. U radu se detaljno razmatra upotreba robotike kao oblika veštačke inteligencije (VI) koja je veoma korisna u poljskim operacijama primene traktora kao što su: obrada zemljišta, setva, zaštita od korova, aplikacija herbicida i žetva.

Tipičan fokus je stavljen na snagu traktora i ograničenja primene aplikacija za zaštitu useva i način korišćenja ekspertskih sistema za veću produktivnost.

Ključne reči: *Veštačka inteligencija, poljoprivreda, traktor, poljske operacije, inženjering*

Prijavljen:
Submitted: **22.03.2022.**
Ispravljen:
Revised: **19.09.2022.**
Prihvaćen:
Accepted: **23.09.2022.**

Univerzitet u Beogradu
Poljoprivredni fakultet
Institut za poljoprivrednu tehniku
Naučni časopis
POLJOPRIVREDNA TEHNIKA
Godina XLVII
Broj 4, 2022.
Strane: 15 – 27

University of Belgrade
Faculty of Agriculture
Institute of Agricultural Engineering
Scientific Journal
AGRICULTURAL ENGINEERING
Year XLVII
No. 4, 2022.
pp: 15 – 27

UDK: 631.4:621.2.

Original Scientific paper
Originalni naučni rad
DOI:10.5937/POLJTEH2204015E

DEVELOPMENT AND PERFORMANCE EVALUATION OF A MOTORIZED TUMBLE BARREL FEED/FOOD MIXER

Ukachi J. Etoamaihe[*1], N. R. Dirioha[2], Uma K. Oke[3], Oluwaseun Babalola[4]

[1,2,4]Department of Agricultural Engineering, Michael Okpara University of Agriculture, Umudike, Umuahia, Abia State, Nigeria
[3]Department of Animal Production, Michael Okpara University of Agriculture, Umudike, Umuahia, Abia State, Nigeria

Abstract: A tumble barrel food /feed mixer was designed and fabricated. It has a volumetric capacity of 0.33 m^3. The tumble barrel mixer consists of a hopper, a stainless steel barrel with baffles. It is mounted on a steel framework and driven by a shaft connected to stirrers inside the baffles. The baffles are alternatively placed in the barrel in such a way that they do not touch the stirrers during operation. The shaft is driven by a 3HP (2,25 kW) variable speed electric motor. Performance tests were conducted on the machine after fabrication using the ASAE (R2006) test standards, and also Completely Randomized Design (CRD). Three speeds of the mixer, 100,150 and 200 rpm (min^{-1}) (and four mixing times of 5,10,15 and 20 minutes were studied as they affected the Degree of Mixing (DM) of ground and shelled corn samples in the mixer. Results obtained showed, there was an increase in the degree of mixing as the speed of the machine increased from 100 to 200 rpm (min^{-1}). Also the degree of mixing increased as the time of mixing increased from 5mins to 20 minutes for the three speeds studied. From the Analysis of variance tables, the calculated F-values were very much higher than the tabulated values at 5% probability.

These indicate a high significance of the effect of speeds of mixing on the degree of mixing of the tumble barrel mixer. The speed of 150 rpm (min^{-1}) gave the highest effect in the tumble mixer. From the difference of means tables, there were significant differences in the degree of mixing for 100 and 150 rpm (min^{-1}) speeds for all the different time of mixing durations. However, in the 200 rpm (min^{-1}) speed, there was no significant difference in the DM between the 15 to 20 minutes mixing time duration.

Key words*: Development, Performance, Tumble Barrel Mixer, Feed, Shaft, CRD.*

[*]Corresponding author. E-mail: etoamaihe.ukachi@mouau.edu.ng

INTRODUCTION

Mixing is a process by which food or feed ingredients are stirred together to get a uniform mixture [1]. Mixers are designed to mix a wide variety free flowing materials for food and feed formulation. To achieve a well-balanced diet with all the relevant nutrients mixing is necessary, providing a uniform mixture by stirring of two or more ingredients [2]. The purpose of mixing is to blend the ingredients of certain formulation into a compound such that each small unit of sample of a given mass has the same composition of each ingredient as the design formula [3]. In this case the mixing is said to be thorough and uniform [4].

There are basically two methods of mixing. They are:

I. Manual mixing

II. Mechanical mixing

According to [5], the manual method of mixing feed entails the use of shovel or hand to intersperse the feed's constituents into one another on open concrete floors. The manual method of mixing feed ingredients is generally characterized by low output, less efficient, labour intensive and may prove unsafe and hazardous to the health of intended consumers. The mechanical method of mixing on the other hand is achieved by using a wide variety of mechanized mixers to achieve mixing while eliminating the drudgeries imminent in manual mixing. Tumble barrel mixers are mechanized mixers that use the principle of rotating barrel movement and internal baffles or stirrers to mix feed homogeneously inside a barrel. They have the advantage of total mixing of constituents and completely eliminating unmixed spots (dark spots) in the mixer because of their tumbling actions. [4].

The purpose of the machine is to make solid food and feed mixing process less laborious especially for medium scale industries and for domestic purposes. The objectives of this study therefore include; to design and fabricate a motorized tumble barrel mixer. To test the developed mixer for performance during operation and to analyze the experimental results obtained using completely randomized design (CRD).

MATERIAL AND METHODS

Design Considerations

The following considerations were made during the development of the machine:

Develop a machine that can mix solid food or feed materials uniformly without dark spots.

Develop a machine that is smooth in operation with little noise.

To use locally available materials for its construction.

To develop a rigid, reliable and efficient mixing machine when in operation.

Description of the Machine

The tumble barrel mixer consists of a cylindrical stainless steel drum of length 0.99m and diameter of 0.5m mounted on a rigid steel frame work, powered by a 3Hp variable speed gear motor. The frame is 0.6m in height,1.8m length and 0.54m width.

The driving shaft length is 1.9m. The cylindrical drum is slanted 30^0 to the horizontal to aid mixing. The mixer has a feed opening at the topmost part of the drum and a discharge point at the bottom. Stirrers are fixed on the driving shaft inside the drum. There are also baffles by the sides of the drum located below and above the stirrers on the driving shaft. The mixer is designed to operate in batches. The isometric and orthographic drawings of the machine are shown in Figs 1 and 2, while the developed machine is shown Fig.3.

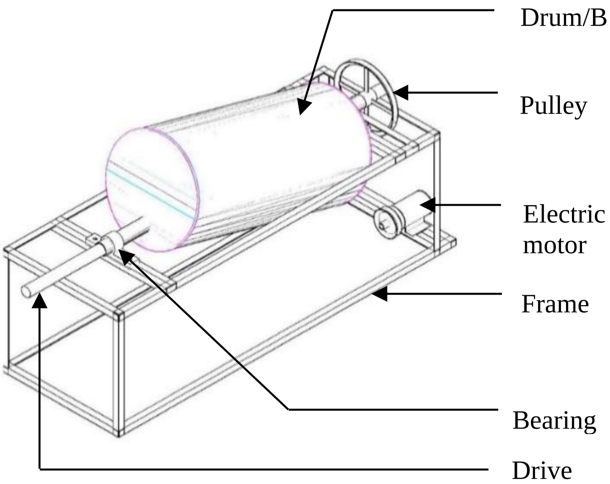

Figure 1. Isometric View of the Tumble Barrel Mixer

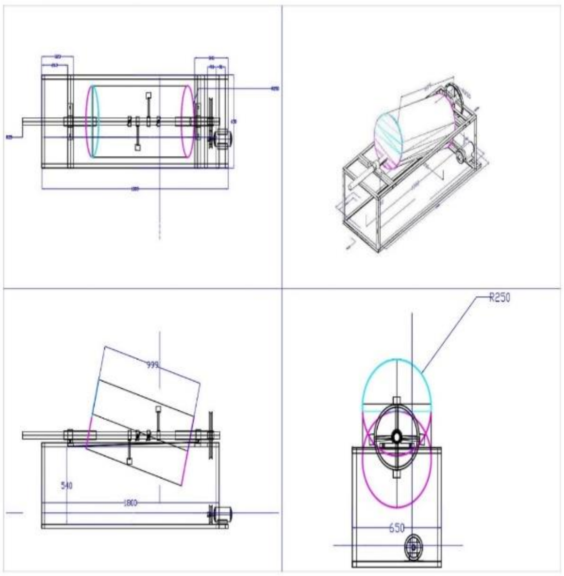

Figure 2. Orthographic View of the Tumble Barrel Mixer (All dimensions in mm)

Figure 3. The Developed Tumble Barrel Mixer

DESIGN ANALYSIS AND CALCULATIONS

Volume of the Mixer

The mixer has a diameter of 0.5m and a length of 0.99m and therefore has a volume of $0.2m^3$

The Power Drive Mechanism

The power is from the variable speed gear electric motor and the power required by the mixer was calculated using the relation by [6];

$$P = \tau\omega \qquad \text{……………..} \textbf{(1)}$$

Where:
P = power required (HP);
τ = Torque (Nm)

And the torque is calculated from the equation by [6] as;

$$\tau = Fr \qquad \text{……………..} \ \mathbf{(2)}$$

F = weight of mixer fully filled with wet feed. (i.e 1.121N.)
r = Radius of mixer.

A 3 HP electric motor was selected because of the estimated power requirements for turning and driving the mechanisms in the tumble mixer.

Belt

The length of belt otherwise known as effective belt length (Le) is a design parameter required for the selection of belt length to fit in sheave so as to avoid error that can lead to accidents.

Effective length of belt can be gotten using the formula outlined by [6] as;

$$Le = 2c + 1.57(D + d) + \left(D - d/_{4c}\right)^2 \qquad \text{……………..}\mathbf{(3)}$$

C = 41.91cm
D = 20.48cm
d = 16.51cm

Where:

L_e = the effective belt length
C = the design distance between the two pulleys (D and d)
D = the diameter of the driver pulley (cm)

$$L_e = 2(41.91) + 1.57(20.48 + 16.51) + \left(20.48 - 16.5/_{4(41.91)}\right)^2$$

$$L_e = 140.67cm$$

Determination of the thickness of the cylindrical wall of the mixer

The mixer barrel has a circular cross section and is therefore subjected to circumferential stress concentration. According to [7], the stress is given as;

$$\sigma = \frac{pd}{4t} \qquad \text{……………..} \ \mathbf{(4)}$$

therefore,

$$t = \frac{pd}{4\sigma} \qquad \text{……………..} \ \mathbf{(5)}$$

Where:

t = thickness of the mixer wall
P = 68.95-275.79 MPa (operational pressures recommended for mixers) [8]
σ = maximum shear stress of stainless steel material (310N/mm^2)
d = 700mm; t was calculated as, t = 68.95 x 700/4 x 310 = 39mm.

To avoid any underestimation a 40mm thick stainless steel mixer was used.

Mixer drive shaft diameter

The drive shaft diameter was obtained using the expression outlined by [9], and is given as;

$$d^3 = {}^{16}/_{\pi\tau_{max}} \sqrt{(M_b K_b)^2 + (M_t K_t)^2} \qquad \text{……………..} \ \mathbf{(6)}$$

Where:

Mt = torsional moment (136.05Nm);
Kb = combined shock and fatique factors applied to bending;
Kt = combined shock and fatique factors applied to torsional moment;
Mb = bending moment;
τ_{max} = allowable shear stress of mild steel.(40MN/m^2)

The diameter of the mixer shaft was obtained as 250mm

Bearing selection

Using the expression by [10], the radial load acting on the drive shaft is obtained as

$$F = {}^{19.1PK \times 10^6}/_{D\,S} \qquad \text{……………..} \ \mathbf{(7)}$$

Where, *F* is the radial force on the shaft (N), *P, the* power transmitted (kW), D is the diameter of the drive shaft.

The Frames

The frames are made of 3mm thick mild steel rectangular bars and have the following dimensions; 1800mm x 650mm x 540mm for length, breadth and height respectively.

MATERIALS AND METHODS

Performance Tests

The performance tests for the tumble drum mixer was carried out according to the standard test procedure for farm batch mixers developed by [11]. In the tests, 100kg of ground corn and 2.8kg of shelled corn were put into the mixer before operation. Four mixing durations of 5min,10min,15min and 20min were used during the mixing operation. Three speeds of the machine, 100,150 and 200 rpm respectively were tested for the three mixing time durations to determine their various degrees of mixing (DM). At the end of each test run, ten samples of 500g each were drawn from the mixed components and analysed.

There were three replications of each test. The coefficient of variation among the blended samples and level of mixing were computed using the expressions developed by [12].

$$CV = \frac{SD}{Y} \times 100 \qquad \text{……………..}\textbf{(8)}$$

$$Y = \frac{\sum yi}{n} \qquad \text{……………..}\textbf{(9)}$$

$$SD \equiv \sqrt{(Y - yi)^2 \big/ n-1} \qquad \text{…………….. }\textbf{(10)}$$

$$DM = 100 - \%CV \qquad \text{…………….. }\textbf{(11)}$$

Where:

CV = percent coefficient of variation,
DM = percentage degree of mixing,
SD = standard deviation
Y = mean, *yi* = individual sample analysis results,
n = total number of samples

Experimental Design

The experiments were designed using Completely Randomized Design (CRD). Three speeds of the machine, namely 100,150 and 200rpm were investigated. For each speed, four mixing time durations of 5,10,15 and 20 minutes were used to determine the corresponding percentage degrees of mixing (DM) of the materials. The CRD was used because the design has the maximum degrees of freedom for estimating the error variance. Also the number of replications and factors are restricted only by the number of experimental units available. In this design variations or factors are applied to experimental units at random without restrictions [13].

The linear model by [13] of the CRD is given as;

$$X_{ij} = \mu + F_i + E_{ij} \quad \text{................(12)}$$

Where:

X_{ij} =Any individual observation;
μ=Mean;
F_i =Variation or Factor effect
E_{ij} = Experimental Error

RESULTS AND DISCUSSION

Results

Table 1: Degree of mixing (DM) at 100 rpm (min^{-1}) for indicated times

Replications	@5mins	@10mins	@15mins	@20mins
1	88.6%	91.5%	92.6%	93.1%
2	88.7%	91.6%	92.6%	93.1%
3	88.8%	91.6%	93.1%	93.1%
4	88.8%	91.7%	93.1%	93.1%
Total	354.9	366.4	371.4	372.4
Mean	88.7%	91.6%	92.9%	93.1%

Table 2. Degree of mixing (DM) at 150 rpm (min^{-1}) for indicated times

Replications	@5mins	@10mins	@15mins	@20mins
1	89.7%	92.4%	92.5%	92.7%
2	89.7%	92.4%	92.6%	92.7%
3	89.8%	92.4%	92.6%	92.8%
4	89.9%	92.4%	92.7%	92.8%
Total	359.1	369.5	370.4	371
Mean	89.8%	92.4%	92.6%	92.8%

Table 3. Degree of mixing (DM) at 200 rpm (min^{-1}) for indicated times

Replications	@5mins	@10mins	@15mins	@20mins
1	88.7%	91.7%	93.6%	93.7%
2	88.6%	91.8%	93.7%	93.6%
3	89.2%	91.7%	94.1%	94.1%
4	89.1%	92.1%	93.8%	94.1%
Total	355.6	367.3	375.2	375.5
Mean	88.9%	91.8%	93.8%	93.9%

Table 4. Analysis of Variance for (DM) at 100 rpm (min^{-1})

Source	Degrees of freedom	Sum of squares	Mean square	F calculated	F tabulated(5%)
CFM	1	134157.4	24.1		
Factors	2	48.2	0.039	617.9***	3.8
Error	13	0.5	3.25	(highly significant)	
Total	15	48.7			

Table 5. Analysis of Variance for (DM) at 150 rpm (min^{-1})

Source	Degrees of freedom	Sum of squares	Mean square	F calculated	F tabulated(5%)
CFM	1	135056.3	11.9		
Factors	2	23.8	0.015	793.3***	3.8
Error	13	0.2	1.6	(highly significant)	
Total	15	24			

Table 6. Analysis of Variance for (DM) at 200 rpm (min^{-1})

Source	Degrees of freedom	Sum of squares	Mean square	F calculated	F tabulated (5%)
CFM	1	135718.6	32.7		
Factors	2	65.4	0.054	605.6***	3.8
Error	13	0.7	4.41	(highly significant)	
Total	15	66.1			

Table 7. Difference of Means Table in F-LSD for 100 rpm (min^{-1}) Speed

Means	88.73	91.6	92.9	93.1
93.1	4.37	1.5	0.2	0
92.9	4.17	1.3	0	
91.6	2.87	0		
88.73	0			

FLSD =0.084

Table 8 : Difference of Means Table in F-LSD for 150 rpm (min^{-1}) Speed

Means	89.8	92.4	92.6	92.8
92.8	3	0.4	0.2	0
92.6	2.8	0.2	0	
92.4	2.6	0		
89.8	0			

FLSD = 0.033

Table 9: Difference of Means Table in F-LSD for 200 rpm (min^{-1}) Speed

Means	88.9	91.83	93.8	93.83
93.88	4.98	2.08	0.08 **NS	0
93.8	4.9	2	0	
91.83	2.93	0		
88.9	0			

FLSD= 0.115

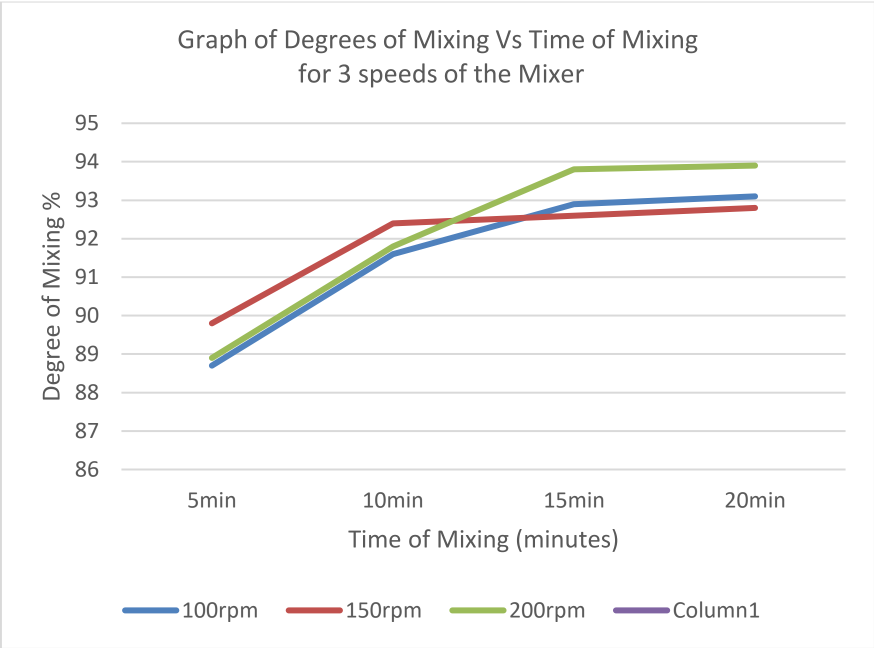

Fig. 4. The Graph of Mixing Time Against Degrees of Mixing for Three Speeds of the Mixer

Discussion of Results

There was a general trend of increase in the degree of mixing as the speed of the machine increased from 100 to 200 rpm (min^{-1}).This is in line with the results obtained by [14] and [15]. It was also observed from tables 1 - 3 that the degree of mixing increased as the time of mixing increased from 5mins to 20 mins for the three speeds studied.
From the analysis of variance tables for the different speeds (tables 4 - 6), the calculated F-values were very much higher than the tabulated values at 5% probability. These indicate a high significance of the effect of speeds of mixing on the degree of mixing of the tumble barrel mixer. These observations are in line with the results obtained by [16].The speed of 150 rpm (min^{-1}) gave the highest effect in the tumble mixer.

In the difference of means tables (tables 7-9), there were significant differences in the degree of mixing for 100 and 150 rpm (min^{-1}) speeds for all the different time of mixing durations (tables 10-11).
However, in the 200rpm speed (table 12), there was no significant difference the degree of mixing between the 15 to 20 minutes mixing time duration.
This can be attributed to the fact that at such high speed the mixing may have consolidated, therefore more residence time of the materials in the mixer will not affect the degree of mixing any more. From the graph in Fig.4, the degrees of mixing (DM) increased proportionally with time up to 10 mins duration. However, the DM tend to be approximately constant after 15 mins of mixing in all cases.

CONCLUSIONS

The tumble barrel food/feed mixer performed satisfactorily well during tests. Results obtained showed, there was an increase in the degree of mixing as the speed of the machine increased from 100 to 200 rpm (min^{-1}) . Also the degree of mixing increased as the time of mixing increased from 5mins to 20 minutes for the three speeds studied. From the Analysis of variance tables, the calculated F-values were very much higher than the tabulated values at 5% probability. These indicate a high significance of the effect of speeds of mixing on the degree of mixing of the tumble barrel mixer. The speed of 150 rpm gave the highest effect in the tumble mixer. From the difference of means tables, there were significant differences in the degree of mixing for 100 and 150 rpm (min^{-1}) speeds for all the different times of mixing. However, in the 200 rpm (min^{-1}) peed, there was no significant difference in the DM between the 15 to 20 minutes mixing time duration.

REFERENCES

[1] Say, D.R. 1987. The Technical Center for Agricultural and Rural Development. www.Rmcord.Com/Twisted.Com.Htm.

[2] Keith, B. And Tim, H. 1994. Testing Mixer Performance, Kansas State University Agricultural Experiment Station And Cooperative Service, Mf-1172, pp. 1-4.

[3] Harner, I. Keith, B. And Tim H. 1995. Rotating Drum Mixers. Kansas State University of Agriculture and Cooperative Extension Service Bulletin.

[4] www.Miraclemixer.Com 2017.Tumble Blenders.Accessed 22nd October 2017

[5] Adebukola A.A and Patrick O.A. 2019. Development and Evaluation of a Fish Feed Mixer.AgricEngInt: CIGR Journal Open Access Vol.21.No.3

[6] Khurmi RS and Gupta JK 2005. A textbook of machine design (S. I. Units), Eurasia Publishing House (PVT.) Ltd., Ram Nagar, New Delhi-110055. 2005; 509-600, 677-714.

[7] Singh,S. (2001).Machine Design.Khanna Publishers ,New Delhi pp 298-333.

[8] Brennam, J. G., Butters J. R., Cowell, N. D. and Lilly, A. E. V.1981. Food Engineering Operations, 2nd Edition. Applied Science Publishers ltd London, pp 116.

[9] Hall, A. S.; Holowenko, A. R. and Laughlin; H. G. 1988. Theory and Problems of Machine Design. S. I. (metric) edition. McGraw-Hill Book Company, Singapore. pp. 255 – 276.

[10] Krutz,G, Thompson,L and Claar, T 1984. Design of Agricultural Machinery. John Wiley and Sons New York. pp 259-277

[11] ASAE Standards,2006 (ASAE S380 R2006). Test Procedure to Measure Mixing Ability of Portable Farm Batch Mixers, pp. 261-262
[12] Ibrahim,S.O and Fasasi M.B. 2004. Design and Development of a Portable Feed Mixer for Small Scale Poultry Farmers.Proceedings of NIAE 26 Ilorin
[13] Cochran, W. G. and Cox, G. M. 1992. Experimental Design 3rd edn. John Wiley and Sons M. Y, pp.335 – 375.
[14] Balami,A.A, Adgidzi,D, and Muazu , A. 2013. Development and Testing of an Animal Feed Mixing Machine, International J. of Basic and Applied Sciences 1(3): pp. 491-503
[15] Chikwado, U.K. 2015. Development and Performance Test of Poultry Feed Mixing and Pelleting Machine. International Journal of Science and Research 4(6): pp.1161-1166
[16] Gosa,B. 2020. Development of Livestock Feed Mixer. International Journal of Scientific and Research Publications vol.10 Issue 10.

RAZVOJ I OCENA PERFORMANSI MIKSERA (MEŠAČA) SA MOTOROM ZA HRANU

Ukachi J. Etoamaihe[1], N. R. Dirioha[2], Uma K. Oke[3], Oluwaseun Babalola[4]

[1,2,4]Department of Agricultural Engineering, Michael Okpara University of Agriculture, Umudike, Umuahia, Abia State, Nigeria
[3]Department of Animal Production Michael Okpara University of Agriculture, Umudike, Umuahia, Abia State, Nigeria

Apstrakt: Dizajniran je i proizveden mešač (mikser) za hranu i stočnu hranu sa cilindričnim oblikom. Ima kapacitet zapreminski od 0,33m3^2. Cilindrični mikser se sastoji od rezervoara, cilindra od nerđajućeg čelika sa pregradama (lopatice). Montira se na čelični okvir i pokreće osovinu koja je povezana sa mešalicama unutar pregrada. Pregrade su alternativno postavljene u cilindru tako da se ne dodiruju tokom rada. Osovinu pokreće elektromotor promenljive snage od 3 KS (2,25 kW). Testovi performansi su sprovedeni na mašini nakon proizvodnje korišćenjem standarda za testiranje ASAE (R2006), kao i potpuno randomizovanog dizajna (CRD). Proučavane su tri brzine miksera, 100, 150 i 200 rpm (min^{-1}) i četiri vremena mešanja od 5, 10, 15 i 20 minuta, jer utiču na stepen mešanja (DM) mlevenih i oljuštenih uzoraka kukuruza u mešalici.

Dobijeni rezultati su pokazali da je došlo do povećanja stepena mešanja kako se brzina mašine povećavala sa 100 na 200 rpm (min^{-1}). Takođe se stepen mešanja povećavao kako se vreme mešanja povećavalo sa 5 minuta na 20 minuta za tri proučavane brzine. Iz tabele Analiza varijanse, izračunate F-vrednosti su bile mnogo veće od tabelarnih vrednosti sa verovatnoćom od 5%. Ovo ukazuje na veliki značaj uticaja brzina mešanja na stepen mešanja cilindrične mešalice. Brzina od 150 rpm (min^{-1}) dala je najveći efekat u mikseru.

Iz razlika u tabelama srednjih vrednosti, uočene su značajne razlike u stepenu mešanja za brzine od 100 i 150 rpm (min^{-1}) za sva različita vremena trajanja mešanja.

Međutim, pri brzini od 200 rpm (min^{-1}), nije bilo značajne razlike u DM između vremena mešanja od 15 do 20 minuta.

Ključne reči: *Razvoj, Performanse, Tumble Barrel mešač, punjenje, osovina, CRD.*

Prijavljen:
Submitted: **07.07.2022.**
Ispravljen:
Revised: **20.10.2022**.
Prihvaćen:
Accepted: **27.10.2022.**

Univerzitet u Beogradu Poljoprivredni fakultet Institut za poljoprivrednu tehniku Naučničasopis **POLJOPRIVREDNA TEHNIKA** Godina XLVII Broj 4, 2022. Strane: 28 – 37		University of Belgrade Faculty of Agriculture Institute of Agricultural Engineering Scientific Journal **AGRICULTURAL ENGINEERING** Year XLVII No. 4, 2022. pp. 28 – 37

UDK: [004.932.2:633.85-157.63]:004.738.5 *Originalni naučni rad*
Original Scientific paper
DOI: 10.5937/PoljTeh2204028M

DETEKCIJA GUBITAKA SEMENA ULJANE REPICE PRE BERBE ANALIZOM SLIKE U OKVIRU FOG RAČUNARSTVA

Dušan Marković[*1], Ranko Koprivica[1], Biljana Veljković[1], Marija Gavrilović[1], Dejan Vujičić[2], Uroš Pešović[2], Siniša Ranđić[2]

[1]Univerzitet u Kragujevcu, Agronomski fakultet u Čačku
[2]Univerzitet u Kragujevcu, Fakultet tehničkih nauka u Čačku

Sažetak: Gubici u proizvodnji uljane repice mogu nastati pre berbe, prouzrokovani spontanim otvaranjem zrelih mahuna i ispadanjem semena na zemljište. Ljuske uljane repice, na istoj biljci sazrevaju u različito vreme, tako da imamo da su one na vrhu prezrele a u donjem delu zrele. Jedan od najkritičnijih momenata u uzgajanju uljane repice predstavlja određivanje pravog vremena za berbu, jer zakasnela berba podrazumeva prezrevanje i otvaranje ljuski, što dovodi do rasipanja i gubitaka semena. Jedan od načina da se prati osipanje semena i samim tim potencijalni gubici jeste postavljanje posuda između redova biljaka uljane repice i nadgledanje (prebrojavanjem) broja semena koje upadnu iz otvorenih ljuski. Predstavljeni model sistema koji čine senzorski uređaji sa pridruženim kamerama, pozicionirani iznad posuda, imaju funkciju da prenesu sliku o trenutnom stanju zrna u njoj. Centralno mesto u ovom radu predstavlja aplikacija za analizu slike koja se može izvršavati u blizini lokaliteta na računarski podržanim uređajima u okviru Fog računarstva. Na taj način rezultati analize slike o broju semenki u posudi dobijaju se gotovo odmah i mogu se proslediti na Cloud platformu ili direktno do korisnika koji će preduzeti odgovarajuće akcije. Dobijanjem pravovremenih informacija o broju rasutih semenki moguće je organizovati berba na optimalan način kako bi se izbegli gubici i predupredilo prezrevanje zasada uljane repice.

Ključne reči: *Analiza slike, seme uljane repice, Fog računarstvo, Raspberry Pi.*

[*]Kontakt Autor. E-mail adresa: dusan.markovic@kg.ac.rs
Istraživanja u ovom radu su deo Projekta 451-03-68/2022-14 i
Projekta 451-03-68/2022-14/200132 , koje finansira Ministarstvo prosvete, nauke i tehnološkog razvoja Republike Srbije.

UVOD

Koncept Interneta stvari (Internet of Things) doneo je jedan novi pristup u povezivanju uređaja na Internet i razmeni podataka, tako da je zahvaljujući svojim odlikama našao veliku primenu u prikupljanju senzorskih podataka. Prikupljanje podataka bi podrazumevalo prenos podataka sa senzorskih uređaja na Cloud platforme, odnosno na udaljene servere gde bi se na centralnom mestu vršila obrada podataka. Na taj način dobija se struktura sistema gde se podaci čuvaju na jednom mestu i gde se obrada podataka može izvršiti sa potrebnom procesorskom snagom. Međutim, kako se broj senzorskih uređaja koji šalju podatke vremenom povećavao, pojavljuju se sve veći nizovi podataka koje je potrebno prihvatiti i procesirati. Da bi se optimizovao prenos podataka i da bi se dobili rezultati obrade bez većeg kašnjenja, koncept Cloud sistema je proširen skoro do mreže senzorskih uređaja. Na taj način su karakteristike skladištenja i obrade pristiglih podataka sa Cloud platformi prenete bliže lokalnim senzorskim mrežama prateći principe Fog računarstva. U toj varijanti podaci se obrađuju u neposrednoj blizini, nema potrebe za slanjem svih sirovih podataka na Cloud platformu već se samo prosleđuju rezultati obrade, a koje takođe mogu odmah dobiti i krajnji korisnici bez kašnjenja. Autori u radu [1] upravo su opisali Fog računarstvo kao sredstvo pomoću koga bi se predupredile nepovoljne situacije vezane za velike obime podataka koji se generišu od strane IoT i senzorskih uređaja [2]. Primena Cloud-Fog sistema ima svoj značaj i u oblasti poljoprivrede, što se može sagledati kroz radove [3], [4] i [5].

Procesiranje podataka dobijenih posredstvom IoT koncepta predstavljeno je u radovima [6], [7] i [8], gde je korišćena analiza slike kako bi se dobile nove informacije. Slična primena može se sagledati i kod analize slike semena malih dimenzija koje je teže ručno izmeriti za kratko vreme, što se može videti na primeru nadgledanje klijavosti semena koja pripadaju familiji kupusnjača (*Brassica*) [9]. Slično je stanje i sa sitnim semenom uljane repice i upravo u ovom radu predstavljen je primer detekcije i prebrojavanja semenki uljane repice na osnovu analize slike kako bi se utvrdili potencijalni gubici pre žetve.

Cilj ovog rada je predstavljanje sistema za prikupljanje i obradu podatka koji se zasniva na Fog računarstvu, pri čemu bi se obrada podatka izvršavala blizu izvora podataka, a pre slanja na Cloud. Model sistema izvršava obradu podataka koji podrazumeva procesiranje slika na računarski podržanim uređajima blizu senzorskih uređaja. Primena takvog modela je prikazana u slučaju analize slike semena uljane repice, na osnovu koje bi se utvrdili gubici semena pre žetve i odredilo pravo vreme za berbu u cilju smanjenja (izbegavanja) većih gubitaka.

MATERIJAL I METODE RADA

U tehnološkom procesu proizvodnje uljane repice, najveći problem je odrediti odgovarajući momenat berbe. Vreme berbe je povezano sa morfološkim osobinama sorti i opštim stanjem useva na polju. Nepravovremena berba i nepravilna primena mašina za žetvu, prouzrokuju velike gubitke prinosa, lošiji kvalitet zrna i ulja [10], [11], [12] i [13] što umanjuje ekonomičnost proizvodnje ove veoma značajne uljarice.

Prema [14] određivanje vremena i načina mehanizovane berbe uljane repice otežavaju: neujednačeno cvetanje, otvaranje ljuski i međusobna isprepletanost biljaka.

Gubici uljane repice usled otvaranja ljuski nastaju zbog: prirodnih procesa sazrevanja i starenja biljke, neujednačenog sazrevanja ljuski uljane repice, slabe mehaničke čvrstoće ljuske i meteoroloških uslova pre žetve. Uljana repica dugo cveta, zbog čega se kasnije plodovi (ljuske) neujednačeno formiraju i dozrevaju u različito vreme. U momentu žetve, na istoj biljci mogu se naći nedovoljno zrele, zrele, kao i prezrele ljuske koje su se otvorile i iz kojih je zrno ispalo. Pored toga, postoji uzajamna isprepletenost bočnih grana susednih biljaka koje se dodiruju, tako da pri jačim udarima vetra dolazi do kontakta i trenja jedne o druge ljuske, što dovodi do njihovog otvaranja i ispadanja zrna pre žetve.

Glavni razlog otvaranja ploda uljane repice i pojava gubitaka pre i u toku žetve je njegova slaba mehanička čvrstoća. Plod kod uljane repice je ljuska sastavljena od dve polovine između kojih se nalazi središnja tanka pregrada. Polovine ljuske su međusobno spojene šavom (linijom spajanja), tako da čine jednu celinu u kojoj je smešteno zrno. U našim istraživanjima prosečan broj zrna u ljusci je 25. Ljuske se otvaraju duž linije spajanja dve polovine ljuske i unutrašnje pregrade, pri čemu dolazi do odvajanja ovih delova i rasipanja zrna.

Otvaranje ljuski i rasipanje zrna je u prirodi koristan proces, jer se biljke na taj način razmnožavaju, stvaraju nove generacije i produžavaju vrstu. Posmatrajući ovaj proces iz ugla proizvodnje uljane repice on se može smatrati štetnim, jer prouzrokuje velike gubitke zrna i smanjuje prinos. U narednoj godini će iz rasutog semena po zemljištu izniknuti nove biljke uljane repice koje predstavljaju korov u osnovnom usevu, kojeg treba uništiti herbicidima, zbog čega se utroši više radnog vremena i goriva, a time i povećava zagađenje životne sredine i troškova proizvodnje.

Primer predstavljen preko modela sistema sa analizom slike sproveden je na uzorcima semena uljane repice sorte Banaćanka. Posude dimenzija 120 mm x 210 mm predviđene su za postavku ispod ljuski tako da bi u njih upadalo seme iz raspuklih (otvorenih) ljuski i iznad kojih je pozicioniran senzorski uređaj sa kamerom.

Model Cloud-Fog sistema je predstavljen sa Fog slojem između Cloud-a i senzorskih uređaja za prikupljanje podataka. Ideja u prikazanom slučaju podrazumeva da se uređaji sa kamerama rasporede u polju sa uljanom repicom tako što bi se pozicionirali u redovima ispod mahuna uljane repice. Pored uređaja bi se postavila posuda poznatih dimenzija u koju bi se skupljale semenke iz otvorenih mahuna. U definisanim vremenskim intervalima fotografisala bi se posuda i slike bi bile prosleđene na Fog uređaj gde bi se vršila analiza slike, koja bi kao rezultat dala broj semenki u posudi. U toj varijanti rezultati analize bi bili prosleđeni na Cloud platformu i do krajnjih korisnika.

Uređaj na kome se vrši analiza slike deo je sloja koji bi pripadao Fog računarstvu, a u osnovi sastoji se od Raspberry Pi 3 računarskog modula. Raspberry Pi predstavlja računar malih dimenzija (85.60 mm x 53.98 mm x 17 mm) i težine svega 45 g. Raspberry Pi modul predstavlja računarski sistem integrisan na jednom čipu (SoC) sa oznakom BCM28351. On sadrži centralni procesor, radnu memoriju, grafički procesor, žičnu komunikaciju preko Ethernet kabla kao i vezu sa IEEE 802.11 bežičnom mrežom (Wireless) i različite interfejse za eksterne uređaje. Raspberry Pi može da se koristi kao klasičan personalni računar uz dodatak tastature i izlazne jedinice za prikaz odnosno monitora. A može se koristiti i kao web server gde periferne jedinice nisu potrebne. SD memorijska kartica može biti korišćena kao medijum za čuvanje podataka.

Operativni sistem koji se koristi kod Raspberry Pi poznat je pod nazivom Raspbian i jedan je od posebno konfigurisanih Linux operativnih sistema. Linux operativni sistem se dobro uklapa pošto je besplatan i otvorenog koda.

Raspberry Pi modul može biti napajan iz više izvora, kao što je USB port sa računara, zidna utičnica sa USB priključnicama, bekap baterija za mobilne telefone ili solarni punjači za telefone. Takođe, Raspberry Pi može biti napajan uz pomoć alkalnih baterija, pri čemu se može napajati i sa šest punjivih AA baterija sa regulatorom napona [15].

Primeri za testiranje su realizovani tako što bi u posudi bio prihvaćen određeni broj semenki koji odgovaraju potencijalnim gubicima shodno površini posude koju ona zauzima i broju semenki koje može da prihvati. U više navrata bi bio uslikan sadržaj posude za isti broj semenki ali uz drugačiji nasumični razmeštaj semenki i na osnovu tih uzoraka analizom slike je utvrđivan broj semenki. Na kraju za jedan uzorak izračunava se srednja vrednost i poredi se sa realnim broj semenki kako bi se utvrdila tačnost dobijenih rezultata.

Aplikacija za analizu slike predstavlja segment koji je realizovan u programskom jeziku Python. Nakon učitavanja slike na Fog uređaj vrši se analiza slike tako što se u programskom kodu pronalaze konture koje odgovaraju semenkama na beloj podlozi. Konture se pronalaze na osnovu grupe piksela na slici koji imaju istu određenu boju i nalaze se između definisanih graničnih vrednosti koje odgovaraju jednoj prosečnoj semenki. Svaka od kontura predstavlja jednu semenku i njihovim prebrojavanjem dobijamo ukupni broj semenki u posudi. Jedan od problema nastaje kada je u posudi veći broj semenki i tada dolazi do njihovog spajanja, pri čemu taj slučaj aplikacija prepoznaje kao jednu konturu. Da bi se korigovalo prebrojavanje ako se dobiju veće konture od prosečne izdvojene vrednosti vrši se multipliciranje minimalnih i maksimalnih vrednosti za detekciju kontura i ako dođe do uklapanja tada se prebrojani broj semenki povećava za veličinu uvećanja graničnih vrednosti.

Seme koje je upalo u posudu kamera može da registruje u svakom momentu, a tako dobijena slika na Fog uređaju se analizira i dobija se broj zrna. Postupak je ponavljan više puta za različite pozicije i rasutost semenki, pri čemu su takođe uzimane i različite vrednosti otvorenih ljuski. Seme koje je upalo u posudu kamera je registrovala u različitim intervalima i pri tome preko aplikacije izbrojana su zrna u svim varijantama čiji se broj kretao od 25 do 125 semenki u posudi. Analiza slike je namenjena izvršavanju u blizini lokacije gde se nalaze senzorski uređaji prateći koncept Fog računarstva, a pre slanja podataka na Cloud platformu.

Na osnovu broja zrna, mase 1000 zrna i površine posude mogu se preračunati prirodni gubici nastali samoosipanjem u kilogramima po hektaru, korišćenjem formule 1.

$$N = \frac{M \cdot n}{100 \cdot A} \quad kg\ ha^{-1} \tag{1}$$

Gde je:

- M - masa 1000 zrna semena (g)
- n - broj semena po posudi
- A - površina posude (m2)
- N - nastali gubici (kg/ha)

Gubici semena su izraženi pri sadržaju vlage od 9%.

REZULTATI ISTRAŽIVANJA I DISKUSIJA

Gubici semena nastali otvaranjem ljuski u godinama kada su povoljni vremenski uslovi mogu biti oko 2% od prosečnog prinosa [10]. Međutim, gubici semena nastali otvaranjem ljuski mogu biti do 30% od prosečnog prinosa, posebno u godinama kada su vremenski uslovi nepovoljni (visoke temperature praćene jakim vetrovima i olujama), i kada se berba produži za mesec dana [16], [17].

U letnjim i sunčanim danima, pri visokim temperaturama i niskim relativnim vlažnostima vazduha, zbog slabe mehaničke čvrstoće zrelih plodova, dolazi do samog otvaranja ljuski i samoosipanja zrna. Na povećanje gubitaka zrna pre žetve još dodatno utiču nepovoljne vremenske prilike kiša, grad i jaki vetrovi [18], [19] i [16]. Usled dodirivanja i međusobnog kontakta grana jedne biljke sa granama druge biljke, dolazi do trenja, otvaranja ljuski i rasipanja zrna [13], [20]. Istraživanja sprovedena u Finskoj [18] ukazuju da brzina vetra od 8 m s^{-1} prouzrokuje otvaranje ljuski i gubitke zrna od 25 kg ha^{-1} na dan. Zbog jakog vetra i kasnije žetve za 10 dana od optimalnog roka berbe gubici zrna nastali razbijanjem ljuski povećani su za tri puta. Takođe su autori u radu [21] utvrdili da se ljuske otvaraju i pri tihom vremenu, bez jakih vetrova, kada nastaju gubici semena usled otvaranja ljuski od 11 kg/ha, odnosno 0,5% od prinosa.

Autori u radu [22] navode da je dnevni gubitak semena uljane repice nastao samoosipanjem u normalnim uslovima 0,1%, a ako u toku žetve padne kiša gubici se povećavaju do 0,3% od prosečnog prinosa. Najmanji gubici semena prilikom samoosipanja od 0,04% bili su kod novih hibrida čije su ljuske otpornije na otvaranje, a najveći kod komercijalnih sorti 0,07% od prinosa na dan.

Autori u radu [17] utvrdili su gubitke otvaranja ljuski pre berbe u tri različita roka žetve i to 42, 50 i 57 dana posle cvetanja. U 2007. godini u kontrolnoj varijanti gubici nastali otvaranjem ljuski su u prvom roku berbe 123 kg/ha ili 4,71 %, u drugom 172 kg/ha ili 5,13% i u trećem 421 kg/ha ili 16,84% od prosečnog prinosa. Usev uljane repice je bio napadnut bolestima, pa su zbog toga i gubici semena nastali samoosipanjem zbog otvaranja ljuski veliki. U 2008. godini kada je usev uljane repice bio zdrav, gubici zrna nastali otvaranjem ljuski su manji i to: 10 kg/ha ili 0,24% u prvom, 25 kg/ha ili 0,58% u drugom i 40,5 kg/ha ili 0,9% od prosečnog prinosa u trećem roku berbe.

U završnoj fazi sazrevanja uljane repice, pored klimatskih faktora, na otvaranje ljuski i rasipanje zrna pre žetve, utiče i pojava bolesti i štetočina [23], [24].

Utvrđivanje visine gubitaka zrna pre žetve nastalo otvaranjem ljuski može se vršiti u polju sledećim metodama:

1. Vizuelni metod - gde se na osnovu iskustva vrši slobodna procena otvorenih ljuski na usevu izraženo u procentima;
2. Brojanjem otvorenih ljuski na određenom broju odabranih biljaka;
3. Postavljanjem posuda između redova biljaka uljane repice u koje upada seme iz otvorenih ljuski.

Za utvrđivanje čvrstoće na otvaranje ljuske i određivanje visine gubitaka zrna pre žetve autori u radu [25] su koristili metod brojanja otvorenih ljuski na usevu uljane repice. Za analizu je uzeto 50 biljaka u prvom roku kao i mesec dana kasnije u drugom roku berbe pri čemu je utvrđen broj otvorenih ljuski. Pored toga, u navedenim istraživanjima autori su primenjivali i vizuelan metod utvrđivanja gubitaka. Dve osobe su u prvom i drugom roku berbe izvršili vizuelnu slobodnu procenu otvorenih ljuski na osnovu čega je utvrđen stepen otvaranja ljuski izražen u procentima.

Na osnovu metode vizuelne procene autori su ustanovili da je procenat otvorenih ljuski u tehničkoj zrelosti varirao od 0,8% do 8,3%, a četiri nedelje posle tehničke zrelosti od 5% do 12,5 %. U oba roka berbe najmanji procenat neotvorenih (celih) ljuski imala je sorta *Californium* 91,7% u prvom i 87,5% u drugom roku berbe.

Prema istraživanjima [26] najveći gubitak zrna je ustanovljen pre žetve kod kontrolne varijante i iznosio je 46,3 kg/ha ili 1,49% od prosečnog prinosa. Najmanji gubici zrna su zabeleženi u usevu tretiranom sa sredstvom za zaptivanje ljuski *Contacto,* pre žetve su iznosili 14,9 kg/ha ili 0,48% prosečnog prinosa.

Jedna od metoda koja se u praksi koristi za utvrđivanje gubitaka zrna na polju je postavljanje posuda između redova za prihvatanje zrna ispalog iz ljuski. Na ovaj način mogu da se ustanove i gubici zrna koji nastaju radom delova kombajna u toku žetve. Da bi se obezbedilo sigurno prihvatanje semena ispalog iz otvorene ljuske u posude, njihova unutrašnja strana se oblaže mekim materijalom (tkaninom) kako bi se sprečilo ispadanje semena. Na dnu posude za prihvatanje semena potrebno je ostaviti otvor kako bi voda mogla da otiče iz posude prilikom kišnog perioda pre žetve. Seme ispalo iz ljuski u posudu sakuplja se dva puta dnevno da bi se izračunao gubitak po jedinici površine u tom danu. Na kraju su sabrani svi izmereni dnevni gubici semena pre berbe i izračunat ukupan gubitak semena nastao otvaranjem ljuski pre žetve. Na osnovu izmerene mase zrna i površine kutije, preračunati su i dobijeni gubici zrna (semena) pre žetve izraženi u kg/ha.

Praćenje procesa sazrevanja, otvaranja ljuski i utvrđivanje gubitaka zrna u polju navedenim metodama je vrlo teško, naporno i nedovoljno precizno. Zbog toga cilj naših istraživanja je utvrđivanje visine gubitaka zrna uljane repice pre žetve nastalih osipanjem (ispadanjem) zrna iz ljuske pre berbe, na jedan lakši, brži, jednostavniji i precizniji način primenom metoda računarske obrade slike.

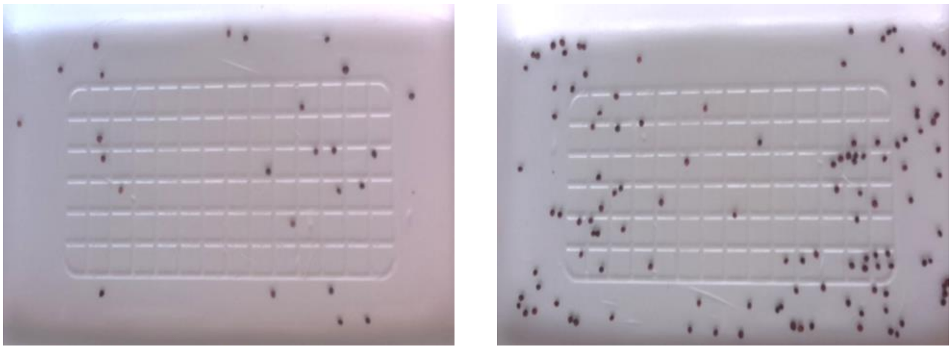

a) b)

Sl. 2. Seme uljane repice u posude sa 25 (a) semenki i 125 (b) semenki
Fig. 2. Image of rapeseed in container with 25 (a) seeds and 125 (b) seeds

Umesto fizičkog obilaska postavljenih posuda i provere stanja u njima, moguće je prenosom slike i njenom analizom na daljinu dobiti rezultate sa lokacija. U ovom radu predstavljen je model takvog sistema u kome posebno mesto zauzima aplikacija za obradu slike pomoću koje se može dobiti trenutno stanje ispalih semenki. Na Sl. 2. predstavljena su dva slučaja, prvo kada se otvori jedna ljuska i u posudi se nalazi 25 semenki (a), kao i druga varijanta kada je više raspuklih ljuski pa se u posudi nalazi 125 semenki (b).

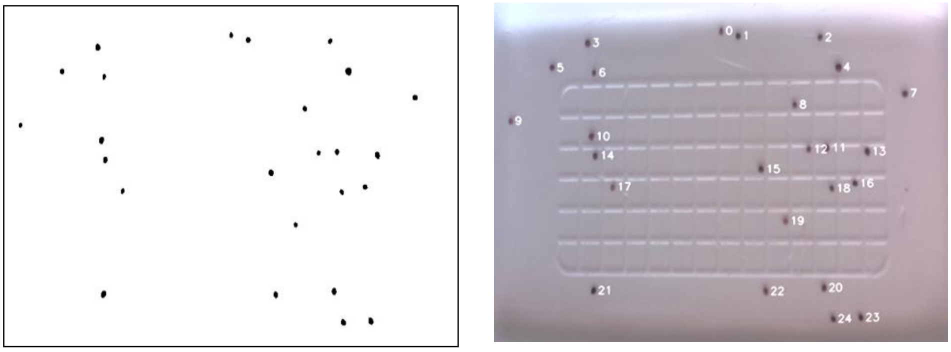

Slika 3. Analiza slike semena uljane repice sa 25 semenki
Figure 3. Image analysis of rapeseed with 25 seeds

Analizom slike od 25 semenki izdvojene su konture koje su prikazane na Sl. 3, u prvoj varijanti prikazane su kao pune crne konture na beloj podlozi, dok su u drugoj prikazane numerisane vrednosti za svaku od njih. Na ovaj način dobija se ukupan broj kontura odnosno semenki po slici.

Pošto je u primeru korišćena posuda površine 0,025 m2 može se na osnovu formule 1 i broja semenki koje su upale u posudu izračunati gubici po jedinici površine. Isto tako na osnovu istog obrasca mogu se proračunati vrednosti broja semenki za očekivane gubitke, pri čemu se vrednosti mogu sagledati u Tab. 1 za posmatranu površinu koja je oivičena posudom od 0,025 m2.

Tabela 1. Gubici semena uljane repice
Table 1. Loses of rapeseed

Gubici u procentima Losses in percentages	Gubici zrna u posudi (g) Losses of grain in the container (g)	Broj zrna u posudi Number of grains in the container
1%	0,1	25
2%	0,2	50
3%	0,3	75
4%	0,4	100
5%	0,5	125

Tab. 2. Prebrojavanje semena uljane repice analizom slike
Tab. 2. Counting of rapeseed by image analysis

Broj semenki Number of seeds	Izračunati broj semenki (Medijana) Calculated number of seeds (Median)	Tačnost rezultata Accuracy of results
25	24,5	98,0%
50	47,0	94,0%
75	69,0	92,0%
100	88,5	88,5%
125	111,5	89,2%

Na osnovu višestrukog ponavljanja za svaku od datih pet varijanti izvršen je proračun u sklopu aplikacije za analizu slike i rezultati su predstavljeni u Tab. 2.

Može se zaključiti da kada je u posudi određene površine manji broj semenki tada je tačnost rezultata dobijenih analizom slike u našem modelu visoka i iznosi 98% za varijantu od 25 semenki i 94% za varijantu od 50 semenki. Kako se broj semenki povećava tačnost opada usled grupisanja i spajanja semenki i usled veće verovatnoće da se u posudi nađu otpale ljuske ili možda slučajno neke druge primese slične semenkama. Pošto je poenta predstavljenog modela sa analizom slike da se pravovremeno reaguje i započne berba na moguću pojavu gubitaka, od interesa su na prvom mestu varijante sa manjim brojem semenki. U tim slučajevima tačnost je dobra i preostaje da se dostave informacije kako bi se izbegli veći gubici. U slučaju da dođe do odlaganja žetve iz nekih razloga dobijeni broj semenki analizom slike možda neće odlikovati tako velika tačnost, ali može da posluži za detekciju trenutnog stanja u kome se uljana repica nalazi. Takođe, poželjno bi bilo na jednoj parceli, u usevu uljane repice, postaviti više senzorskih uređaja koji mogu da uslikaju stanje sa semenkama, na primer tri kontrolne tačke. Na taj način se smanjuje mogućnost pojave pogrešnih vrednosti, jer se proveravaju vrednosti na svim kontrolnim tačkama na jednoj parceli i ako jedna vrednost odstupa ona se ne uzima u obzir. Time je smanjena verovatnoća da dođe do generisanja pogrešnog rezultata u slučaju nepravilnosti na pojedinim slikama sa lokacije.

ZAKLJUČAK

Aplikacija za analizu slike ima svoju primenu u detekciji broja semenki uljane repice na osnovu slika preuzetih sa lokaliteta kako bi se pravovremeno reagovalo sa berbom i izbegli dodatni gubici nastali samoosipanjem. Slike sa implementiranih senzorskih uređaja sa polja ne moraju se slati na udaljeni server na Internetu već se analiza slika može izvršiti na računarski podržanim uređajima u okviru Fog računarstva. Na taj način izbegava se fizički obilazak parcela i nadgledanje posuda sa prikupljenim semenima, već rezultat koji predstavlja broj semena korisnik može da dobije gotovo odmah preko sistema za nadgledanje koji sadrži aplikaciju za analizu slike. Na osnovu praćenje broja smena ispalih pre berbe mogu da se utvrde gubici samoosipanja i početak vremena žetve.

LITERATURA

[1] Dastjerdi, A.V., Buyya, R. 2016. Fog Computing: Helping the Internet of Things Realize Its Potential. *Computer*, 49(8): pp.112-116.

[2] Marković, D., Koprivica, R., Pešović, U., Ranđić, S. 2015. Application of IoT in monitoring and controlling agricultural production. *Acta Agriculturae Serbica*, XX, 40: pp.145-153.

[3] Guardo, E., Di Stefano, A., La Corte, A., Sapienza, M., Scatà M. 2018. A Fog Computing-based IoT Framework for Precision Agriculture. *Journal of Internet Technology*, 19(5): pp.1401-1411.

[4] Morais, R., Silva, N., Mendes, J., Adão, T., Pádua, L., López-Riquelme, J.A., Pavón-Pulido, N., Sousa, J.J., Peres, E. 2019. mySense: A comprehensive data management environment to improve precision agriculture practices. *Computers and Electronics in Agriculture*, 162: pp.882-894.

[5] Ahmed, N., De, D., Hussain, M.I. 2018. Internet of Things (IoT) for Smart Precision Agriculture and Farming in Rural Areas. *IEEE Internet of Things J.*, 5(6):pp. 4890-4899.

[6] Kapoor, A., Bhat, S. I., Shidnal, S., Mehra, A. 2016. Implementation of IoT (Internet of Things) and Image processing in smart agriculture. Published in: *2016 International Conference on Computation System and Information Technology for Sustainable Solutions (CSITSS)*, pp. 21-26, Bangalore.

[7] Tran, H. A. M., Ngo, H. Q. T., Nguyen, T. P., Nguyen, H. 2018. Design of Green Agriculture System Using Internet of Things and Image Processing Techniques. Published in: *2018 4th International Conference on Green Technology and Sustainable Development (GTSD)*, pp. 28-32, Ho Chi Minh City.

[8] Liming, X., Yanchao, Z. 2010. Automated strawberry grading system based on image processing. Computers and Electronics in Agriculture, *Computers and Electronics in Agriculture*, 71: S32-S39.

[9] Dell' Aquila, A. 2009. Digital imaging information technology applied to seed germination testing. A review. *Agronomy for Sustainable Development*. 29: pp.213-221.

[10] Price, J. S., Neale, M. A., Hobson, R.N., Bruce, D. M. 1996. Seed losses in commercial harvesting of oilseed rape. *Journal of Agricultural Engineering Research,* 65(3): pp.183-191.

[11] Turan, J., Mehandžić, R., Malinović, N. 2007. Žetva uljane repice namenskim hederom. *Savremena pojoprivredna tehnika*, 33(1-2): pp.92-98.

[12] Koprivica, R., Božić, M., Bošković, N., Veljković, B., Marković D. 2013. Gubici semena uljane repice i primena digitalnog senzora brzine radi kvalitetnijeg rada kombajna. *Traktori i pogonske mašine*, Novi Sad, 18(4): pp.69-74.

[13] Holzapfel, C., Kirk, A., Nybo, B., Lafond, G., May, W., Johnson, E. 2013. Quantifyng genetic differences in seed losses due to pod drop and pod shattering in canola. *Annual Project Report*, pp. 26-28.

[14] Malerž, J. 1977. Effektivnost uborki ozimovo rapsa prisposoblenim zernouboročnim kombajnom. *Meždunarodnij seleskohozjajstvenij žurnal*, 6: pp.90-96.

[15] Vujovic, V., Maksimovic, M. 2015. Raspberry Pi as a Sensor Web node for home automation. *Computers & Electrical Engineering*, 44: pp.153-171.

[16] Špokas, L., Velicka, R., Rimkeviciene, M., Marcinkeviciene, A. 2005. Ripening dynamics and natural falling of spring rape seeds. *Zemes ukio Mokslai*, 3: 29-38.

[17] Kosteckas, R., Liakas, V., Šiuliauskas, A., Rauckis, V., Liakiene, E., Jakiene, E. 2009. Effect of Pinolen on winter rape seed losses in relation to maturity. *Agronomy Research* 7(1): 347-354.

[18] Pahkala, K., Sankari, H. 2001. Seed loss as a result of pod shatter in spring rape and spring turnip rape in Finland. *Agricultural and Food Science in Finland*, 10: pp.209-216.

[19] Tys, J., Piekarski, W., Jackowska, I., Kaczor, A., Zającand, G., Starobrat, P. 2003. Technologiczne i ekonomiczne uwarunkowania produkcji biopaliwa z rzepaku. *Monografie*. p. 153, Institut agrofizyki im. Bohdana Dobrzanskiego w Lublinie.

[20] Tan, X., Zhang, J., Zhang, Z., Zhou, J., Jiang, S., Qi, C., Li, J. 2007. Quantitative determination of the strength of rapeseed pod dehiscence. Published in: *Proceedings of the 12th International Rapeseed Congress*, 26-30 March 2007, pp. 280-283, Wuhan, China.

[21] Bruce, D.M., Hobson, R.N., Morgan, C.L. Child, R.D. 2001. Threshability of Shatter-resistant Seed Pods in Oilseed Rape. *Journal of Ag. Eng. Research*, 80(4), pp. 343-350.

[22] Špokas, L., Steponavičuis, D. 2014. Evaluating the effectiveness of pinolene based pod sealant for reducing shattering losses in several cultivars of rape of (*Brassica napus* L.). *Bulgarian Journal of Agricultural Science*, 20(2): pp.310-320.

[23] Rameeh, V. 2013. Evaluation of different spring rapeseed (*Brassica napus* L.) genotypes for shattering tolerance. *Journal of Oilseed Brassica*, 4(1): pp.19-24.

[24] Tariq, A. M., Hussain, T., Iqbal, M., Aadal, K. N., Tariq, M., Rizwan, M. 2015. Screening of different promosing linies of *Brassica napus* for the grain shattering tolerance. *International Journal of Modern Agriculture*, 4(1): pp.1-4.

[25] Luczkiewicz, T. 2012. Analiza sposobu dziedziczenia cech u otrzymanych mutantów rzepaku ozimego (*Brassica nap*us L.) oraz ocena ich przydatności do hodowli. *Sprawozdanie ostanie realizaciji zdania w 2012 roku*. Uniwersytet Przyrodniczy w Poznaniu, pp. 5-11.

[26] Gentvainyte, S., Bauša, L., Čingienė, R., Domeika, R., Zaleckas, E., Steponavičius D. 2015. The economical-technological evaluation of rape pod sealants. *Žmogaus ir gamtos sauga* – 1: pp.13-16.

DETECTION OF OIL RAPE SEED LOSSES BEFORE HARVEST BY IMAGE ANALYSIS WITHIN FOG COMPUTING

Dušan Marković[1], Ranko Koprivica[1], Biljana Veljković[1], Marija Gavrilović[1], Dejan Vujičić[2], Uroš Pešović[2], Siniša Ranđić[2]

[1]University of Kragujevac, Faculty of Agronomy Čačku
[2]University of Kragujevac, Faculty of Technical Sciences Čačak

Abstract: Losses in the production of oilseed rape can occur before harvest, caused by the spontaneous opening of mature pods and the fall of seeds on the ground. Different seed pods, among other things, ripen on the same plant at different times. So, in the cultivation of similar crops, one of the most critical moments is determining the right time for harvesting, because late harvest implies overripeness and opening of the shell, which leads to seed spoilage, losses and mechanical damage during threshing. One way of monitoring seed shedding and thus potential losses is by placing a container between rows of oilseed rape plants and monitor the number of seeds that fall from open shells. The presented model of the system, which consists of sensor devices with associated cameras, positioned above the position, has a function to transmit images of the current state. Central to this paper is an image analysis application that can be performed near sites on computer-aided devices within Fog Computing. In this way, the results of the analysis of images on the number of seeds in the container are obtained almost immediately and can be forwarded to the Cloud platform or directly to the user who will take appropriate action. By obtaining timely information on the number of scattered seeds, it is possible to organize the harvest in an optimal way in order to avoid losses and prevent over-ripeness of oilseed rape.

Key words: *Image analysis, rapeseed, Fog computing, Raspberry Pi.*

Prijavljen: **08.06.2022.**
Submitted:
Ispravljen: **31.08.2022.**
Revised:
Prihvaćen: **18.09.2022.**
Accepted:

Univerzitet u Beogradu
Poljoprivredni fakultet
Institut za poljoprivrednu tehniku
Naučni časopis
POLJOPRIVREDNA TEHNIKA
Godina XLVII
Broj 4, 2022.
Strane: 38 – 47

University of Belgrade
Faculty of Agriculture
Institute of Agricultural Engineering
Scientific Journal
AGRICULTURAL ENGINEERING
Year XLVII
No. 4, 2022.
pp. 38 – 47

UDK:631.6:631.563:633.491

Original Scientific paper
Originalni naučni rad
DOI:10.5937/PoljTeh2204038B

COMPARATIVE ANALYSIS OF HYBRID UNDERGROUND PIT STORAGE STRUCTURE FOR YAM AND SWEET POTATO TUBERS

Oluwaseun Stephen Babalola[*1], Omokhagbor Moses[2], Tosin Paul[3], Joseph Antigha Edet[4]

[1,2,3,4] Michael Okpara University of Agriculture, College of Engineering and Engineering Technology, Department of Agricultural Engineering, Umudike, Abia State, Nigeria

Abstract: Storage of crop as post-harvest operation is very important, in order to reduce wastage during the season of the crop, maintain the quality of the crop, to meet up with demand in times of scarcity and reduce price cost. This can be achieved with the design and construction of a good storage structure. In order to improve one of the storage structures used for yam and sweet potato tuber crops, underground pit storage structure was modified by hybridizing the bottom and side wall lining using closed-cell foam and sawdust material at ratio 50:50 in terms of thickness. Twenty tubers of yam and sweet potato were stored in the hybrid underground pit structure. The lowest and highest temperatures of the underground pit were 20 and 23°C, while the lowest and highest temperatures of the ambient environment were 27.9 and 29.8°C. The lowest relative humidity in the hybrid underground pit and ambient environment were 70.6% and 57.3%, while the highest were 86 and 79.6% respectively.

It was discovered that at the end of eight week of storage, the weight loss in the tubers of yam and sweet potato was 10.5 and 22.5%, while the sprouting rates were 15 and 20%, percentages of rottenness were 10.5 and 15% respectively.

It can be concluded that the hybrid underground pit storage structure improved the storage period of yam and sweet potato but can prolong the storage and life span of yam tuber than sweet potato.

Key words*: Hybrid Underground Storage Structure, Closed-Cell foam, Sawdust, Yam, Sweet Potato.*

[*] Corresponding Author. E-mail: ojedelestephen@gmail.com

INTRODUCTION

One of the post-harvest operation is storage, but some problems like loss of quality and quantity of tuber crops are the challenges of farmers. Wastage is unavoidable at post-harvest stage because all the harvested crops cannot be suddenly consumed. Hence, the supply of tuber crops diminishes from time of harvest. According to [1], moisture, temperature, relative humidity, relative humidity and soil type are some factors that can initiate the growth of microorganisms causing spoilage of yam under storage. In addition, water table height can also influence spoilage of tuber in case of storage in underground pit.

According to [2] and [3], Yam is better stored in environment that can inhibit sprouting (breakage of dormancy), reduce dryness of the tuber, and prevent rottenness and storage life span of up to seven (7) months.

Therefore, to increase the quality and quantity of tuber crops available at off season, tuber crops are preserved in storage structures like underground pits, underground ditches, mud structures, thatched huts, cribs, leaving the tubers on the bare ground, platform, tree shade, and barns. Most of these storage structures are used by peasant farmers, although they have their demerits, for example, underground structure and mud structures are prone to flooding, high moisture content that can cause fungi infections and decay; so, structures made with palm fronds and other fire prone materials used by peasant farmers are not reliable. The use of shelters that are durable, well ventilated, insect and rodent proof are not financially affordable by some peasant farmers [4]. Hence, there is need to improve on the affordable storage structures like underground pit as yam and sweet potato storage structures for the peasant farmers who are the main tuber crop farmers.

Sweet potato is a tuber crop that is easy to plant, affordable with many health benefits, such as; good source of fiber, prevents cancer, good for heart, contains vitamins (E, B_6, C), relieves stress, good for baking, good for livestock feeds and regulates blood sugar. These benefits in addition to population increase has increased the demand for sweet potato beyond supply, hence, it has opened opportunity for potato farmers to increase their commercial farming of sweet potato. The other tuber crop under discussion is yam; yam is also a tuber crop of the species of *Discorea spp*. It is a worldwide acceptable tuber crop with different varieties depending on the region. It is grown in Africa and many continents in the world. It is a source of carbohydrate and also protein to some extent in the world [5]. According to [6], in terms of nutritional content, carbohydrate content of yam is 80 – 90%, protein content is 5 – 8% and mineral content of 3.5%.

There has been different study of underground storage structure, but there is lack of knowledge in hybrid form of its bottom and wall layers with closed cell foam and sawdust as lining materials.

Closed cell foam is a dense foam made from polyurethane material. It has higher R-values and insulation than other types of foam. It has high resistance to water penetration to avoid moisture build-up, because moisture can cause bacterial and mold growth. The ability of closed cell foam in controlling temperature and relative humidity prevents the growth of mold. Its use will prevent extreme rise in temperature and relative humidity. Closed cell foam is highly dense, strong, flexible plastic rubber material possessing internal pores or cells. The internal cells are very close but not interconnected together.

The closed cells contain trapped gas at the production stage, which is helpful in increasing the insulation capacity of the foam material. In addition, it is resistant to water leakage and serves as moisture barrier.

Sawdust is a by-product of sawing or milling of wood or tree. It contains moisture content of 10.8, porosity of 84% and water retention of 50%. It has been used as blotting material because of its absorptive nature, as hand cleaner when mixed with dish detergent, wood filler by mixing it with adhesives and as compost. It has also been used as a fuel source because of its firing capacity, and also as an insulating material. Sawdust has been used for treating of inorganic metal impurities from waste water [7]; feasibility of using sawdust for supercapacitor application [8]; use of sawdust as bedding materials [9] and in vermicompost [10].

The lining materials of the wall and bottom consisting of closed cell foam and sawdust are at synergic ratio 50:50 with respect to thickness.

Despite the remarkable progress made in increasing food production at the global level, approximately half of the population in developing countries does not have access to adequate food supplies. There are many reasons for this, one of which is food losses occurring after harvest. Therefore, underground pits could increase the shelf life of agricultural products as well as save cost of food production.

In order to ensure constant availability of these tuber crops, storage is very important in a conducive environment. One of the storage facilities used for tuber crops is underground pit storage. The aim of this work is to perform a comparative analysis on the use of hybrid lining underground pit for storage of potato and cassava crop. In order to achieve this aim; measurement of temperature and relative humidity was done, degree of weight loss was determined, sprouting and rotting rate were observed.

MATERIAL AND METHODS

Study Area: The experiment was carried out at G2 western farm located at National Root Crop Research Institute, Umudike, during the dry season in 2021. Umudike is situated at 7°24′East, 5°29′North at an altitude of 120 m belonging to humid forest agro-ecological zone. It has an annual rainfall of 2,200 mm and average annual temperature of 31°C with dystric luvisol.

Materials

Thermometer, Hygrometer table and Psychometric chart, Cutlass, Shovel, Ropes, Measuring tape, Bamboo, Colour analyzer, Weighing Balance, Pen, Recording book, Closed-Cell Foam, Sawdust, Yam and Sweet Potato.

Methods

Construction of Underground Storage Pit and Storage of the Tubers

An underground pit was constructed with a rectangular shape of dimension 1.0m × 1.0m × 1.5m. The bottom and side walls were lined with sawdust and foam material with total of 60mm thickness at ratio 50:50. The lining materials of the wall and bottom consisting of closed cell foam and sawdust are at synergic ratio 50:50.

Twenty cassava tubers were put in the pit and the same number and process was done for potato and then covered with sawdust and thin layer of soil for evaluation of the storage structures. The tubers used in the research have been allowed to stay for three days before storing, cleaned and free from injury and sprout.

The lining materials of the underground pits were evenly distributed on the study site and the research was carried out at the period when the water table is low. The storage and research were carried out within eight (8) weeks.

Parameters for Assessment

The parameters used for assessing the tubers for underground pit storages structures were temperature, relative humidity, weight loss, sprouting index and rate of rottenness.

Temperature: It was carried out by reading the degree of hotness or coldness of the two underground storage structures daily and their ambient environment for the period of eight (8) weeks of storage with the use of thermometer.

Relative Humidity: The use of hygrometer and psychometric chart were used to determine the moisture contents of the environments of the storage structures and the ambient environment on a daily basis after reading the temperatures respectively.

Weight Loss: The stored cassava and potato tubers were weighed on a daily basis using the weighing balance and the average was recorded as the weight. The change of weight indicates the rate of moisture loss in the tubers. The weight loss, due to different factors, was calculated using the thousand tuber mass (TTM) method developed by [11] in equation 1.

$$\%\ weight\ loss = \frac{(M - M_x)}{M} \times 100 \quad \textbf{(1)}$$

Where,

M = Thousand Tuber Mass (TTM) at the beginning of the study and
M_x = The TTM of stored tuber for x duration.

Sprouting Index: The use of visual observation was carried out every day to checkmate sprouting or any growth protruding in the tubers.

The Sprouting was calculated by taking the percentage of the number of sprouted tubers from the total number of tubers in each storage structures. Thus the sprouting was determined from the expression according to [12] and [2] in equation 2;

$$\text{Sprouting Index} = \frac{Number\ of\ Sprouted\ Tubers}{Total\ number\ of\ Tubers} \times 100 \quad \textbf{....(2)}$$

Rate of rottenness: Observation of discolouration of the surface of the yam tubers and potatoes were checked on a weekly basis for eight weeks of storage. The part of each yam and potato showing discolouration was measured using measuring tape at the end of each week. The rate of rottenness was measured using equation 3:

$$\text{Rate of rottenness} = \frac{Length\ of\ surface\ discolouration}{Total\ length\ of\ the\ Tuber\ Crop} \times 100 \quad \textbf{... (3)}$$

Sample Collection: Samples required for the experiment were gotten from National Rot Crop Research Institute Umudike, Abia State.

Reading Pattern: The samples were weighed before storage and values for Temperature and Relative Humidity were measured before storage. The number of crops stored in each pit and appearance were noted.

Data/ Statistical Analysis: Simple statistical analysis of mean and standard deviation were used in computation of results [13].

$$Mean = \frac{\sum x}{n};\quad S.D = \sqrt{\frac{\sum(x-\bar{x})2}{n}};$$

Where: x = Temperature and humidity values;
n = Number of weeks;
$\bar{x}$ = Mean and
S.D = Standard deviation

In addition, comparative analysis of the results between cassava and potato tubers were discussed.

RESULTS AND DISCUSSION

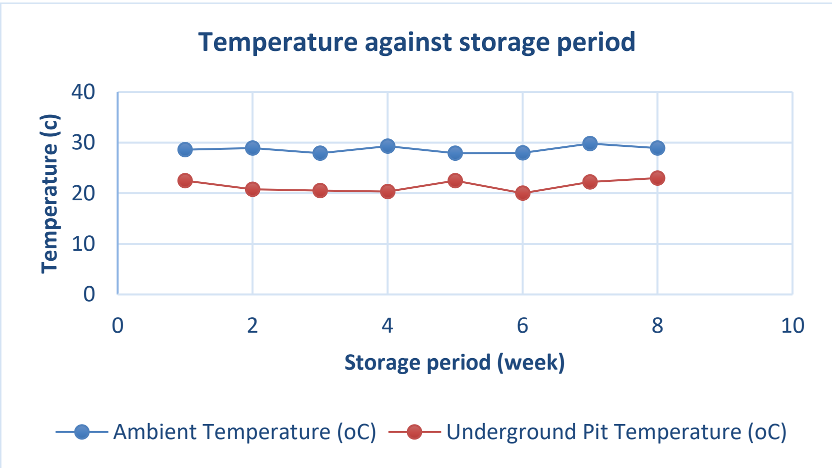

Figure 1. Temperature in the Structure against Storage Period

The highest and lowest temperatures were 29.8 and 20.0°C in the underground storage structure, while the highest and lowest temperatures of the ambient environment were 29.8 and 27.9 °C respectively. It was observed that the temperatures of the underground pit structure were lower than the surrounding temperatures during the storage period as shown in figure 1. This could be as a result of the hybrid nature of the bottom and lining walls respectively, since sawdust and closed cell foam are not good conductors of heat, hence they prevented rise in temperature of the underground pit.

The increase in temperature of the surrounding soil of the pit that can cause high heat was blocked by the wall, hence the hybrid lining wall serves as a lagging material prevented transfer of heat and temperature from the surrounding soil to the storage environment. Rise in temperature can increase the rate of transpiration of crop during storage, resulting to increase in sprout rate and weight loss respectively.

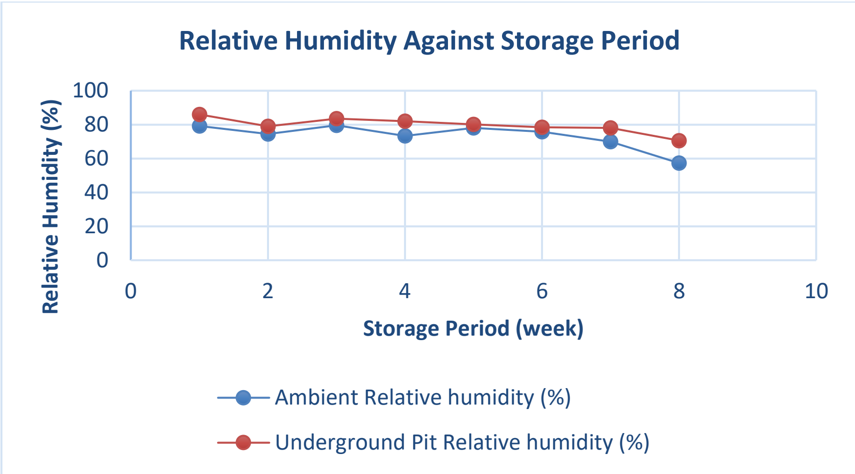

Figure 2.Relative Humidity against Storage Period

The underground pit had average relative humidity a little higher than the ambient environment all through the storage period. During the first week, the underground structure had a higher RH than the ambient environment by 6.9%, while at the 8th day of storage, the widest difference of 13.3% between the underground structure and the ambient environment was observed. The lowest difference was at 5th week with a slight difference of 2.2% between the underground storage structure and the environment. The slight difference in the RH between the two environment helps in reducing the rottenness and sprout rate of the tubers. The hybrid lining was helpful to maintain good RH for the storage of the tuber crops, as the soil moisture could not gain access to the pit environment because of the reduced penetration from the sawdust and very low porosity and permeability of the closed cell foam.

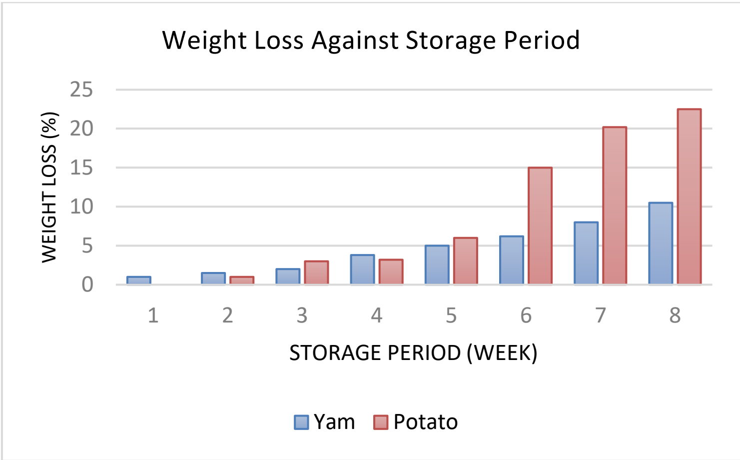

Figure 3. Weight Loss against Storage Period of Yam and Potato

The weight loss experienced at first week was 1% for yam with no weight loss experienced by the potato tuber crops. The rate of weight loss till fifth week was almost equal with a slight difference within the range of 0.5 to 1% as seen in figure 3. At 6 to 8th week of storage, the rate of weight losses in the sweet potato were as twice as the yam weight loss. The highest weight loss was experienced at 8th week of storage with 10.5% for the tubers of yam and 22.5% for the potatoes. This might be caused by slight increase in sprouting rate and rottenness.

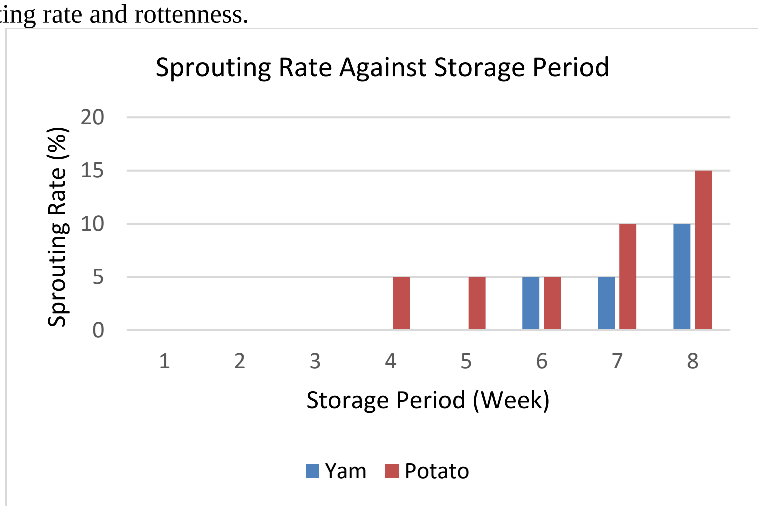

Figure 4. Sprouting Rate against Storage Period

Dormancy is necessary to maintain the quantity and quality of stored produce, but before this dormancy can be maintained for a long time, the environmental condition must be at a level that is not favorable for sprouting to take place. The prevention of high rise in temperature inside the underground pit by the hybrid lining wall prevented sprouting of yam for the first five weeks of storage while dormancy was maintained in potato for three weeks. The maintenance of low temperatures below the environmental temperature all through the storage period prevent high rise of heat, which kept the sprouting rate of yam and sweet potato to be low with maximum sprouting rate of 10% and 15% as shown in figure 4.

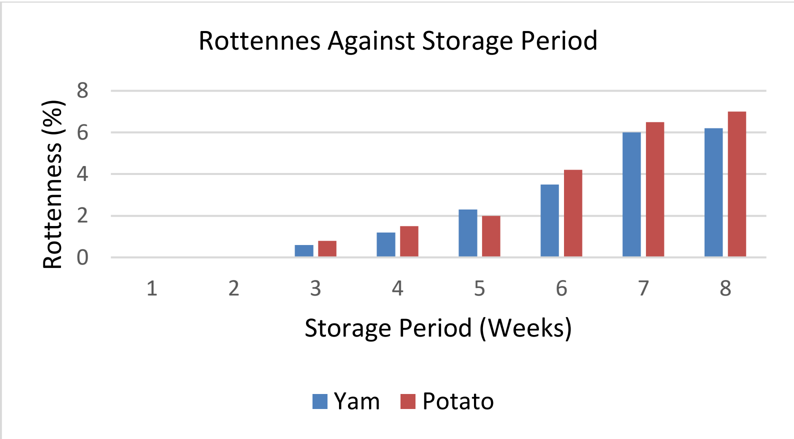

Figure 5. Rottenness against Storage Period

There was no record of deterioration of the crops till the end of second week. However, rottenness was discovered a little at the end of the third week in the yam and potato by 0.6 and 0.8% respectively. Rottenness increased as the storage period increased, but at a very slow rate. The highest rates of rottenness were 6.2 and 7.0% in the yam and sweet potato respectively. This showed that the hybrid lining of the bottom and side walls of the underground pit storage prevented conducive environment that can make microorganisms causing deterioration of crop during storage to thrive very well.

CONCLUSIONS

The use of underground pit storage structures designed with good materials in hybrid lining form is effective to a good period of time in keeping storage crop at the environmental requirements favourable for the storage of such crop. The research findings with 6.2% and 7% of rottenness of yam and potato, and also highest sprouting rate of 10% and 15% for yam and sweet potato respectively, has proven that hybrid lining of the bottom and side walls of underground pit with sawdust and closed-cell foam material can prolong the storage of yam and sweet potatoes beyond eight (8) weeks.

The research showed that underground pit storage is a good storage structures for yam and sweet potato tuber crops and also for curing if the tubers will still be transferred to another storage structure, but the findings showed that underground pit storage is a better storage structure for yam than sweet potato.

REFERENCES

[1] Kay D.E. 1973. Crop and Product Digest. No.2. root Crops 2nd Edition, London. Tropical Agriculture. Pp.84.
[2] Opera L.U.1999. Yams: Post Harvest Operations. Massey University. http://www.fao.org/inpho, 2011
[3] Plucknett, D.L. 1979. Smallscale Processing and storage of Tropical Root Crops (Ed. D.L. Plucknett) West view Tropical Agricultural series, No1 Boulder, Colorado: West view press. pp110-123.
[4] Umogbai, V. I. 2013. Design, Construction and Performance Evaluation of an Underground Storage Structure for Yam Tubers. International Journal of Scientific and Research Publications, Volume 3, Issue 5, May 2013 1 ISSN 2250-3153.
[5] International Institute of Tropical Agriculture (IITA) (1995). Annual Report of the IITA, Ibadan, Nigeria. Pp84.
[6] FAO, 1990. Production Year Book, (Food and Agricultural Organization of the United Nations). Vol. 44.
[7] Surinder Singh, Sushil K. K. 2020. Low Cost Adsorbents for Removal of Inorganic Impurities from Wastewater. Inorganic Pollutants in Water, 2020.
[8] Nelson P.R., Mohd Rafie Bin Johan. 2020. Recent Advancements of Supercapacitor Electrode Materials Derived from Agricultural Waste Biomass. Reference Module in Earth Systems and Environmental Sciences, 2020.
[9] Mandal A.B., Bhanja S.K. 2017. Poultry Husbandry-Indian Perspective. The Indian Nitrogen Assessment, 2017.
[10] Kavita Sharma and Garg V.K. 2019. Vermicomposting of Waste. Sustainable Resource Recovery and Zero Waste Approaches.
[11] Proctor, D.L. and Rowley, J. G. 1983. The Thousand Grain Mass Method (TGM): A basis for better assessment of weight losses in stored grain, Tropical Stored Product information 45, pp.19-23, TDRI, Slough.
[12] Clark, G. E. 1994b. Assessment of tuber storage and sprouting treatments for Sandersonia aurantiaca. New Zealand Journal of Crop and Horticultural Science 22: pp.431-437.
[13] Curran - Everett, D., Taylor, S. and Kafadar, K. 1985. Fundamental Concepts in Statistics: Elucidation and Illustration. Journal of Applied Physiology. 85; pp.775 -786

KOMPARATIVNA ANALIZA HIBRIDNE PODZEMNE KONSTRUKCIJE SKLADIŠTA ZA ČUVANJE YAMA I SLATKOG KROMPIRA

Oluwaseun Stephen Babalola*[1], Omokhagbor Moses[2], Tosin Paul[3], Joseph Antigha Edet[4]

[1,2,3,4] *Michael Okpara University of Agriculture, College of Engineering and Engineering Technology, Department of Agricultural Engineering, Umudike, Abia State, Nigeria*

Abstrakt: Skladištenje poljoprivrednih proizvoda kao operacija posle žetve je veoma važno, da bi se smanjio gubitak tokom sezone, održao kvalitet proizvoda, zadovoljila potražnja u vremenu oskudice i tako uticalo na cenu proizvoda.
Ovo se može postići projektovanjem i izgradnjom dobre strukture skladišta za čuvanje.

U cilju poboljšanja jedne od skladišnih struktura koje se koriste za useve Yama i krtola slatkog krompira, struktura podzemnog skladišta forme jame (trap) je značajno modifikovana promenom obloge dna i bočnih zidova upotrebom strukturne pene sa zatvorenim tipom ćelija i dodatkom piljevine u odnosu 50:50 na debljinu materijala .
U hibridnoj podzemnoj strukturi jame (trap) uskladišten je uzorak od dvadeset krtola jama i slatkog krompira. Najniža i najviša temperatura podzemnog skladišta iznosila je 20 ^{o}C i 23^{o}C.
Najniža i najviša temperatura ambijentalne sredine 27,9 ^{o}C i 29,8^{o}C. Najniža relativna vlažnost u hibridnoj podzemnoj jami i ambijentalnoj sredini iznosila je 70,6% i 57,3%, dok je najviša iznosila 86% i 79,6% respektivno.
Utvrđen je na kraju osmonedeljnog skladištenja gubitak mase u krtolama Yama i slatkog krompira od 10,5% i 22,5%, dok su stope nicanja bile 15% i 20%.
Pojava truleži je registrovana kod Yam useva sa 10,5% odnosno 15% kod krtola slatkog kromira.
Može se zaključiti da je hibridna struktura podzemnog skladištenja tipa jame (trap) poboljšala dužinu perioda skladištenja Yama i slatkog krompira, ali više može produžiti skladištenje i životni vek krtola Yama, u odnosu na krtole slatkog krompira.

Ključne reči:*Hibridna podzemna skladišta, pena sa zatvorenim ćelijama, piljevina, Yam, slatki krompir*.

Prijavljen:
Submitted: **19.07.2022.**
Ispravljen:
Revised: **30.09.2022.**
Prihvaćen:
Accepted: **22.09.2022.**

Univerzitet u Beogradu
Poljoprivredni fakultet
Institut za poljoprivrednu tehniku
Naučni časopis
POLJOPRIVREDNA TEHNIKA
Godina XLVII
Broj 4, 2022.
Strane: 48 – 57

University of Belgrade
Faculty of Agriculture
Institute of Agricultural Engineering
Scientific Journal
AGRICULTURAL ENGINEERING
Year XLVII
No. 4, 2022.
pp. 48 – 57

UDK:631.1:631.370:631.315

Original Scientific paper
Originalni naučni rad
DOI:10.5937/PoljTeh2204048A

SOME PHYSICAL PROPERTIES OF TARO COCOYAM REVELANT TO THE DESIGN OF ITS PROCESSING MACHINES

Ubong Edet Assian[1]*, Tosin Paul[2]

[1]Department of Agricultural and Food Engineering, Faculty of Engineering, University of Uyo, Uyo, Akwa Ibom State, Nigeria
[2]Department of Agricultural and Bioresources Engineering, Michael Okpara University of Agriculture, Umudike, Abia State, Nigeria

Abstract: Information on physical properties of cocoyam is essential for efficient development of equipment / machines for its processing. In this work, some physical properties of Taro Cocoyam (*Colocassia esculenta*) were investigated using standard engineering principles. The results revealed that average length, width, thickness and unit mass obtained at the sample moisture content of 70.50 $\pm$ 3.8% (w.b.) were 63.67 $\pm$ 12.91 mm, 31.88 $\pm$ 5.99 mm, 34.27 $\pm$ 6.12 mm and 52.65 $\pm$ 22.59g, respectively. The values of computed geometric mean, arithmetic mean, square mean and equivalent diameters were 40.88 $\pm$ 6.55 mm, 43.27 $\pm$ 6.79 mm, 41.88 $\pm$ 6.62 mm and 42.01 $\pm$ 6.65 mm, respectively. The value of the sample distribution skewness was -0.29. The aspect ratio, sphericity, surface area, volume, solid density, bulk density, porosity and angle of repose were 0.55 $\pm$ 0.13 (dec.), 65.46 $\pm$ 10.26%, 5384.85 $\pm$ 1646.64 mm^2, 38449.90 $\pm$ 16926.30 mm^3, 0.0014 $\pm$ 0.0003 g / mm^3, 0.00085 $\pm$ 0.00015 g / mm^3, 60.7 $\pm$ 8.40% and 32.15 $\pm$ 4.51^0, respectively. The coefficient of static friction on plywood, glass and galvanized iron surfaces were 0.22 $\pm$ 0.045, 0.15 $\pm$ 0.045 and 0.19$\pm$ 0.046, respectively. The values of coefficient of variation for all the parameters, except unit mass, were low. This implies that the data were uniformly dispersed around their average values.

Key words*: Physical properties, taro cocoyam, design, processing machines*

*Corresponding Author. Email address: assian4real@yahoo.com

In West Africa, Taro Cocoyam, otherwise known as *Colocassia esculenta*, is one of essential root crops (Figure 1), especially in the tropics. Many varieties of cocoyam can give up to 37-75 ton/ ha. Taro Cocoyam cormels and corms are good sources of digestible starch, vitamins and minerals [1]. The growing significance of taro cocoyam, other root crops as well as their accessibility to contemporary processing and stowage techniques requires a sound understanding of their engineering properties. However, it is essential to comprehend the physical principles regulating the raw products responses during handling and various unit operations to have better final end products. For example, shape as a physical property, is a very crucial parameter in predicting the behavior of biomaterials under certain stress or loading conditions. This is very useful in the development of various handling and processing equipment [2].

Fig. 1. Few samples of Taro Cocoyam

A lot of works have been done by many researchers on some physical and engineering properties of seeds, grains, nuts, tuber crops and vegetables so as to offer valuable information which may be used in the development of crop and food processing machines [3, 4, 5, 6]. These physical and engineering properties are geometric mean diameter, sphericity, coefficient of friction, static and dynamic angles of repose, unit mass (weight), specific gravity, volume, aspect ratio, surface area, porosity, bio-yield, true, solid and bulk densities, elastic deformation, hardness, stiffness, compressibility, shear resistance, etc., [7, 8, 6]. Therefore, in order to develop improved Taro Cocoyam processing equipment and vessels, some of these physical properties such as unit mass, size and shape functions [axial dimensions (length, width and thickness), geometric mean, arithmetic mean, square mean and equivalent diameters, aspect ratio, sphericity], surface area, volume, solid density, bulk density, porosity, angle of repose and coefficient of static friction with respect to sample initial moisture content were studied. Nevertheless, food processors and scientists may use these information provided in this study for further works and product development.

MATERIALS AND METHODS

Exactly one hundred and fifteen (115) setts of Taro Cocoyam were purchased from Akpan Andem Market, Uyo, Akwa Ibom State. The samples were picked at random, cleaned to eliminate foreign materials such as dust, dirts, wounded or blemished samples and stones.

The initial moisture content of the 10 unpeeled samples was found using gravimetric method [9, 6, 10]. Fifty (50) unpeeled samples were chosen and their masses measured using electronic digital weighing balance. Besides, their length (L), width (W) and thickness (T) were measured using digital vernier calipers of 0.01 mm calibration and tape rule as shown in Figure 2. These dimensions were employed in the determination of some physical properties of the unpeeled cocoyam samples using Equation 1 to 15. However, in order to examine the sample size distribution, they were grouped based on equivalent diameter (D_E), into three size ranges: small ($25.0\text{ mm} \leq D_E < 35.0$ mm), medium ($35.0\text{ mm} \leq D_E < 45.0$ mm) and large size ranges ($45.0\text{ mm} \leq D_E < 55.0$ mm). The mean, standard deviation and coefficient of variation of each property were computed using Data Acquisition Template powered by Microsoft Excel ™. Furthermore, based on equivalent diameter (D_E), skewness of the sample size distribution was also found, and the mean differences (MD) among geometric mean, arithmetic mean, square mean and equivalent diameters were also assessed using analysis of variance (ANOVA) at 5% level of probability.

Determination of Some Physical Properties of Taro Cocoyam Samples

(a) Moisture Content (MC) Determination

The initial moisture content of Taro Cocoyam samples was determined using Equation 1.

$$\%\,MC_{wb} = \frac{M_i - M_f}{M_i} \times 100\% \qquad (1)$$

Where,

$\%\,MC_{wb}$ = moisture content (% wet basis),
M_i = initial mass of the sample (g)
M_f = mass of the sample at bone dry condition (g).

(b) Sample Size and Shape

Sample geometric mean diameter (D_G) was calculated using Equation 2 [6]:

$$D_G = (L \times T \times W)^{1/3} \qquad (2)$$

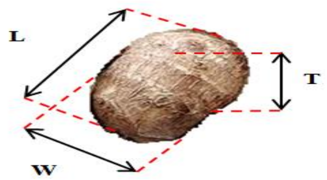

Fig. 2. The principal dimensions of Taro Cocoyam sample

Where, L = sample length (mm),
T = sample thickness (mm),
W = sample width (mm).

Sample size distribution skewness was determined using Equation 3:

$$\text{Skewness } (S_k) = 3 \times \left(\frac{\text{Mean} - \text{Median}}{\text{Standard deviation}}\right) \qquad (3)$$

Sample arithmetic mean diameter (D_A) was found using Equation 4:

$$D_A = (L + T + W) / 3 \tag{4}$$

Sample square mean diameter (D_S) was calculated using Equation 5 [11, 12]:

$$D_S = \left(\frac{(LT) + (LW) + (WT)}{3}\right)^{1/2} \tag{5}$$

Sample equivalent diameter (D_E) was [11, 12] determined using Equation 6:

$$D_E = \left(\frac{D_G + D_A + D_S}{3}\right) \tag{6}$$

Sample aspect ratio (AR) was computed using Equation 7 [11, 12]:

$$AR = \frac{T}{L} \tag{7}$$

Sample sphericity was calculated using Equation 8 [13]:

$$\text{Sphericity } (\psi) = \frac{D_G}{L} \times 100\ \% \tag{8}$$

Note: An object is regarded as a sphere when its sphericity is ≥ 0.6 (i.e. 60%) [14, 6].

(c) Sample Surface Area

Taro Cocoyam samples may be are described as a sphere, based on the sample sphericity value obtained in this work; hence, the sample surface area (S_c) was computed using Equation 9 [7, 15]:

$$S_c = \pi \times (D_G)^2 \tag{9}$$

(d) Sample Volume

The volume of Taro Cocoyam sample (V_c) was computed using Equation 10 [7]:

$$V_c = \frac{\pi\ (D_G)^3}{6} \tag{10}$$

Where, π (pie) = 3.142

(e) Sample Density

The density of Taro Cocoyam sample (ρ_c) was computed by dividing its unit mass by its volume [7]:

$$\rho_c = \frac{M_c}{V_c} \tag{11}$$

Where, M_c= mass of Taro Cocoyam sample (g)

(f) Sample Bulk Density

The bulk density is basically the density of the sample when loaded in a container. It was found as described by the relation [6]:

$$\rho_{sb} = \frac{M_{cs} - M_{ec}}{V_{ec}} \tag{12}$$

Where,
ρ_{sb}= sample bulk density (g/ mm^3),
M_{ec} = mass of empty container (g),
M_{cs}= mass of container and samples (g)
V_{ec} = volume of empty container (mm^3).

(g) Porosity

The porosity of the samples was computed thus [6]:

$$P_s = \left(1 - \left[\frac{\rho_{sb}}{\rho_c}\right]\right) \times 100\ \% \tag{13}$$

Where, P_s= sample porosity (%)

(h) Sample Angle of Repose

Angle of repose of Taro Cocoyam samples was found using a cylindrical container which was opened at both ends as described by [16], [17].

$$\theta = \tan^{-1}\left(\frac{2H}{R}\right) \tag{14}$$

Where,
H = vertical depth (cm)
R = pile radius (cm).

(i) Sample Coefficient of Static Friction

With the aid of static frictional apparatus (Figure 3), plywood was placed on the sliding surface and the sample carefully rested on it. Then, the surface was gently raised up until the sample began to slide down the plane. The angle between the sliding surface and the base was measured as Ɵ.

The procedure was repeated with the rest of the samples. The plywood was replaced with glass and galvanized iron surfaces, and the experimental run repeated. The coefficient of static friction of Taro Cocoyam samples was calculated using Equation 15.

$$\mu = \tan \Theta \tag{15}$$

Fig. 3. Static frictional apparatus

RESULTS AND DISCUSSIONS

The results of the investigation are presented in Table 1 and Figure 4.

Table 1: Some physical properties of Taro Cocoyam samples

Properties	Total No. of Observations	Mean ± S.D.	C.V. (%)
Moisture content (% w.b.)	10	70.50 ± 3.80	5.39
Unit mass, M_c (g)	50	52.65 ± 22.59	42.92
Length, L (mm)	50	63.67 ± 12.91	20.27
Width, W (mm)	50	31.88 ± 5.99	18.80
Thickness, T (mm)	50	34.27 ± 6.12	17.86
Geometric mean diameter, D_G (mm)	50	40.88 ±6.55[a]	16.02
Table 1. A continuation			
Arithmetic mean diameter, D_A (mm)	50	43.27 ±6.79[a]	15.70
Square mean diameter, D_S (mm)	50	41.88 ±6.62 [a]	15.82
Equivalent diameter, D_E (mm)	50	42.01 ±6.65 [a]	15.84
Aspect ratio, AR (decimal)	50	0.55 ±0.13	23.20
Sphericity, ψ (%)	50	65.46 ± 10.26	15.68
Surface area, S_c (mm^2)	50	5384.85 ± 1646.64	30.58
Volume, V_c (mm^3)	50	38449.90 ± 16926.30	44.00
Solid density, ρ_c (g/mm^3)	50	0.0014 ± 0.0003	19.53
Bulk density, ρ_{sb} (g/mm^3)	50	0.00085 ± 0.00015	12.11
Porosity, P_s (%)	50	60.7 ± 8.40	10.33
Angle of repose, θ (^{0})	50	32.15 ± 4.51	14.02
Coefficient of static friction, μ			
Plywood surface	50	0.22 ± 0.045	20.40
Glass surface	50	0.15 ± 0.045	30.20
Galvanized iron surface	50	0.19 ± 0.046	23.74

Note: The values of mean and standard deviation are designated as Mean ± S.D.; C.V = coefficient of variation; Same superscripts in the Mean ± S.D column show no statistical significant mean difference (MD) at P = 0.05.

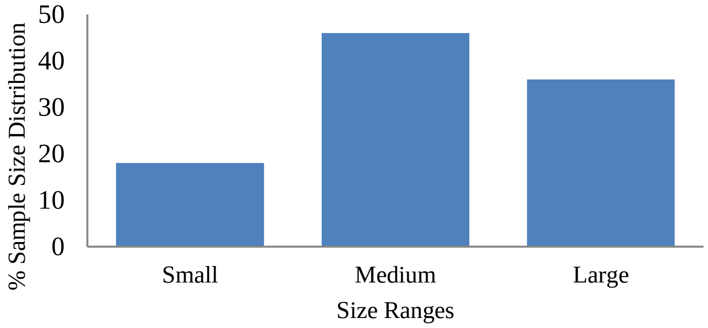

Fig. 4. Histogram showing the % sample size distribution of Taro Cocoyam samples

Moisture Content of Taro Cocoyam Samples

The average moisture content of Taro Cocoyam samples was determined as 70.50 $\pm$3.8% (w.b.). The minimal value (5.39%) of coefficient of variation (C.V.) shows uniform dispersion of the data collected were around their average value. However, moisture content is a very useful parameter which finds application in the design of some efficient unit operations such as dehydration, packaging and culinary. The observed value is an indication that Taro Cocoyam could quickly deteriorate due to high moisture level which creates conducive environment for micro-organisms to strive freely.

Unit Mass of Taro Cocoyam Samples

The average unit mass of Taro Cocoyam samples was found as 52.65 $\pm$ 22.59 g. The C.V. (42.92%) of the samples distribution was a bit high. This implies that the sample mass distribution was not uniformly dispersed about its average value. The observed value of mass may be used in the design of cocoyam weighing, conveying and foreign particle separating system.

Size Distribution of Taro Cocoyam Samples

The average length (L), thickness (T), width (W), geometric mean diameter ($\mathrm{D_G}$), arithmetic mean diameter ($\mathrm{D_A}$), square mean diameter ($\mathrm{D_S}$) and equivalent diameter ($\mathrm{D_E}$) of Taro Cocoyam samples were 63.67 $\pm$ 12.91 mm, 31.88 $\pm$ 5.99 mm, 34.27 $\pm$ 6.12 mm, 40.88 $\pm$ 6.55 mm, 43.27 $\pm$ 6.79 mm, 41.88 $\pm$ 6.62 mm and 42.01 $\pm$ 6.65 mm, respectively, while their corresponding C.V. were 20.27%, 18.80%, 17.86%, 16.02%, 15.70, 15.82% and 15.84%, respectively (Table 1). The observed C.V. values were low. These imply that each of them was found to disperse evenly about their mean values. The sample length was approximately two times the width as well as thickness. Hence, the width was 0.9 of the sample thickness. In addition, there were no statistical significant mean differences (MD) among different types of diameters. Percentage size distributions obtained were 18% small, 46% medium and 36% large size ranges. The computed value of skewness for the sample size distribution was -0.29 (i.e. negative skewness). Figure 3 reveals that the skewed distribution was towards the right side which indicates that the mean, mode and median of the data collected were slightly different. Hence, larger % of the data was between the medium and large size ranges (45.0 mm $\leq$ $\mathrm{D_E}$ $\leq$ 55.0 mm). However, the observed axial dimensions, $\mathrm{D_G}$ and $\mathrm{D_E}$ could be used in the design of sieve aperture of a grading and screening system; peeling and cleaning system for taro cocoyam.

Shape of Taro Cocoyam Samples

The average values of aspect ratio (AR) and sphericity (ψ) were 0.55 $\pm$ 0.13 (decimal) and 65.46 $\pm$ 10.26%, respectively. Their C.V. values were low (i.e., 23.20% and 15.68%, respectively). The observed value of AR means that the samples may not roll on a plane surface if there is a resistance, while the sphericity value attests that the samples are a sphere, but not perfect, and may likely to roll on any surface. This data could be employed in the design of Taro Cocoyam hopper for separating and conveying systems.

Surface Area of Taro Cocoyam Samples

The average surface area of Taro Cocoyam samples was found to be 5384.85 $\pm$ 1646.64 mm^2. The C.V. value (30.58%) got was low. This parameter could be used in designing peeling machine, heat and mass transfer equipment for heat treatment processes.

Volume and Solid Density of Taro Cocoyam Samples

The average volume and density of Taro Cocoyam samples were 38449.40 $\pm$ 16926.30 mm^3 and 0.0014 $\pm$ 0.0003 g/ mm^3, with their corresponding C.V. as 44.00% and 19.53%, respectively. The volume obtained could find application in designing sorting equipment, storage systems (e.g., silos and bins) and in screening solids. The observed estimated value of solid density of Taro Cocoyam samples (0.0014 g /mm^3 = 1400 kg/ m^3) is higher than density of water (1000 kg/ m^3). This implies that the samples can sink in water, and as such lighter foreign particles can be separated easily. The calculated density value could aid in product characterization and process calculation. Besides, its true volume can be found by water displacement method.

Bulk Density of Taro Cocoyam Samples

The average values of bulk density of Taro Cocoyam samples were 0.00085 $\pm$ 0.00015 g/ mm^3 with C.V. of 12.11%. The C.V. determined was low.

The observed value is lesser that the solid density. Hence, more spores (void spaces) are expected in the container when packaged with the samples. This value is useful in the design of system for transportation, containerization and packaging or storage system.

Porosity of Taro Cocoyam Samples

The average value of porosity of Taro Cocoyam samples was 60.7 $\pm$ 8.4% with C.V. of 10.33%. This means that the samples would generate more air-spaces among their particles when loaded in a container. Therefore, the observed value is useful in storage system design.

Angle of Repose of Taro Cocoyam Samples

The mean value of angle of repose of Taro Cocoyam samples was determined as 32.15 $\pm$ 4.51^0 with its C.V. of 14.02%. The calculated angle of repose can find application in efficient design of hopper, conveyor belt system, silos and bins.

Coefficient of Static Friction of Taro Cocoyam Samples

The mean values of coefficients of static friction of Taro Cocoyam samples were 0.22 $\pm$ 0.045, 0.15 $\pm$ 0.045 and 0.19 $\pm$ 0.046 for plywood, glass and galvanized iron surfaces, respectively. Their respective C.V. values were 20.40%, 30.20% and 23.74%.

These values were low. Glass surface had the least static frictional coefficient compared to other surfaces. This was followed by galvanized iron surface.

This shows that glass and galvanized iron surfaces are better surfaces to be used in fabricating hopper and conveyor belt system. However, the glass surface is expensive and delicate. Hence, galvanized iron surface is preferable.

CONCLUSION

In this work, some physical properties of Taro Cocoyam samples were studied at the moisture content of 70.50 $\pm$ 3.80%. The data acquired are vital information for the lucid design of Taro Cocoyam processing systems for proficient unit processes.

CONFLICT OF INTEREST

There is no conflict of interest.

REFERENCES

[1] Onwueme, I. C. and Simha, T. C. 1991. Field Crop Production in Tropical Africa. CTA Ed., Netherland: pp. 276 - 288.

[2] Esref, I. and Halil, U.2007. Moisture-dependent Physical Properties of Whitem Speckled Red Kidney Bean Grains. Journal of Food Engineering, 82: pp. 209-216.

[3] Alonge, A. F. and Etim, P. J.2011. Some engineering properties of African oil bean relevant to its processing. *Journal of Agricultural Engineering and Technology (JAET),* 19 (2): pp. 51-5.

[4] Alonge, A. F. and Folorunso, A. O. 2012. Some engineering properties of coconut relevant to its cracking. Paper presented at the Canadian Society for Bio Engineering (CSBE), Orillia, Toronto, Canada. July 15 -18, 2012.

[5] Antia, O.O. and Assian, U. E.2018. Development of an Empirical Model for Palm Nut Volume Determination. European Journal of Advances in Engineering and Technology, Vol (Issue 7), pp. 466-469.

[6] Assian, Ubong E. and Alonge, Akindele F.2021. Some Physical Properties of Kariya (*Hildegardia Barteri*) Nut/Kernel Relevant to the Design of its Processing Equipment. Global Journal of Engineering and Technology Advances, 7(2): pp.83–90.

[7] Rao, M., Syed, R. and Ashim, D. 2005. Engineering Properties of Foods (3rd Edition). CRC Press, United States of America.

[8] Alonge, A. F. and Antia, E. O. 2014. Some physical and frictional properties of African bread fruit (*Treculia Africana*) seed relevant to its processing. Paper No. 1897372. St. Joseph, Michigan, USA: American Society of Agricultural and Biological Engineers.

[9] ASABE 2010. ASABE Standard. Year Book, American Society of Agricultural and Biological Engineers.

[10] Antia, O.O., Olosunde W. and Offiong, A. 2014. Determination of Optimum Moisture Content of Palm Nut Cracking for Efficient Production of Whole Kernel. *Nigerian Journal of Technological Development,* 11(2): pp.27-30.

[11] Mohsenin, N.N. 1986. Physical Properties of Plant and Animal Materials. Gordon and Breach Science Publisher, New York.

[12] Ciro, V. H. J. 1997. Estudio Dinámico de la Café para el Desarrollo de la Cosecha Mecánica por Vibración Thesis B. Sc. (Agricultural Engineering). Universidad Nacional de Colombia, Medellín, Colombia.

[13] Irtwange, S.V. and Igbeka, J.C. 2000. Some physical properties of two African yam bean (*Sphenostylis stenocappa*) accessions and their interrelations with moisture content. *Applied Engineering in Agriculture,* 18(5): pp.567-576.

[14] Akubuo, C.O. and Eje, B.E. 2002. Palm kernel and shell separator. *Bio-system Engineering*, 81(2): pp.193-199.
[15] Alonge, F.A. and Edidiong, J.U. 2012. Some physical properties of African nutmeg (*Monodara myristica*) seed relevant to its processing. ASABE Annual International Meeting. Paper No. 121340755.
[16] Sohelli, B., Mohammad, B., Massah, J. and Javad, K. 2011. Experimental Study of the Repose Angles of Corn Seeds in Rotating Drums. World Applied Sciences Journal, 13(9): pp.1996-2004.
[17] Falguni, R. and Atul, K. S. 2021. Determination of Various Physical Properties of Okra Seeds. International Journal of Current Microbiology App.Science, 10(2): pp.3575-3582.

NEKE FIZIČKE OSOBINE TARO COCOYAM (*Colocassia esculenta*) RELEVANTNE ZA DIZAJN MAŠINA ZA PRERADU

Ubong Edet Assian[1], Tosin Paul[2]

[1]Department of Agricultural and Food Engineering, Faculty of Engineering,
University of Uyo, Uyo, Akwa Ibom State, Nigeria
[2]Department of Agricultural and Bioresources Engineering,
Michael Okpara University of Agriculture, Umudike, Abia State, Nigeria

Apstrakt: Podaci o fizičkim osobinama Taro Cocoyam (*Colocassia esculenta*) su neophodni za efikasan razvoj opreme/mašina za njegovu preradu. U ovom radu, neke fizičke osobine su istraživane primenom standardnih inženjerskih principa.
Rezultati su otkrili da su prosečna dužina, širina, debljina i masa dobijene pri sadržaju vlage vrednosti od 70,50 ± 3,8% (w.b.) , i dimezija uzorka: 63,67 ± 12,91 mm, 31,88 ± 5,99 mm, 34,27 ± 6,12 mm i 52,25 ± 52,65 g, respektivno.
Vrednosti izračunate geometrijske i aritmetičke sredine, sume kvadrata, sredine ekvivalentnih prečnika, bile su: 40,88 ± 6,55 mm, 43,27 ± 6,79 mm, 41,88 ± 6,62 mm i 42,01 ± 6,65 mm, respektivno. Vrednost asimetrije distribucije uzorka bila je -0,29.
Odnos širine i visine, sferičnosti, dodirne površine, ukupne zapremine, nasipne zapremine, poroznosti i ugala trenja bili su: 0.55 ± 0.13 (dec.), 65.46 ± 10.26%, 5384.85 ± 1646.64 mm^2, 38449.90 ± 16926.30 mm^3, 0.0014 ± 0.0003 g/mm^3,
0.00085 ± 0.00015 g / mm^3, 60.7 ± 8.40% and 32.15 ± 4.51^0, respektivno .
Vrednost koeficijenta statičkog trenja na šper ploči, staklu i pocinkovanoj čeličnoj površini, bile su: 0,22 ± 0,045, 0,15 ± 0,045 i 0,19 ± 0,046, respektivno.
Vrednosti koeficijenta varijacije za sve parametre, osim jedinične mase, bile su niske.
Ovo implicira da su podaci ravnomerno raspoređeni oko svojih prosečnih vrednosti.

Ključne reči: *Fizičke osobine, Taro Cocoyam, dizajn, mašine za obradu.*

Prijavljen:
Submitted: **30.07.2022.**
Ispravljen:
Revised: **20.10.2022.**
Prihvaćen:
Accepted: **28.10.2022.**

Univerzitet u Beogradu
Poljoprivredni fakultet
Institut za poljoprivrednu tehniku
Naučni časopis
POLJOPRIVREDNA TEHNIKA
Godina XLVII
Broj 4, 2022.
Strane: 58 – 66

University of Belgrade
Faculty of Agriculture
Institute of Agricultural Engineering
Scientific Journal
AGRICULTURAL ENGINEERING
Year XLVII
No. 4, 2022.
pp. 58 – 66

UDK:631.1:631.370:631.315

Original Scientific paper
Originalni naučni rad
DOI:10.5937/POLJTEH2204058A

PRACTICAL MODEL FOR ESTIMATING TARO COCOYAM VOLUME BASED ON ITS AXIAL DIMENSIONS

Ubong Edet Assian*[1], Tosin Paul[2]

[1]*Department of Agricultural and Food Engineering, Faculty of Engineering, University of Uyo, Uyo, Akwa Ibom State, Nigeria*
[2]*Department of Agricultural and Bioresources Engineering, Michael Okpara University of Agriculture, Umudike, Abia State, Nigeria*

Abstract: Taro Cocoyam is prone to attack by rodents, insect pests and environmental elements. After drying, it is stored to evade wastage. In an effort to efficiently develop storage system, fundamental physical parameter such as volume of the fresh cocoyam with respect to its axial dimensions should be well expressed and modelled for easy estimation. In this study, fresh Taro Cocoyam samples were sourced, cleaned and packaged. Ten unpeeled samples were used in determining initial moisture content (% w.b). The axial dimensions of fifty unpeeled samples were measured and used to compute arithmetic mean diameter (D_A). Corresponding true volume (V_T) was found using water displacement approach. The bulk samples were grouped based on D_A, into seven (7) size ranges. Mean and standard deviation of each parameter were computed. The model was established, verified and validated. Statistical analysis showed that the value of coefficient of determination (R^2) was almost equals correlation coefficient ($r \approx 1$). The values of reduced Chi-square (χ_c^2), root mean square error (RMSE) and mean bias error (MBE) were not that high. The values of coefficient of residual mass (CRM) and modelling efficiency (EF) were almost perfect.

Therefore, the model established is practically good for estimating volume of Taro Cocoyam which could find application in the design of feed hopper and storage system.

Key words*: Model, estimation, Taro Cocoyam, volume, storage system*

---

*Corresponding Author. Email address: assian4real@yahoo.com

INTRODUCTION

The demand for fresh Taro Cocoyam today has progressively been on the increase in our locality (Nigeria). After harvest, it is allowed to naturally undergo dehydration to reduce the moisture level and stored properly to avoid attack by rodents / insect pests or other environmental elements. Poorly designed storage facility, processing equipment for cocoyam or other factors may contribute to the wastage or loss in its quality.

Some physical properties such as axial dimensions (length, width and thickness), arithmetic mean diameter, geometric mean diameter, moisture content, surface area, initial mass, static frictional coefficient, angle of repose, etc. are relevant in the development of a good storage facility and processing equipment [1, 2, 3, 4, 5]. Models could be established amongst these properties for easy prediction or equipment development. However, precise modelling of Taro Cocoyam volume with respect to its axial dimensions could assist in the development of feed hoper and storage systems. Model permits possibility for improving the system, process or equipment efficiency and total engineering design performance, before fabrication. It enhances rapid and simple evaluation of various options that could result in a desired solution. It helps in the elimination of wastage in the design and results testing [5]. Several researchers have established many models which could find application in food and crop processing / process optimization as well as equipment development [6, 7, 8, 9, 10, 11, 12, 5]. Thus, the main objective of this research was to establish a model that could be used in estimating Taro Cocoyam volume with respect to its axial dimensions for efficient development of storage system.

MATERIALS AND METHODS

Exactly one hundred and fifteen (115) setts of fresh Taro Cocoyam (*Colocassia esculenta)* were bought from Akpan Andem Market, Uyo, Akwa Ibom State. Taro Cocoyam samples were chosen at random, mopped and scrapped with a clean cloth and knife to eliminate foreign materials such as dust, dirts, wounded or blemished samples, stones, and stored in black polyethene bags. The initial moisture content of 10 unpeeled samples was found using gravimetric method as described by [13], [14], [15] using Equation 1. Seventy (70) unpeeled samples were chosen and their axial dimensions (length [L], width [W] and thickness [T]) measured using digital vernier calipers of 0.01 mm calibration and tape rule as shown in Figure 1, and documented. The corresponding true volume of each sample was determined by water displacement as described by [2] and recorded. The axial dimensions were used to compute arithmetic mean diameter (D_A) using Equation 2. The bulk samples were categorized based on D_A into seven (7) size ranges: I ($D_A < 3.0$ cm), II ($3.0 \text{ cm} \leq D_A < 3.5$ cm), III ($3.5 \text{ cm} \leq D_A < 4.0$ cm), IV ($4.0 \text{ cm} \leq D_A < 4.5$ cm), V ($4.5 \text{ cm} \leq D_A < 5.0$ cm), VI ($5.0 \text{ cm} \leq D_A < 5.5$ cm) and VII ($D_A \geq 5.5$ cm).

Mean and standard deviation of each parameter were computed using Data Acquisition Template powered by Microsoft Excel ™.

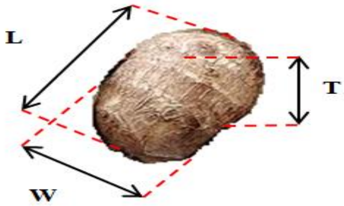

Fig. 1: The principal dimensions of Taro Cocoyam sample

Moisture Content Determination

The sample moisture content in percent wet basis (% M_{wb}) was found using Equation 1.

$$\% \, MC_{wb} = \frac{M_i - M_{bd}}{M_i} \times 100\% \tag{1}$$

Where, M_i = initial mass of the sample (g) and M_{bd} = sample mass at bone dry condition (g).

Arithmetic Mean Diameter Determination

The sample arithmetic mean diameter (D_A) was found using Equation 2.

$$D_A = \left(\frac{L + W + T}{3}\right) \tag{2}$$

Sample True Volume Determination

The sample true volume (V_T) was found using Equation 3 [2].

$$V_T = V_f - V_i \tag{3}$$

Where, V_i = initial volume of water in the measuring cylinder or beaker (ml) and V_f = final volume of water in the measuring cylinder or beaker (ml). Note: 1.0 ml = 1.0 cm^3

Data Analysis

A. Model Formulation

From the data generated, the following in form of exponential model, linear-power model, quadratic model, polynomial of degree 3 and hyperbolic model were suggested as given in Equation 4 to 8 [16].

$$Y = ae^{bX} \tag{4}$$

$$Y = a(X)^b + c \tag{5}$$

$$Y = a(X)^2 + b(X) + c \tag{6}$$

$$Y = a(X)^3 + b(X)^2 + c(X) + d \tag{7}$$

$$Y = \frac{1}{a + b(X)} \tag{8}$$

Where,
Y represents
V_T in (cm^3),
X denotes D_A,
and a, b, c and d are constants of the suggested model equations.

B. Model Development

The measured data obtained were fitted into the proposed model Equation 4 to 8 using Non-Linear Regression Statistics embedded in Statistical Package for Social Scientists (SPSS) Version 20. Each model and its respective constants were found.

The model(s) with reasonable and highest value of coefficient of determination (R^2) were selected and subjected to verification and validation

C. Model Verification and Validation

The experimental run was repeated with 5 samples per size range from the bulk sample, giving a sum of 35 samples. The model was verified and validated using statistical computations and analyses namely: coefficients of correlation (r) and determination (R^2), scattered graph of measured and predicted values, reduced Chi-square (χ_c^2), mean bias error (MBE), coefficient of residual mass (CRM), root mean square error (RMSE) and modelling efficiency (EF) [5, 17].

Where,

Reduced Chi-square (χ_c^2)

$$(\chi_c^2) = \frac{\sum_{i=1}^{\hat{T}} (MR_{mea} - MR_{pre})}{\hat{T} - G} \tag{9}$$

Mean bias error (MBE)

$$MBE = \frac{1}{\hat{T}} \sum_{i=1}^{\hat{\hat{T}}} (MR_{mea} - MR_{pre})^2 \tag{10}$$

Root mean square error (RMSE)

$$RMSE = (MBE)^{1/2} \tag{11}$$

Coefficient of residual mass (CRM)

$$CRM = \frac{\sum_{i=1}^{\hat{\hat{T}}} MR_{mea} - \sum_{i=1}^{\hat{T}} MR_{pre}}{\sum_{i=1}^{\hat{\hat{T}}} MR_{mea}} \tag{12}$$

Modelling efficiency (EF)

$$EF = 1 - \frac{\sum_{i=1}^{\hat{\hat{T}}} (MR_{mea} - MR_{pre})^2}{\sum_{i=1}^{\hat{T}} (MR_{mea} - MR_{mea.mean})^2} \tag{13}$$

Where,

MR_{mea} = measured values,

MR_{pre} = predicted values,

$MR_{mea.mean}$ = mean measured values,

$\hat{T}$ = total number of observation,

G = number of constants.

For exact goodness of fit, the value of r should be equal to R^2. Besides, the value of CRM must be close to zero and EF roughly equal to 1.

RESULTS AND DISCUSSIONS

The results of the study are shown in Table 1.

Table 1. The mean values of axial dimensions, arithmetic mean diameter and true sample volume

Group		Axial Dimensions				Volume of Liquid in the Cylinder		$V_d = V_T$ (cm^3)
		L (cm)	W (cm)	T (cm)	D_A (cm)	V_i (cm^3)	V_f (cm^3)	
I	Mean	3.806	2.275	2.505	2.862	124.00	142.50	18.50
	SD	0.556	0.191	0.021	0.115	0.00	3.54	3.54
II	Mean	5.587	2.218	2.415	3.407	125.67	146.00	20.33
	SD	0.303	0.098	0.083	0.062	2.58	5.22	4.23
III	Mean	5.470	2.820	3.088	3.793	128.17	154.83	26.67
	SD	0.766	0.502	0.481	0.116	4.92	16.01	12.68
IV	Mean	6.006	3.264	3.498	4.256	127.44	165.50	38.06
	SD	0.889	0.479	0.508	0.138	7.69	6.07	7.08
V	Mean	6.812	3.535	3.798	4.715	105.92	154.85	48.92
	SD	0.625	0.206	0.196	0.126	9.90	10.99	6.05
VI	Mean	8.248	3.700	3.915	5.288	127.75	203.25	75.50
	SD	0.702	0.129	0.157	0.185	8.54	16.64	8.10
VII	Mean	8.917	3.873	4.110	5.633	130.67	208.67	78.00
	SD	0.091	0.078	0.036	0.03	5.77	11.02	5.29
Overall Mean		6.367	3.188	3.427	4.327	121.80	163.80	42.00
Overall S.D		1.291	0.599	0.612	0.679	111.96	20.80	18.59

Note: L= length, W=width, T=thickness, D_A= arithmetic mean diameter, V_i and V_f are initial and final volume of liquid, V_d = volume of liquid displaced equals true volume of Taro Cocoyam (V_T).

The plot of true volume of Taro Cocoyam (V_T) against its arithmetic mean diameter (D_A) is given in Figure 1.

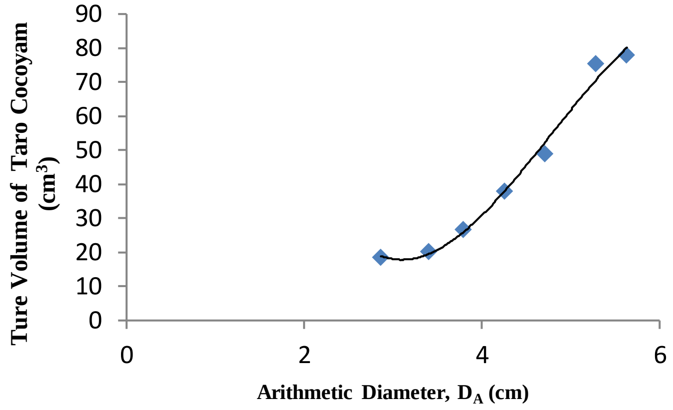

Fig. 2. Plot of true volume of Taro Cocoyam against its arithmetic mean diameter.

As observed in Figure 2, increase in D_A, led to increase in the true volume of taro cocoyam. The model that could reasonably describe the relationship is the polynomial of degree 3 and is stated in Equation 14 as:

$$V_T = a(D_A)^3 + b(D_A)^2 + c(D_A) + d \quad (14)$$

Where,
a = −3.87,
b = 55.453,
c = −232.11 ,
d= 319.76

The predicted values of Taro Cocoyam volume using the model Equation 14 are presented in Table 2.

Table 2. Mean measured and predicted values of volume of taro cocoyam

Volume of Taro Cocoyam (cm^3)	
Measured Values	Predicted Values
18.50	18.96
20.33	19.60
26.67	25.99
38.06	38.02
48.92	52.51
75.50	*70.76*
78.00	*80.15*

Besides, a graph of mean predicted against mean measured value of Taro Cocoyam volume from Table 2 is presented in Figure 3 to examine its curve fitness.

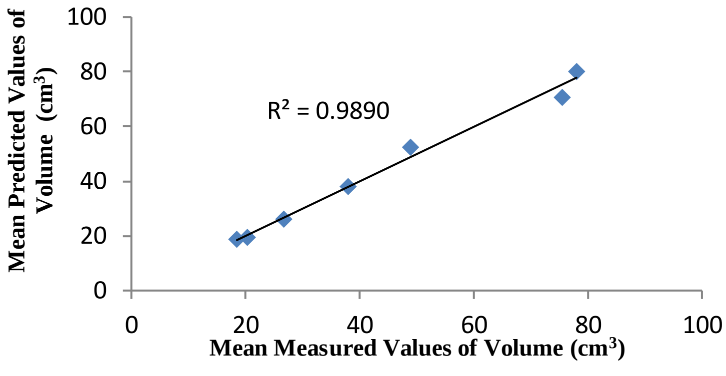

Fig. 3: Plot of mean predicted and measured value of Taro Cocoyam volume

The graph, in Figure 3, evidently shows that the points for predicted and measured values have positive correlation and $R^2 \approx 1$. The line where the slope is equivalent to one is that which the predicted values would be equal the measured values. Moreover, the computed statistical parameters for goodness of fit from Figure 3 are shown in Tables 3.

Table 3: Statistical parameters for goodness of fit for the model Equation 14

Parameters	**Values**
Coefficient of correlation, r	0.9945
Coefficient of determination, R^2	0.9890
Reduced Chi-square, χ_c^2	0.7050
Mean bias error, MBE	5.2000
Root mean square error, RMSE	2.2900
Coefficient of residual mass, CRM	0.0000
Modelling efficiency, EF	0.9900

From Table 3, the value of R^2 was almost equal to r, which indicated that $R^2 \approx 1$. The values of χ_c^2, RMSE and MBE were too high. The value of CRM was zero and EF almost equal one. These are good characteristics of an acceptable quality fit. Therefore, the empirical model as describes in Equation 14 could be employed in estimating the volume of Taro Cocoyam with respect its axial dimensions.

CONCLUSION

The model Equation 14 was established using experimental approach. It was validated and found to be rationally good for estimating Taro Cocoyam volume if its axial dimensions are measured. Besides, the model could also be used in efficient design of feed hopper, silo and bin capacity for storing dried Taro Cocoyam samples.

CONFLICT OF INTEREST

None is declared.

REFERENCES

[1] Irtwange, S.V. and Igbeka, J.C.2000. Some physical properties of two African yam bean (*Sphenostylis stenocarpa*) accessions and their interrelations with moisture content. *Applied Engineering in Agriculture*, 18(5): pp. 567-576.

[2] Antia, O.O. and Assian, U.E.2018b. Development of an empirical model for palm nut volume determination. *European Journal of Advances in Engineering and Technology,* 5, (7) : pp. 466-469.

[3] Antia, O.O., Assian, U.E. and William, O. 2019c. Modeling of Water Absorption by Dried Palm Nut Soaked at Room Temperature. International Journal of Trend in Scientific Research and Development (IJTSRD), Vol. 3, (Issue 3), pp.1499-1504.

[4] Antia, O.O., William, O., and Emem, E.O. 2021. Application of basic drying theory to determine drying mass constants of selected seafoods. Global Joumal of Engineering and Technology Advances, 07(1). pp.137–143.

[5] Assian, U., Antia, O. and Olosunde, W. 2021a. Predicting Cracking Efficiency and Kernel Breakage of Centrifugal Nut Cracker. International Journal of Advances in Engineering and Management (IJAEM), Volume 3, Issue 5, pp. 1211-1217.

[6] Alonge, A.F. and Oje, K. (2003). Computer modelling of solar radiation available for crop drying at a Tropical Station (Ilorin, Nigeria). *Journal of Engineering and Engineering Technology* (FUTAJEET), Akure, Nigeria, 3: pp. 41- 46.

[7] Ndukwu, M. C. and Asoegwu, S. N.2011. A mathematical model for predicting the cracking efficiency of vertical-shaft centrifugal palm nut cracker. *Research in Agricultural Engineering*, 57(3): pp.110–115.
[8] Alonge, A. F. and Onwude, D.I. 2013. Estimation of solar radiation for crop drying in Uyo, Nigeria using a mathematical model. *Advanced Materials Research,* 824: 420-428.
[9] Antia, O.O. and Assian, U.E. 2018a. Empirical modeling of 4-dimensional relationship for dried palm nut of dura variety. *American Journal of Engineering Research*, 7, (6): pp.311-316.
[10] Antia, O.O., Assian, U.E. and William, O. 2019a. Development of an Empirical Model Relating Palm Nut Moisture Content, Shell Thickness and soaking Time. International Journal of Mechanical and Civil Engineering, Vol. 2, (Issue 1), pp.36-47.
[11] Antia, O.O., Assian, U.E. and William, O. (2019b). Effect of Moisture Content on Palm Nut Shell Fragmentation for Effective Separation of Kernel. International Journal of Mechanical and Civil Engineering, Vol. 2, (Issue 1), pp.48-55.
[12] Antia, O.O., Assian, U.E. and William, O. 2019c. Modeling of Water Absorption by Dried Palm Nut Soaked at Room Temperature. International Journal of Trend in Scientific Research and Development (IJTSRD), Vol. 3, (Issue 3), pp.1499-1504.
[13] ASABE 2010. ASABE Standard. Year Book, American Society of Agricultural and Biological Engineers.
[14] Assian, U.E. and Alonge, A. F. 2021. Some physical properties of kariya (*Hildegardia barteri*) nut/ kernel relevant to the design of its processing equipment. Global Journal of Engineering and Technology Advances, 7(2): pp. 83–90.
[15] Antia, O.O., Olosunde W. and Offiong, A. 2014. Determination of optimum moisture content of palm nut cracking for efficient production of whole kernel. *Nigerian Journal of Technological Development*, 11(2): pp.27-30.
[16] Spiengel, M.R. and Stephens, L. J. 1999. *Statistics*. *Schaum's Outline Series*. 3rd Edition. McGraw- Hill Companies, New York: 362-401, pp.281-286.
[17] Assian, U.E., Antia , O.O. and William, A. O. 2021b. Empirical Model for Predicting Volume of Palm Nut With Respect to its Moisture Content. *Research Inventy: International Journal of Engineering and Science,* Vol.11, Issue 5, pp. 31-36.

PRAKTIČNI MODEL ZA PROCENU ZAPREMINE TARO KOKOYAM NA OSNOVU NJEGOVIH AKSIJALNIH DIMENZIJA

Ubong Edet Assian[1], Tosin Paul[2]

[1]Department of Agricultural and Food Engineering, Faculty of Engineering, University of Uyo, Uyo, Akwa Ibom State, Nigeria
[2]Department of Agricultural and Bioresources Engineering, Michael Okpara University of Agriculture Umudike, Abia State, Nigeria

Sažetak: Taro Cocoyam (*Colocassia esculenta)* plod je podložan napadima glodara, insekata i elemenata iz životne sredine .
Nakon sušenja plod Taro Cocoyam, se čuva kako bi se izbegli gubici. U nastojanju da se efikasno razvije sistem skladištenja, osnovni fizički parametar kao što je zapremina svežeg ploda (zrna) Taro Cocoyam u odnosu na njegove aksijalne dimenzije treba da bude dobro izražena i modelovana zbog lake procene.

U ovoj studiji, sveži uzorci zrna Taro Cocoiam su nabavljeni, očišćeni i upakovani. Za određivanje početnog sadržaja vlage (%) korišćeno je deset (10) neoljuštenih uzoraka.
Aksijalne dimenzije pedeset (50) neoljuštenih uzoraka su izmerene i korišćene za izračunavanje srednjeg aritmetičkog prečnika (D_A). Odgovarajuća stvarna zapremina (V_T) je određena korišćenjem postupka sušenja. Veliki uzorci su grupisani na osnovu pri (D_A), u sedam (7) različitih veličina. Izračunate su srednja vrednost i standardna devijacija svakog parametra. Model je uspostavljen, verifikovan i validiran.
Statistička analiza pokazuje da je vrednost koeficijenta determinacije (R^2) skoro jednaka koeficijentu korelacije ($r \approx 1$). Vrednosti redukovanog hi-kvadrata testa (χ_c^2), srednje kvadratne greške (RMSE) i srednje greške pristrasnosti (MBE) nisu bile tako visoke. Vrednosti koeficijenta preostale mase (CRM) i efikasnost modeliranja (EF) bile su skoro savršene.
Zato je uspostavljeni model praktično dobar za procenu zapremine ploda Taro Cocoiam i može da nađe uspešnu primenu kod projektovanja oblika rezervoara za hranu i sistema za skladištenje.

Ključne reči: *Model, procena, Taro Cocoiam, zapremina, sistem skladištenja.*

Prijavljen:
Submitted: **29.07.2022**
Ispravljen:
Revised: **22.10.2022**.
Prihvaćen:
Accepted: **30.10.2022.**

Univerzitet u Beogradu
Poljoprivredni fakultet
Institut za poljoprivrednu tehniku
Naučni časopis
POLJOPRIVREDNA TEHNIKA
Godina XLVII
Broj 4, 2022.
Strane: 67 – 81

University of Belgrade
Faculty of Agriculture
Institute of Agricultural Engineering
Scientific Journal
AGRICULTURAL ENGINEERING
Year XLVII
No. 4, 2022.
pp. 67 – 81

UDK:631.3:631.51:628.50.

Original Scientific paper
Originalni naučni rad
DOI:10.5937/PoljTeh2204067O

LEACHING RISK ASSESSMENT OF PESTICIDES FROM SOIL AS FUNCTION OF SOIL PROPERTIES, PESTICIDE PROPERTIES AND RAINFALL CHARACTERISTICS USING HYDRUS 1D NUMERICAL MODEL

Jekwu Sunday E. Ona*[1]

Monitoring and Evaluation Department/Environmental Consultancy, Community and Social Development Agency (CSDA) Government of Enugu State Nigeria

Abstract. It has been observed through experiments that many chemicals especially pesticides found in streams and groundwater bodies are transported through surface runoff and/or preferential flow processes. Researchers have also proved that the timing and nature of rainfall since the last pesticide application are often described as significant controls on pesticide transport through flow processes. Rainfall variability is now considered as the climate drivers on contaminant transport. The amount of pesticides transported through surface runoff and/or preferential flow pathways to streams and groundwater respectively has been shown to be strongly correlated with the concentration of that chemical in a thin near-surface layer of the soil immediately prior to such an event.

The thin near-surface layer of a soil is regarded as the source where all the dynamics of solute transport starts. The thin near-surface layer is the store of pesticide from which they are leached by both fast episodic as well as slow steady processes. In this research, we seek to better understand the idea of driver-source-trigger concept of pesticide solute transport in the subsurface. The driver (rainfall variability) triggers (surface runoff and/or preferential flow) from the source (a thin near-surface layer) for pesticides transport to stream and/or groundwater. The methodology for this study is by the use of HYDRUS 1D Numerical Model.

Key words*: Soil Physics, risk assessment, leaching, pesticides, transport modeling, water quality.*

*[1]Corresponding Author. E-mail: jekwuona@gmail.com

INTRODUCTION

Agricultural practices are one of the main origins of chemicals found in the soil. The original purpose of this agricultural chemicals application (fertilizers, pesticides etc.) is to enhance crop growth and production [23]. Generally, organic chemicals of concern include petroleum products, chlorinated, aromatic and polycyclic organic compounds that originate for example, from industrial sites or from the use of pesticides. Inorganic chemicals such as nitrates and heavy metals have also been reported to contaminate aquifers. In the soil environment, some of these solutes are beneficial as they provide plants and soil organisms with food and pest resistance; yet, the movement of solutes off-site to surface and/or ground water sources can have substantial agronomic, environmental and economic consequences [25]. For instance, water sources contaminated by certain nutrients and pesticides can be rendered unsafe for human and animal consumption, and may also be toxic to aquatic organisms.

Based on the consequences emanating from the movement of these solutes, there is concern for the quality of the vadose zone and possible contamination of groundwater and hence a major impetus for studying solute transport in soils. The aim of this study is to improve how to efficiently use chemicals needed in the soil for crop production. This will help in protection of water quality both on the surface and on the underground. The study will also help to better understand how these solutes moves in the soil to minimize off site contaminations. The regulation of pesticide use is often conducted at national and regional scales. In order to better manage the use of pesticides for the mitigation of environmental impact it is important to understand the episodic, spatial and temporal variability's of the risk of off-site movement of these chemicals [22].

Rainfall events usually trigger off or initiates surface runoff and/or rapid preferential flow processes in the vadose zone. These flows are mainly responsible for example, pesticides dissipation to stream and/or groundwater although we cannot rule out the role of other factors like soil properties, land management practices and the properties of the chemicals in question. Pesticides transport, have been found to be episodically transported mainly through discrete flow pathways (surface runoff and preferential flow) and this transport is often initiated in a thin near-surface soil layer and driven by naturally variable and intermittent rainfall intensities [19]. Therefore one can say that the episodic or periodic behaviors of pesticide transport in the environment are controlled by surface runoff and/or preferential flow processes which on their own are being triggered by rainfall events. According to [20], factors that influence pesticide transport both in the surface and subsurface include climatic, soil and topography, pesticide and land practices factors.

It is important to note that these factors are all interrelated and embracing ranging from climate, soil properties, and chemical properties to land management practices. But in the final analysis, it is experimentally proven that; the timing and magnitude of rainfall events that have the potential to trigger rapid flow processes such as surface runoff and preferential flow have significant controls on pesticide transport [22].

Transport modeling can be referred to as the quantification of the migration of contaminants in the subsurface [27]. A large number of physical, chemical and microbiological processes affect the movement and fate of solutes in the subsurface.
These processes require a broad array of mathematical and physical sciences to study in order to efficiently describe solute transport [13].

Many models have been developed to evaluate the computations of water flow and solute transport in the vadose zone.
Generally, they are either analytical or numerical models for predicting water and solute movement between the soil surface and the groundwater table. Amongst the most commonly used ones are the Richards equation for variably saturated flow, and the Fickian-based advection-dispersion equation (ADE) for solute transport.

According to [27], most transport models assume that the concentration of solutes or contaminants in variably saturated zones never reaches values large enough to induce variations in the density or viscosity of groundwater. In another related development, [26] posited that many contaminants do not make it to groundwater because of the combination of adsorption and decay. These theories are always based on some assumptions and then this implies the need for further research.

HYDRUS is one of the computer codes which simulate water, heat, and solutes transport in one, two, and three dimensional variably saturated porous media on the basis of the finite element method. The Richards's equation for variably-saturated water flow and advection-dispersion type equations (ADE) for heat and solute transport are solved numerically using finite difference or finite element methods which requires an iterative implicit technique [26, 32]. To get results that are very close to reality it is important to keep modeling to a minimum set of processes in order to reduce the number of highly uncertain parameters.

MATERIALS AND METHODS

Ten types of pesticides with different solute sorption (k_d) and solute decay (μ) values (kd0.1_μ1, kd1_μ1, kd10_μ0.1 and kd100_μ0.1 kd0_μ0, kd0_μ0.1, kd0.1_μ0.1 and kd1_μ0.1, kd10_μ1 and kd100_μ1) were modeled in thin near-surface layers of sand, loamy-sand, sandy-loam, loam, silt and silt-loam agricultural soil types. This is to investigate the dissipation of pesticides from the thin near-surface layer of each of the soil types as function of soil properties, pesticide properties and rainfall characteristics. The investigation and analysis was carried out by the use of HYDRUS 1D numerical model.

Input parameters

Table (1) shows the parameters of four types of pesticides simulated in each of the six soil types maintaining the same boundary conditions, soil hydraulic and solute parameters. Van Genuchten (1980a) equation was used to calculate the volumetric water content for each of the six soil types;

$$\theta(h) = \frac{\theta s - \theta r}{[1 + (\alpha h)n]m} + \theta r \qquad \textbf{(1)}$$

Relationship between m and n; $m = 1 - \frac{1}{n}$ ....**(2)**

The volumetric water content was used to calculate the solute concentration [C], of the various pesticides.

$C_T = \theta c + \rho bs$…………………… … ……………..**(3)**

$s = k_d c$……………………………… ……………...….**(4)**

$c = \frac{C_T}{\theta + \rho b k_d}$……………………………… ….……….**(5)**

Meaning of the symbols			
θ	Volumetric water content of the soil	n [-]	Parameter n in soil water retention curve
θ_r [-]	Residual water content of the soil	m	Parameter (= 1 - 1/n)
θ_s [-]	Saturated water content of the soil	Pb [ml^{-3}]	bulk density of the soil
α [1/mm]	Parameter alpha in soil water retention curve	K_d	Solute sorption
μ	Solute decay	C_T	Total concentration loaded to the soils
S	Solid phase solute concentration	c	Solute concentration

Each of the six soil type is assumed to be dry, 1000mm in depth and consists of double layering, the second layer in all being sandy soil and the simulation period was for 100 days. A single rainfall event of 15mm/day occurred during the simulation period in each of the six soil type and no root water uptake was considered.

Table 1. Input parameters for the pesticides: kd0.1_μ1, kd1_μ1, kd10_μ0.1 and kd100_μ0.1

Soil type	θ_r [-]	θ_s [-]	α [1/mm]	n [-]	Pb [ml^{-3}]	Rainfall duration [mm/day]	C_T [mmol]	K_d	μ	C [$mmol/mm^3$]
Sand	0.45	0.43	0.0145	2.68	1.6	15	1	0.1, 1, 10, 100	1, 1, 0.1, 0.1	4.8709, 0.6078, 0.0623, 0.0062
Loamy Sand	0.057	0.41	0.0124	2.28	1.4	15	1	0.1, 1, 10, 100	1, 1, 0.1, 0.1	5.0302, 0.6855, 0.0711, 0.0071
Sandy Loam	0.065	0.41	0.0075	1.89	1.5	15	1	0.1, 1, 10, 100	1, 1, 0.1, 0.1	4.3725, 0.6334, 0.0663, 0.0067
Loam	0.078	0.43	0.0036	1.56	1.4	15	1	0.1, 1, 10, 100	1, 1, 0.1, 0.1	3.4783, 0.6462, 0.0707, 0.0071
Silt	0.034	0.46	0.0016	1.37	1.3	15	1	0.1, 1, 10, 100	1, 1, 0.1, 0.1	2,7902, 0.6543, 0.0756, 0.0077
Silt Loam	0.067	0.45	0.002	1.41	1.3	15	1	0.1, 1, 10, 100	1, 1, 0.1, 0.1	2.9036, 0.6603, 0.0757, 0.0077

Pre and post processing in HYDRUS 1D numerical model

The input parameters and the codes required to execute HYDRUS 1D are placed in the pre-processing dialog windows and after execution comes the results in the output files. The output files are organized into 3 groups; T-level information, P-level information, and A-level information. T-level information output file contains information, which is printed at the end of each time step. Some examples include; RUN_INF.OUT, SOLUTE.OUT, OBS_NODE.OUT etc. The output files under P-level information are printed only at prescribed print times and some of their examples include; NOD_INF.OUT and BALANCE.OUT, files. A-level information is printed each time a time-dependent boundary condition is specified. Examples are A_LEVEL.OUT and METEO.OUT output file.

RESULTS AND DISCUSSIONS

The BALANCE.OUT output file displayed in the mass balance information window contains the mean concentration (cMean) of the pesticide solutes dissipated from the thin near-surface layers of the soil types at given time steps and table 2 is showing that of the pesticide solute (kd1_µ1) in the six soil types.

Table 2. cMean of the pesticide solute (kd1_µ1) dissipated in each time step for the six soil types

Time (days)	Loamy Sand mmol/mm^3	Silt Loam mmol/mm^3	Sand mmol/mm^3	Sandy Loam mmol/mm^3	Loam mmol/mm^3	Silt mmol/mm^3
0	6.86E-01	6.60E-01	6.08E-01	6.33E-01	6.46E-01	6.54E-01
5	1.73E-02	9.72E-03	1.69E-02	1.41E-02	1.17E-02	9.62E-03
10	9.71E-04	3.24E-04	9.08E-04	6.27E-04	4.47E-04	3.19E-04
15	8.89E-05	2.18E-05	8.78E-05	5.25E-05	3.33E-05	2.14E-05
20	1.18E-05	2.40E-06	1.27E-05	6.79E-06	3.95E-06	2.35E-06
25	2.07E-06	3.74E-07	2.46E-06	1.20E-06	6.51E-07	3.65E-07
30	4.55E-07	7.57E-08	5.91E-07	2.69E-07	1.38E-07	7.36E-08
35	1.19E-07	1.87E-08	1.68E-07	7.20E-08	3.53E-08	1.81E-08
40	3.61E-08	5.42E-09	5.46E-08	2.23E-08	1.05E-08	5.24E-09
45	3.37E-08	4.26E-09	5.19E-08	1.95E-08	8.57E-09	4.09E-09
50	3.18E-08	3.39E-09	4.97E-08	1.73E-08	7.09E-09	3.22E-09
55	3.01E-08	2.71E-09	4.78E-08	1.55E-08	5.90E-09	2.55E-09
60	2.86E-08	2.19E-09	4.60E-08	1.40E-08	4.94E-09	2.04E-09
65	2.71E-08	1.77E-09	4.42E-08	1.26E-08	4.16E-09	1.63E-09
70	2.58E-08	1.44E-09	4.26E-08	1.14E-08	3.52E-09	1.32E-09
75	2.45E-08	1.18E-09	4.11E-08	1.04E-08	2.99E-09	1.07E-09

Cont. Table 2.

80	2.34E-08	9.70E-10	3.96E-08	9.41E-09	2.54E-09	8.72E-10
85	2.23E-08	8.01E-10	3.82E-08	8.57E-09	2.17E-09	7.15E-10
90	2.12E-08	6.64E-10	3.69E-08	7.82E-09	1.86E-09	7.15E-10
95	2.03E-08	5.53E-10	3.56E-08	7.15E-09	1.60E-09	4.86E-10
100	1.93E-08	4.62E-10	3.44E-08	6.54E-09	1.38E-09	4.86E-10

The cMean of the pesticide solute (kd1_µ1) was plotted against time to observe the mode of its dissipation from the thin near-surface layers of the six agricultural soil types and the result is as shown below.

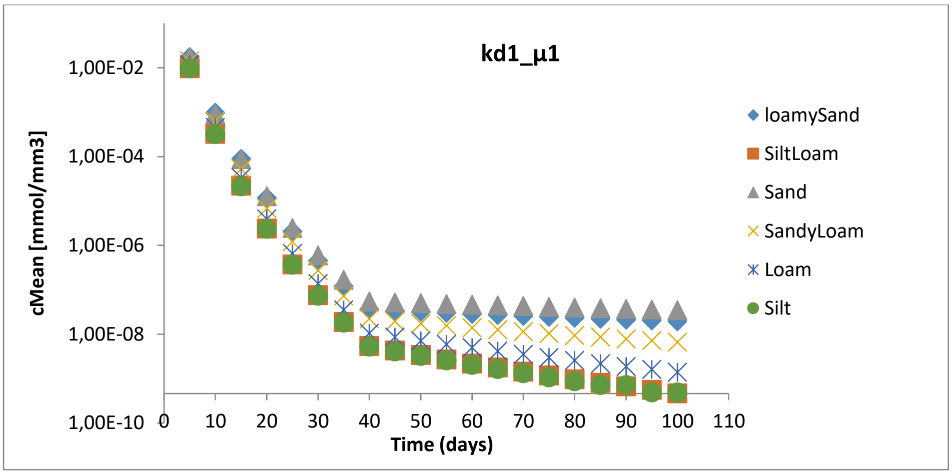

Figure 1. Dissipation of pesticide solute (kd1_u1) from the thin near-surface layers in the six soil types

From figure (1), the values from the graph are indicating that there was pesticide solute dissipation after each time step. It is obvious from the curve of the graph that the dissipation from the thin near-surface layers of the soil types were rapid at first for some time and then it became gradually slower as time progressed. Precisely from the first day of application to about the 35th day, the graph displayed steady and rapid dissipation from the thin near-surface layers and then it became slower and slower after the 35th day till the end of the simulation period.

Dissipation pattern of the pesticide solutes

In figure (2) below the cMean of the pesticide solutes were plotted against time in the six soil types but in this case from the first day of application to the 35th day of the simulation which were the periods there was clear observation of rapid dissipation. This is to understand the pattern of dissipation that occurred during the simulation. Exponential trendline was drawn in these graphs to see how best they fit into the parameters.

From the fit of exponential trendline drawn on the parameters one can summarize that the dissipation pattern was exponential.

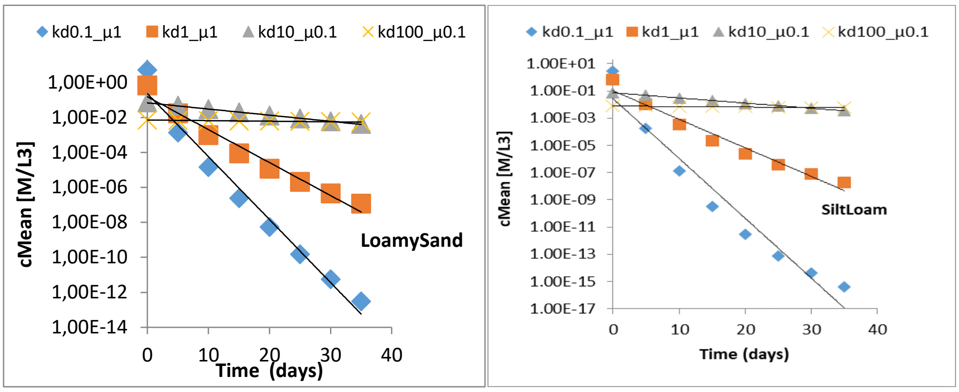

Figure 2. Exponential dissipation of pesticide solutes from the thin near-surface layers of Loamy Sand and Silt Loam

The exponential dissipation rate per day for each of the pesticide solutes in the six agricultural soil types were calculated by the use of exponential equation;

$$\mathbf{a_0\ exp^{-a1t}} \qquad \ldots\ldots\ldots\ldots\ldots\ldots \qquad \mathbf{(6)}$$

Where ao is the cMean at initial time zero and the a1t is the dissipation rate or constant per day. The table below is showing the relationship in loam soil type.

Table 3. Soil types, pesticides properties and exponential dissipation in Loam soil

Soil type	kd	µ	a_o [$cMean_o$] mmol/mm^3	a1 [1/day]	R^2
Loam	0	0	0.6644	1.522	0.9979
	0	0.1	0.5926	1.528	0.9977
	0.1	0.1	0.0687	0.94	0.9551
	1	0.1	0.7358	0.453	0.9701
	10	0.1	0.0681	0.082	0.9989
	100	0.1	0.0071	0.008	0.9999
	0.1	1	0.0293	0.998	0.9453
	1	1	0.1139	0.466	0.9658
	10	1	3.0864	0.132	0.9969
	100	1	3.4831	0.017	0.9999

The table above describes the relationship in loam soil between the solute sorption (kd), the solute decay (µ), and the exponential dissipation equation-the a_0 (cMean at initial time zero), the $a1_t$ (the dissipation rate or constant per day) and the R^2 (the R-squared values).

The dissipation rate per day for the pesticide solutes were plotted against pesticide characteristics (kd and µ values) as shown in figure (3). It is observed that as the solute sorption is increasing, the dissipation rate is decreasing.

When two pesticides having the same solute sorption but different solute decay are compared, more solute dissipation is observed in the one with higher solute decay value. For instance, in loam soil, the pesticide kd10_µ1 dissipated more pesticide solutes of 0.132mmol/mm^3 per day to that of kd10_µ0.1 which dissipated 0.082mmol/mm^3.

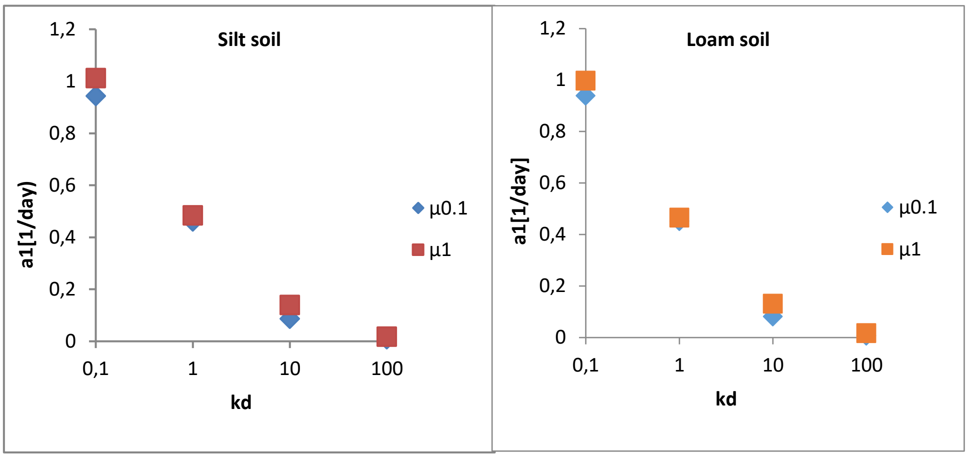

Figure 3. Graph showing dissipation rate per day of pesticides kd0.1 µ1, kd1 µ1, kd10 µ0.1 and kd100 µ0.1 in the thin near-surface layers of silt and Loam soil.

Retardation Factors for the Pesticides

The retardation factors were calculated for each of the pesticides solutes in the six agricultural soil types by the use of retardation formula

$$R = 1 + \frac{Pbkd}{\theta} \qquad (7)$$

Where,
Pb = the soil bulk density,
θ = volumetric water content
kd = the solute sorption.

Table 4. Retardation factors for the ten types of pesticide in loam soil

S/N	Pesticides	pb	kd	θ	R
1	kd0.1_µ1	1.4	0.1	0.1475	1.95
2	kd1_µ1	1.4	1	0.1475	10.49
3	kd10_µ1	1.4	10	0.1475	95.92
4	kd100_µ1	1.4	100	0.1475	950.15
5	kd0_µ0	1.4	0	0.1475	1.00
6	kd0_µ0.1	1.4	0	0.1475	1.00
7	kd0,1_µ0.1	1.4	0.1	0.1475	1.95
8	kd1_µ0.1	1.4	1	0.1475	10.49
9	kd10_µ0.1	1.4	10	0.1475	95.92
10	kd100_µ0.1	1.4	100	0.1475	950.15

Model Evaluation

In order to find out if there is any close relationship between the model results and what is obtained in reality, the results have to be evaluated using indices established for the objective of the modeling. In this case, two known concepts for evaluation of pesticide leaching risk assessments; the attenuation factor and preferential flow index were considered. The former was used for evaluation while the later was not used for reasons to be explained later in the discussion. The attenuation [AF] for each of the pesticides was calculated by using its formula:

$$AF = exp^{-Kb\frac{z\Delta\theta R}{i}} \qquad \textbf{(8)}$$

Where,
kb = the solute decay,
z = depth of the thin near-surface layer (10mm),
i = net rate of groundwater recharge which is 2mm/day [6],
$\Delta\theta$ = volumetric water content ,
R = retardation factor.

Table 5. Attenuation factor [AF] for each of the pesticides in SandyLoam

S/N	Sandy Loam	kb	z [mm]	Δθ	R	i	AF
1	kd0.1_µ1	1.00	10.00	0.0787	2.91	2.00	3.19E-01
2	kd1_µ1	1.00	10.00	0.0787	20.06	2.00	3.73E-04
3	kd10_µ1	1.00	10.00	0.0787	191.60	2.00	1.81E-33
4	kd100_µ1	1.00	10.00	0.0787	1906.97	2.00	0.00E+00
5	kd0_µ0	0.00	10.00	0.0787	1.00	2.00	1.00E+00
6	kd0_µ0.1	0.10	10.00	0.0787	1.00	2.00	9.61E-01
7	kd0.1_µ0.1	0.10	10.00	0.0787	2.91	2.00	8.92E-01
8	kd1_µ0.1	0.10	10.00	0.0787	20.06	2.00	4.54E-01
9	kd10_µ0.1	0.10	10.00	0.0787	191.60	2.00	5.32E-04
10	kd100_µ0.1	0.10	10.00	0.0787	1906.97	2.00	2.58E-33

Pesticides are among contaminants that undergo important transformations in soils. In figure (1), it was clearly observed that there was dissipation of pesticide solutes from the thin near-surface layers of the six soil types. The dissipation of the pesticide solutes were rapid initially for some time and then it became slower and slower till the end of the simulation period. Exponential functions was used in figure (2) to describe the simulation results. The trendline is showing that the fit was not perfect as signs of deviation can be seen. These points to the fact that results gotten from modeling are just a simplified picture of reality and cannot show perfectly what can be in the real world. In overall the fit can be regarded as a good approximation of the modeled data as the values of R^2 were high.

In a related study of empirical observation of pesticide dissipation by [20], rainfall was characterized by a random time between events and a random storm depth, both of which are assumed to be exponentially distributed.

The conclusion of this study is that on average pesticide solutes tend to dissipate exponentially with time, most likely rapid dissipation initially and then followed by slower dissipation.

The dissipation of pesticide solutes from the thin near-surface layers in this study is in line with what [26] stated that; soil properties (mainly water content and bulk density) and pesticide properties (sorption and decay) influences the solute concentrations of the chemicals when they are applied to agricultural soils. It is also in line with the observation that the mobility of pesticide solutes in soil is largely controlled by their water solubility and sorption properties [16]. And just as [28] stated, the magnitude of pesticide solute losses varied from soil to soil, depending on structural development and the organic carbon content. Dissipation of conservative solute like bromide tracer can be used as a reference point in studying the pattern of dissipation of pesticides from the thin near-surface layers. This is buttressed in a research carried out by [21], on analysis of the leaching behavior of bromide and two herbicides, methabenzthiazuron (MBT) and ethidimuron (ETD) using data from twelve uncropped lysimeter and high-resolution climate data, in order to identify the rainfall controls on rapid solute leaching. Laboratory experiments determined that the sorption of the herbicides followed Freundlich isotherms and degradation was found to decrease exponentially with time. The bromide tracer known not to adsorb to soil, displayed a smoother breakthrough curve and its retardation factor was 1. The same characteristics and smoother breakthrough curve was observed in this study for the pesticide solutes kd0_µ0 and kd0_µ0.1 as they did not bind to the soil and their retardation factors were 1. The researchers concluded that; the variability of the mobility of pesticides (MBT and ETD) are large when compared with bromide because of processes such as adsorption and decay.

The exponential dissipation behavior of pesticide solutes in this study can also be compared to solute transport triggered by surface runoff to streams. [24], in their research, retained three contrasting values of retardation factor for three pesticides to investigate the different behavior of the pesticides in solution during rainfall events according to their sorption. They concluded that because weakly sorbing solutes are more likely to be transported into the soil matrix and away from the soil surface before the initiation of runoff, stronger sorbing solutes are more likely to be transported by surface runoff. The end result in this research is that strongly sorbing solutes are found more in the receiving waters like streams and rivers. But we must note that triggering of fast flow pathways like surface runoff involves highly nonlinear threshold processes. These thresholds processes are why pesticide leaching appears episodic and short lived. The fast flow process (surface runoff) when initiated, are always short lived with durations of the order of the rainfall event, usually between several minutes and hours.

Therefore in solute transport by surface runoff, the pattern of dissipation is also rapid initially and then slower and slower based on the duration and magnitude of the rainfall event.

Table (3) shows that the relationship between the solute sorption and the dissipation rate per day of the pesticide solutes from the thin near-surface layers are negative. In each of the six soil types, as the solute sorption increases the dissipation rate per day decreases.

This is well defined in figure (3) as the two variables in the graph are seen to have a negative relationship. This is in agreement with prior observations in literatures that pesticides with lower kd values bind less to soil organic matter (SOM) in the thin near-surface layers of the soil and therefore are more susceptible to leaching than pesticides with higher kd values [15]. Moreover in table (4), it is observed that the relationship between solute sorption and the retardation factor is positive. As the solute sorption values of the pesticides increases, the retardation factor also increases. This also buttressed the fact that stronger sorbing pesticide solutes will be retained more in the soil surface while weakly sorbing pesticide solutes will be likely found more in receiving waters.

The leaching risk measurement index, attenuation factor [AF] can be used to evaluate the results from this study. Attenuation factor is primarily used for relative measures of leaching risks in simple models which consider flow only in the soil matrix and not through episodically activated rapid flow pathways like preferential flow. In table (5), the relationship between solute sorption and attenuation factor indicates that the more the pesticides bind to the soil i.e. the higher the solute sorption, the less their attenuation factor and this implies also the less they can be found in the groundwater. It is also important to mention that as the retardation factor increases due to higher solute sorption, the attenuation factor invariably decreases and this implies also the lesser the pesticide solute can be found in the groundwater. Just like [12], stated about their PIRI risk tool which uses modified attenuation factor index; the outputs from this kind of risk evaluation like the PIRI tools do not represent the absolute risk but a relative risk rating among pesticides or land uses in a catchment.

The leaching risk measurement index, preferential index [PF] describes only the leaching potential by rapid flow processes through macropores and does not consider the possibility of slower transport through the soil matrix. Soil and chemical parameters as well as the timing and magnitude of rainfall and preferential flow events are the basis for the preferential flow (PF) leaching index. As there is no significant parameterization of timing and magnitude of rainfall and preferential flow events in this study, the preferential flow index cannot be used to evaluate this model result.

CONCLUSION

Pesticide degradation experimentson disturbed and undisturbed soil samples, [28] showed that there is rapid decline of leached loads with time. They went further to put up five physical-chemical processes that could explain the different patterns of pesticide leached loads observed in the soils and they include:

(1) relative extent of preferential flow,

(2) sorption capacity of the compounds to the different soils,

(3) extent of degradation of the compounds in the soil,

(4) variation in sorption kinetics between compounds associated with pesticide diffusion into soil aggregates, and

(5) protection of the compounds by a combination of intra-aggregate diffusion and the presence of preferential flow pathways.

Multiple processes generate exponential dissipation of pesticide solutes under transient flow conditions. In order to have a better prediction of pesticide leaching risk assessments, further research, analysis and investigation should be carried out on subsurface solute transport models that assume that the soil consists of two mobile pore regions, one representing the matrix and the other one the macropores. Then most importantly, there should be significant parameterization on all the indices required to get a better result that is very close to reality.

REFERENCES

[1] Allison E., Jones C. Soil and Water Management Modules (5). Obtained in PDF. Format at; www.montana.edu/wwwpb/pubs/4481.html.

[2] Boesten, J. et al. 1997. Soil persistence models and EU registration. Technical Report 7617/vi/96. Committee of the European Communities, Brussels.

[3] Brady N.C and Weil R.R .2008. *The Nature and Properties of Soils*. Pearson Prentice Hall, New Jersey.

[4] Coquet Y., Simunek J., Coutadeur C., van Genuchten M. Th., Pot V., and Roger-Estrade J. 2005. Water and Solute Transport in a Cultivated Silt Loam Soil: 2. Numerical Analysis. *Vadose Zone Journal* 4:pp. 587-601.

[5] Delleur Jacques [ed]. 2000. *The handbook of groundwater engineering*. CRC Press, Boca Raton, Florida.

[6] Diaz-Diaz R and Loague K. 2000. Comparison of two pesticide leaching indices. *Journal of the American water resources association*. Vol 36. No 4.

[7] Domagalski, J. L., N. M. Dubrovsky, and C.R. Kratzer. 1997. Pesticides in the San Joaquin River, California: Inputs from dormant sprayed orchards. *Journal of Environmental Quality*. 26, 454-465.

[8] Edwards, W., M. Shipitalo, L. Owens, and W. Dick .1993. Factors affecting preferential flow of water and atrazine through earthworm burrows under continuous no-till corn. *Journal.of Environmental Quality*. 22, 453-457.

[9] Flurry M., (1996). Experimental Evidence of Transport of Pesticides through Field Soils-A Review. *Journal of Environmental Quality* 25, pp. 25-45.

[10] Foussereau X., Graham W. D., Akpoji G. A., Destouni G., and RAO PSC. 2001. Solute transport through a heterogeneous coupled vadose-saturated zone system with temporally random rainfall. *Water Resources Research*. 37: no 6; pp. 1577-1588.

[11] Grace W.Su., Geller J.T., Pruess K., and Hunt J.R.2001. Solute transport along preferential flow paths in unsaturated fractures. *Water Resources Research*, 37 no; 17 pp. 2481-2491.

[12] Kookona, R., R. Correl, and R. Miller.2005. Pesticide impact rating index: A pesticide risk indicator for water quality. *Water Air Soil Pollution Focus*, 5, pp. 45-65, doi: 10.1007/s11267-005-7397-7.

[13] Leij F.J and van Genucthen M. T. 2000. Solute Transport . In M Summer (ed), *Handbook of soil science*. pp. A183-A227. CRC Press, London.

[14] Lennartz, B. 1999. Variation of herbicide transport parameters within a single field and its relation to water flux and soil properties. *Geoderma*, 91(3-4), pp. 327-345, doi: 10.1016/S0016-7061(99)00008-7.

[15] McCauley A., Jones C., and Jacobsen J., 2005. Soil and Water Management Modules (1-3). Obtained in PDF format at; www.montana.edu/wwwpb/pubs/4481.html.

[16] McCauley A., Jones C. 2005. Soil and Water Management Modules (4). Obtained in PDF format at; www.montana.edu/wwwpb/pubs/4481.html.

[17] McGrath G, Hinz C and Sivapalan M.2010. Assessing the impact of regional rainfall variability on rapid pesticide leaching potential. *J. of Contaminant Hydrology* 113, pp.56-65.

[18] McGrath G.S, and Hinz C and Sivapalan M.2007. Modeling the impact of within-storm variability of rainfall on the loading of solutes to preferential flow pathways. *European Journal of Soil Science.* doi:10.1111/j.1365-2389.2007.00987.x

[19] McGrath G.S, Hinz C and Sivapalan M .2007. Temporal dynamics of hydrological threshold events. *Hydrol. Earth Syst. Sci.*, 11, pp. 923-938.

[20] McGrath G.S, Hinz C, and Sivapalan M.2008. Modeling the effect of rainfall intermittency on the variability of solute persistence at the soil surface. *Water Resources Research*, vol. 44, W09432, doi: 10.1029/2007WR006652.

[21] McGrath G S, Hinz C, Sivapalan M. 2010. Identifying a rainfall event threshold triggering herbicide leaching by preferential flow. *Water Resources Research*, vol. 46, W02513, doi: 10.1029/2008WR007506.

[22] McGrath G S, Hinz C and Sivapalan M. 2009. A preferential flow leaching index. Water Resources Research, vol, 45, W11405, doi: 10, 1029/2008WR007265.

[23] Mengel D and Rehm, G (2012). Fundamentals of fertilizer application. In P M Huang, Y Li and M Summer, eds., *Handbook of soil sciences*. p 14-1-14-11. CRC Press.

[24] Payraudeau S, McGrath G. S and Hinz C.2011. Climate and contaminant transport: the role of within-storm variability on contaminant transport by surface runoff. Water Quality: Current Trends and Expected Climate Change Impacts (Proceedings of symposium H04 held during IUGG2011 in Melbourne, Australia, July 2011) (IAHS Publ. 348, 2011).

[25] Pimentel D., Acquay H., Biltonen M., Rice P., Silva M., Nelson J., Lipner V., Giordano S., Horowitz A., D'Amore M.1992. Environmental and economic costs of pesticide use *BioScience*. 42; pp. 750-760.

[26] Radcliffe D. E and Simunek J. 2010. *Soil Physics with HYDRUS Modeling and Applications*. Boca Raton FL: CRC Press.

[27] Rausch R., Schafer W., Therrien R., and Wagner G. 2005. *Solute transport modeling: An introduction to models and solution strategies*. Gebruder Borntraeger verlagsbuchhandlung Berlin.

[28] Renuad, F. G., C. D. Brown, C. J. Fryer, and A Walker .2004.A lysimeter experiment to investigate temporal changes in the availability of pesticide residues for leaching. *Enviromental Pollution*. 131(1), pp. 81-91, doi: 10.1016/j.envpol.2004.02.028.

[29] Ritter W.F.1990. Pesticide contamination of ground water in the United States-A review. *J. Environ. Sci. Health* B25:1-29.

[30] Ritter W.F. 2001. Pesticides and Water Quality Impacts. In *Watershed Management and Hydrology*. CRC Press. Boca Raton, Florida.

[31] Ross Calvin. 2004. *An introduction to the Environmental Physics and Water sheds*. Cambridge, U.K: University Press.
[32] Saifadeen A and Gladnyeva R. Modeling of solute transport in the unsaturated zone using HYDRUS-1D: Effects of hysteresis and temporal variability in meteorological input data. *TVV-12/5020*. ISSN-1101-9824.
[33] Scorza, R.P., J. H. Smelt, J.T. I. J. Boesten, R.F.A. Hendriks, and A.T.M.S.E.van der Zee 2004. Preferential flow of bromide, bentazon, and imidacloprid in a Dutch clay soil. *Journal of Environmental Quality*. 33, pp.1473-1486.
[34] Šimunek J and Martinus van Genuchten, M.Th. 2006. Contaminant transport in the unsaturated zone. *The handbook of groundwater engineering*. Second edition. CRC Press. pp.1-46.
[35] Simunek J., van Genutchten, M.Th and Sejna, M.2005. The HYDRUS-1D software package for simulating the one-dimensional movement of water, heat, and multiple solutes in variably-saturated media. University of California-Riverside Research Reports.
[36] Udskriftsvenlig version af siden . 2003. Degradation and sorption parameters: chapter 8, PLAP-Monitoring results May 1999-June 2002. Obtained in PDF format at; http://pesticidvarsling.dk/publ_result/2002/vap-result-99-02-8-dk.html.
[37] United States Department of Agriculture (USDA). Natural Resources Conservation Service (NRCS). 2003. Soil Quality Agronomy Technical Note no 17. Series written by Soil Quality Institute 411 S Donahue Dr. Auburn, Al 36832.
[38] William A Jury and Robert Horton. 2004. *Soil Physics*. New Jersey: John Wiley and sons, Inc.
[39] Weber J.B, Wilkerson G G and Rheinhardt C F (2004). Calculating pesticide sorption coefficients (K_D) using selected soil properties. *Chemosphere 55*. pp.157-166.
[40] Yagi K., Williams N, Y., and Cicerone R.J.1993. Agricultural soil fumigation as a source of atmospheric methyl bromide. *Proc. Natl. Acad. Sci*. 90: pp. 8420-8423.
[41] Zhang X C., Norton L. D and Hickman M.1997. Rain pattern and soil moisture content effects on atrazine and metolachlor losses in runoff. *Journal of Environ. Qual*. 26, pp.1539-1997.

PROCENA RIZIKA SADRŽAJA PESTICIDA U ZEMLJIŠTU KAO FUNKCIJA OSOBINA ZEMLJIŠTA, PESTICIDA I PADAVINA (KIŠE), UPOTREBOM NUMERIČKOG MODELA HYDRUS 1D

Jekwu Sunday E. Ona

Monitoring and Evaluation Department/Environmental Consultancy, Community and Social Development Agency (CSDA) Government of Enugu State, Nigeria

Sadržaj. Uočeno je kroz eksperimente da se mnoge hemikalije, posebno pesticidi koji se nalaze u potocima i sadržaju podzemnih voda, prenose površinskim oticanjem i/ili preferencijalnim procesima protoka. Istraživači su takođe dokazali da se vreme i priroda padavina od poslednje primene pesticida često opisuju kao značajna kontrola transporta pesticida kroz procese protoka. Promenljivost padavina se sada smatra klimatskim pokretačima transporta zagađivača.

Pokazalo se da je količina pesticida transportovanih površinskim oticanjem i/ili preferencijalnim putevima toka do potoka i podzemnih voda u velikoj korelaciji sa koncentracijom te hemikalije u tankom prizemnom sloju zemljišta neposredno pre takvog događaja.

Tanak podpovršinski sloj zemljišta smatra se izvorom gde počinje sva dinamika transporta rastvorenih materija. Tanak površinski sloj je skladište pesticida iz kojeg se ispiraju kako brzim epizodnim tako i sporim stabilnim procesima.

U ovom istraživanju, nastojalo se boljem razumevanju ideje o pokretaču u sistemu izvor-okidač kod koncepta transporta rastvorenih pesticida u podpovršinskim horizontima zemljišta. Pokretač (npr. varijabilnost-promenljivost padavina) inicira (površinsko oticanje i/ili preferencijalni protok) iz izvora (tanak sloj blizu površine) za transport pesticida do potoka i/ili podzemnih voda.

Metodologija za ovu studiju je korišćenje numeričkog modela HYDRUS 1D.

Ključne reči: *Fizika zemljišta, procena rizika, ispiranje, pesticidi, transportno modeliranje, kvalitet vode.*

Prijavljen:
Submitted: **12.08.2022.**
Ispravljen:
Revised: **20.11.2022.**
Prihvaćen:
Accepted: **28.11.2022.**

Univerzitet u Beogradu
Poljoprivredni fakultet
Institut za poljoprivrednu tehniku
Naučni časopis
POLJOPRIVREDNA TEHNIKA
Godina XLVII
Broj 4, 2022.
Strane: 82 – 93

University of Belgrade
Faculty of Agriculture
Institute of Agricultural Engineering
Scientific Journal
AGRICULTURAL ENGINEERING
Year XLVII
No. 4, 2022.
pp. 82 – 93

UDK: 620.92

Pregledni rad
Review paper
DOI:10.5937/PoljTeh2204082P

ELEKTRIČNA MOTORNA VOZILA NA VODONIK -TRENDOVI ISPITIVANJA I KONTROLISANJA

Predrag Popović[1], Živko Stjelja[1], Branimir Miletić[1], Đorđe Vranješ[1], Veljko Stojanović[1], Vladimir Nikolić[1,2*], Milica Marčeta-Kaninski[2]

[1]Environ d.o.o., istraživačko-razvojni centar, Čukarička 9, 11000 Beograd, R. Srbija
[2]Institut za opštu i fizičku hemiju, Studentski trg 12, 11000 Beograd, Republika Srbija

Sažetak: Ispitivanje električnih vozila (EV) daleko prevazilazi zahteve homologacionih ispitivanja motornih vozila i njihovih komponenti. Električna motorna vozila na vodonične gorivne ćelije (FCV-eng. Fuel Cell vehicles) su veoma slična električnim vozilima, u smislu da za pokretanje vozila koriste elektromotor umesto motora sa unutrašnjim sagorevanjem. Glavna razlika je ta da EV koriste baterije, koje se moraju priključiti na mrežu radi punjenja, dok FCV proizvode električnu energiju na licu mesta.

Ovaj rad predstavlja pregled regulativa o ispitivanju i kontrolisanju električnih vozila na vodonik. Ispitivanje motornih vozila danas predstavlja spektar raznih testiranja koja se odigravaju u različitim stadijumima razvoja vozila, proizvodnje i upotrebe vozila, a čiji je zadatak da obezbedi dobijanje objektivnih informacija o kvalitetu vozila, njihovih sklopova i komponenti, o uslovima rada, okruženju i sl. Legislativa koja se odnosi na ispitivanje motornih vozila na vodonik postoji, ali se odgovarajuće procedure i standardi i dalje razvijaju, u korak sa napretkom tehnologije

Ključne reči: *sertifikacija, kontrolisanje i ispitivanje, vodonik, gorivne ćelije, električna vozila na vodonik*

UVOD

Homologacija vozila, delova za vozila, sklopova ili zasebnih tehničkih jedinica, predstavlja postupak ispitivanja i potvrđivanja da li određeno vozilo u celini, ili neki njegov deo, odgovaraju zahtevima regulativa/pravilnika Ekonomske komisije Ujedinjenih nacija za Evropu (UN/ECE).

*Kontakt Autor: Vladimir Nikolić, e-mail: nikolic79@gmail.com
Ugovor broj: 451-03-68/2022-14/200051i Environ d.o.o.
Ministarstvo, prosvete, nauke i tehnološkoj razvoja, Republika Srbija,

Pri homologaciji vozila, odnosno delova i opreme vozila, ispituju se i potvrđuju se uređaji bitni za bezbednost vozila, kao i uređaji od kojih zavisi ekološki kvalitet vozila: u takve spadaju uređaji bitni za aktivnu bezbednost vozila (kočnice, upravljački mehanizam, svetla, signalni uređaju, pneumatici i sl), za pasivnu bezbednost vozila (sigurnosni pojasevi, sedišta za decu, unutrašnja oprema, protivpožarna zaštita i sl.), za opštu bezbednost vozila (zaštita od neovlašćene upotrebe i sl.) i za ekološki kvalitet vozila (toksična izduvna emisija, buka, radiofrekvencijske smetnje i sl.).
Institut za standardizaciju Republike Srbije, kao nosilac sistema sprovođenja Sporazuma iz 1958. godine, vrši notifikaciju svih ECE pravilnika koji regulišu ekološka i bezbedonosna pitanja u vezi motornih vozila i opreme. Iz toga sledi da je cilj homologacije povećanje opšte bezbednosti saobraćaja i smanjenje neželjenog uticaja na okolinu.

ECE komisija izdaje godišnji radni dokument o glavnim regulatornim razvojima i aktivnostima vezanim za automobilsku industriju na Svetskom forumu za harmonizaciju propisa o vozilima Ekonomske komisije Ujedinjenih nacija za Evropu (UN/ECE). Pored toga, Komisija objavljuje godišnji izveštaj o statusu usvojenih UN regulativa u oblasti vozila od strane Evropske unije (EU).

Globalni tehnički propisi (GTR- The global technical regulations) razvijeni su u skladu sa međunarodnim sporazumom o konstrukciji vozila iz 1998. godine[1]. Propisi pokrivaju odobravanje bezbednosnih i ekoloških aspekata vozila. Njima upravlja Svetski forum za harmonizaciju (usklađivanje) propisa o vozilima kao stalna radna grupa UNECE. Na Svetskom forumu za harmonizaciju propisa o vozilima, na 160-oj sednici, juna 2013. godine u Ženevi, predstavljen je predlog GTR o vodoniku i električnim vozilima na gorivne ćelije, koji je usvojen 26.06.2013. godine [2].

ECE usvojeni dokumenti, ključni za vozila sa pogonom na vodonične gorivne ćelije, nisu još uvek usvojeni od strane nadležnih državnih organa u Srbiji. Stupanjem na snagu ECE pravilnika, ukoliko se pojavi domaći proizvođač vozila na vodonične gorivne ćelije (FCV – fuel cell vehicle), moraće da bude homogovan prema usvojenim ECE parvilnicima. Ukoliko dođe do prepravke vozila na FCV, moraće da bude ispitivan od strane ovlašćene organizacije prema ECE pravilnicima, a svaki uvezeni FCV mora biti podvrgnut kontroli saobraznosti. Laboratorije u Srbiji koje rade u oblasti vozila moraju da budu ovlašćene od strane nadležnih organa za sprovođenje homologacionih ispitivanja FCV vozila po ECE pravilnicima i kontrolu saobraznosti.

Električna vozila

Ispitivanje električnih vozila (EV) prevazilazi postupak homologacije za vozila i njihove komponente. Takođe pokriva interfejse za punjenje i prateće sisteme koji omogućavaju stanicama za punjenje i back-office sistemima da komuniciraju jedni sa drugima - testiranje interoperabilnosti. Baterijski paketi i moduli od kojih su napravljeni, koji sadrže veliki broj baterijskih ćelija, predstavljaju izvor energije koji može predstavljati potencijalnu opasnost i takođe moraju biti odvojeno ispitivani. Pored toga, mora postojati ispitivanje usaglašenosti svih električnih komponenti kao što su utikači, kablovi, konektori, ožičenje, prekidači itd. Takođe, kako bi se povećao domet električnih vozila, baterije postaju veće i teže, što predstavlja veći potencijalni rizik po bezbednost. Za ispitivanje EV-a neophodan je širok spektar metodologije za ispitivanje i kontrolisanje, kao i za homologaciona ispitivanja za proizvođače na nivou celog vozila i komponenti.

Danas to uključuje: funkcionalnu bezbednost (ISO 26262), električnu bezbednost (EN 50604, ISO 18243 , IEC 62660), testiranje performansi (ISO 12405, ISO 18243, ISO 15118, IEC 62660), ispitivanje životne sredine, testiranje homologacije (R100, UN 38.3, R10), EV interfejs za punjenje, testiranje elektronike i komponenti. Električno vozilo pokriva veoma širok spektar tehnologije i opreme.

Električna vozila sa vodoničnim gorivnim ćelijama - Hydrogen Mobility

Britanski fizičar William R. Grove je 1839. je pronašao da se elektrohemijskim spajanjem vodonika i kiseonika dobija električna energija a gorivnu ćeliju je nazvao voltina plinska baterija [3]. Prvo vozilo na gorivne ćelije napravljeno 1959. godine prikazano je na slici 1.

Slika 1. Prvo vozilo na gorivne ćelije, [4].
Figure 1. First fuel cell vehicle ,[4].

Zeleni vodonik predstavlja obećano gorivo budućnosti. Korišćenje vodonika kao zelenog goriva ili kao komponente za zelena sintetička goriva u sektoru mobilnosti nije sporno ali još uvek nije jasno koja će tehnologija bez emisija prevladati za koju vrstu vozila i primenu.

Vozila na vodonične gorivne ćelije (FCVs - Hydrogen Fuel Cell Vehicles) su slična električnim vozilima u smislu da koriste elektromotor umesto motora sa unutrašnjim sagorevanjem koji daje pogon točkovima. Razlika je u tome da električni automobil napaja baterija koja se mora puniti sa strujnog izvora, dok FCVs pravi struju na licu mesta. U gorivnoj ćeliji se vodonik (H_2 - hydrogen) u gasnom stanju iz rezervoara kombinuje sa kiseonikom (O_2 - oxygen) iz vazduha i generiše struju i vodu i toplotu kao dodatni proizvod, [5].

Emisija

Kao i električna vozila, FCV su vozila sa nultom emisijom – nemaju emisiju izazvanu smogom ili emisijom gasova staklene bašte. Emisije mogu da nastanu u procesu proizvodnje i transporta vodoničnog goriva ukoliko se ne koriste zelene tehnologije (npr obnovljivi izvori energije). Iako je vodonik najrasportranjeniji element u univerzumu, na Zemlji on mora biti odvojen od drugih jedinjenja da bi se koristio kao gorivo. Ovaj proces može biti energetski zahtevan. Količina emisija povezanih sa proizvodnjom vodoničnih goriva zavisi od izvora vodonika i načina proizvodnje. Trenutno, većina vodonika koji se pravi za upotrebu kao gorivo dolazi iz prirodnog gasa, ali vodonično gorivo se takođe može napraviti od vode, nafte, uglja i biljnog materijala. Vodonik se čak može proizvesti iz komunalnog otpada. Postoje pilot projekti koji su koristili deponijski gas i otpadne vode za proizvodnju vodoničnog goriva.

Punjenje rezervoara gorivom i domet vožnje FCV

Punjenje rezervoara vodonikom kod FCV slično je punjenju rezervoara vozila na gas. Jednostavno se priključi mlaznica iz određenog dozatora vodonika na pumpi/stanici i napuni rezervoar. Vremena punjenja su takođe slična: FCV se može napuniti za samo 5 minuta. Domet vožnje za vodonična vozila danas prelazi preko 500 km sa jednim punjenjem rezervoara, (Tabela 1).

Tabela 1. Pregled osnovnih karakteristika vozila na vodonične gorivne ćelije, [6].
Table 1. Overview of the Toyota hydrogen based FCEV vehicles characteristics, [6].

	2022 Toyota Mirai LE			2022 Toyota Mirai Limited			2022 Toyota Mirai XLE		
Vozilo Vehicle									
	Potrošnja goriva Fuel consumption								
km/kg*	K	G	A	K	G	A	K	G	A
	116	120	113	103	105	101	116	120	113
Domet /Range/ km	531			575			647		
	Karakteristike vozila Vehicle characteristics								
Klasa/ Class	Kompakt/Compact			Kompakt/Compact			Kompakt/Compact		
Motor /Motor	AC sinhroni (134 kW)/AC synchronous (134 kW)								
Baterija/ Battery	311 V, Li-jonska/311 V, Li-ion								

K- Kombinovana vožnja, G- Gradska vožnja,A- Vožnja autoputem,
*1 kg vodonika je približno ekvivalentna 4,55 lit. benzina

Međunarodni standardi i propisi koji se odnose na vodonik i vozila na vodonične gorivne ćelije

Da bi proizvodili i prodavali vozila sa pogonom na vodonične gorivne ćelije u inostranstvu, svi proizvođači vozila i proizvođači originalne automobilske opreme, moraju poštovati niz propisa koji se odnose na alternativna goriva. Danas već postoji čitav niz protokola koji pomažu u testiranju i sertifikaciji za vodoničnih vozila., (Slika 2.).

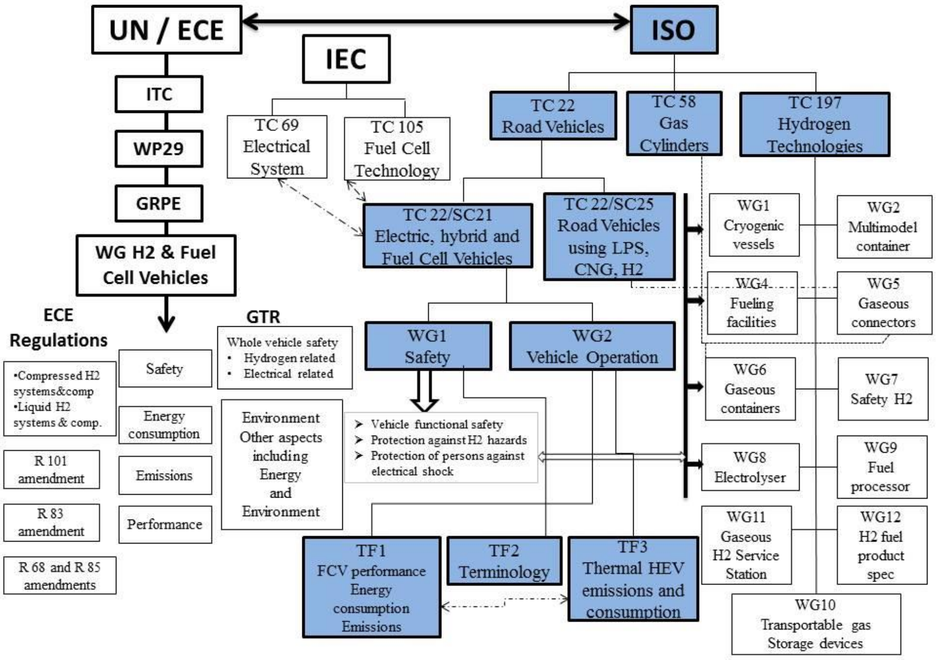

Slika 2. Međunarodni standardi i Regulatorna tela koja se bave vodonikom i vozilima sa gorivnim ćelijama, [7].
Figure 2. International Standard and Regulation Bodies dealing with H2 and FC vehicles, [7].

UN ECE 134 for Hydrogen Fuel Cell Vehicle Safety

Regulativa br. 134 Ekonomske komisije za Evropu Ujedinjenih nacija (UN/ECE) — Jedinstvene odredbe u vezi sa homologacijom motornih vozila i njihovih komponenti u pogledu bezbednosnih performansi vozila na vodonik (HFCV) [2019/795], [8].

Ovaj pravilnik se primenjuje na (1): 1.1. Deo I — Sistemi za skladištenje komprimovanog vodonika za vozila na vodonik na njihove performanse vezane za bezbednost. 1.2. Deo II — Specifične komponente za sisteme za skladištenje komprimovanog vodonika za vozila na vodonik na njihove performanse vezane za bezbednost. 1.3. Deo III — Vozila na vodonik kategorije M i N (2) koja sadrže sistem za skladištenje komprimovanog vodonika u pogledu njegovih bezbednosnih performansi.

GTR No. 13 for Hydrogen and Fuel Cell Vehicles Global Technical Regulation

Razvoj GTR za vozila na vodonik i gorivne ćelije odigrao se u okviru Svetskog foruma za harmonizaciju propisa o vozilima (VP.29) Komiteta za unutrašnji transport (ITC) UNECE.

Ciljevi GTR su da se razvije i uspostavi regulativa za vozila na vodonik koja:

(i) dostiže ili premašuje ekvivalentne nivoe bezbednosti onih za konvencionalna vozila na benzin; i

(ii) (ii) zasnovana je na performansama FCV i ne ograničava budući napredak u tehnologiji.

Opis tipičnog vozila na vodonične gorivne ćelije (HFCVs)

Tipičan raspored komponenti vozila na vodonik sa skladištem komprimovanog vodonika i pogonom gorivne ćelije prikazan je na Slici 3.

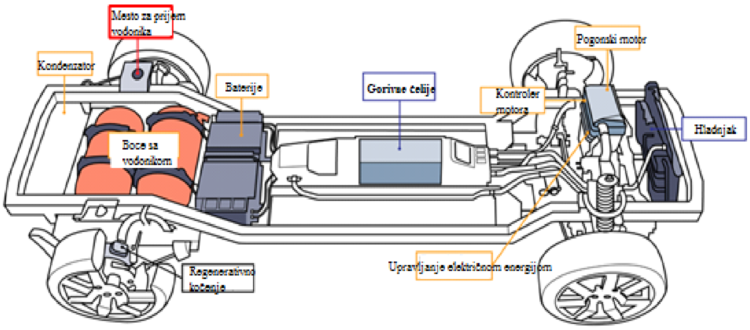

Slika 3. Šema vozila sa vodoničnim gorivnim ćelijama, [8].
Figure 3. Scheme of a hydrogen fuel cell vehicle, [8].

Sistem za punjenje vodonikom

Vozilo se može snabdevati tečnim ili komprimovanim gasom na pumpi za gorivo, u zavisnosti od tipa sistema za skladištenje vodonika u vozilu. Trenutno, vodonik se najčešće isporučuje u vozila kao komprimovani gas koji se sipa pod pritiscima do 125 % nominalnog radnog pritiska (NVP) vozila da bi se kompenzovalo prolazno zagrevanje od adijabatske kompresije tokom punjenja goriva.

Bez obzira na to u kom se stanju vodonik nalazi, vozila se napajaju kroz specijalnu mlaznicu za dovod goriva na pumpi koja se povezuje sa rezervoarom na vozilu kako bi se obezbedio prenos vodonika u potpuno zatvorenom sistemu u vozilo. Rezervoar na vozilu sadrži nepovratni ventil koji sprečava curenje vodonika iz vozila kada je mlaznica za dovod goriva isključena.

Sistem za skladištenje vodonika

Sistem za skladištenje vodonika sastoji se od komponenti koje moraju da izdrže pritisak na kojem se nalazi uskladišteni vodonik. Ključne funkcije sistema za skladištenje vodonika su da primi vodonik tokom punjenja goriva, zadrži vodonik dok ne bude potrebno, a zatim otpusti vodonik u sistem gorivih ćelija za upotrebu u pogonu vozila. Trenutno, najčešći metod skladištenja i isporuke vodoničnog goriva je u obliku komprimovanog gasa.

Vodonik se takođe može skladištiti kao tečnost (u kriogenim uslovima). Dodatni tipovi skladištenja vodonika, kao što je krio-komprimovano skladištenje, nisu obuhvaćeni GTR 13 a mogu biti predstavljeni u revizijama kada njihova tehnologija to dozvoli.

To je na primer skladištenje krio-komprimovanog vodonika (CcH2) kao hibridnog načina skladištenja između tečnog i komprimovanog gasa koji se može puniti i kriogeno kompresovanim i komprimovanim gasom vodonika.

Sistem isporuke vodoničnog goriva

Sistem za isporuku vodoničnog goriva prenosi vodonik iz sistema za skladištenje u pogonski sistem na odgovarajućem pritisku i temperaturi za rad gorivne ćelije. U slučaju sistema za skladištenje komprimovanog vodonika, pritisak mora da se smanji sa 87,5 MPa na manje od 1 MPa na ulazu u sistem gorivih ćelija. Ovo zahteva više faza regulacije pritiska da bi se postigla precizna i stabilna kontrola, nizom ventila za kontrolu protoka, regulatora pritiska, filtera, cevovoda i izmenjivača toplote. U vozilima sa sistemima za skladištenje tečnog vodonika, i tečni i gasoviti vodonik se može osloboditi iz sistema za skladištenje i zatim zagrejati na odgovarajuću temperaturu pre isporuke u sistem gorivih ćelija.

Sistem gorivnih ćelija

Sistem gorivih ćelija generiše električnu energiju potrebnu za rad pogonskih motora i punjenje baterija i/ili kondenzatora vozila. Postoji nekoliko vrsta gorivih ćelija, ali gorivne ćelije sa protonskom jonoizmenjivačkom membranom (PEM) su uobičajeni tip koji se koristi u automobilima. Njihove performanse, kao što radna temperatura, omogućava kraće vreme pokretanja. PEM gorivne ćelije elektrohemijski kombinuju vodonik i kiseonik (iz vazduha) za generisanje električne jednosmerne struje. Gorivne ćelije su sposobne za kontinuiranu proizvodnju električne energije kada se snabdevaju vodonikom i kiseonikom, istovremeno generišući električnu energiju i vodu bez proizvodnje ugljen-dioksida (CO2) ili drugih štetnih emisija tipičnih za motore sa unutrašnjim sagorevanjem. Na Slici 4 je dat šematski prikaz vodonične gorivne ćelije.

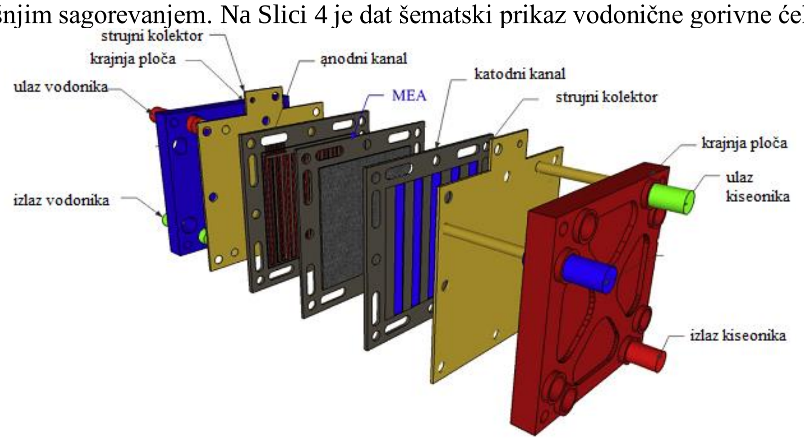

Slika 4. Šematski prikaz vodonične gorivne ćelije, [8].
Figure 4. Shematic representation of the hydrogen fuel cell, [8].

Tipični sistemi gorivih ćelija uključuju ventilator za dovod vazduha u sklop gorivih ćelija (više jediničnih sistema). Približno 50 do 70 % kiseonika koji ulazi u gorivnu ćeliju se troši unutar ćelija. Ostatak se potroši iz sistema.

Većina količine vodonika koji ulazi u sistem gorivih ćelija se troši unutar ćelija, ali je neophodno napraviti balansom sistema mali višak kako bi se osiguralo da se gorivne ćelije neće oštetiti u radu.

Sistem gorivih ćelija takođe uključuje pomoćne komponente kao što su one za odvođenje viška toplote. Većina sistema gorivnih ćelija se hladi mešavinom glikola i vode. Pumpe cirkulišu rashladnu tečnost između gorivih ćelija i hladnjaka.

Pojedinačne gorivne ćelije su električno povezane serijskom vezom u sklop tako da je njihov kombinovani napon, ukupan napon, između 300 i 600 V DC. Pošto sklopovi gorivih ćelija rade na visokom naponu, svi priključci za reaktanate i rashladne tečnosti u sklopu moraju biti adekvatno izolovani od šasije vozila kako bi se sprečili kratki spojevi koji bi mogli da oštete opremu ili naškode ljudima ako je izolacija je narušena.

Električni pogon i sistem upravljanja električnom energijom

Električna energija koju proizvodi sistem gorivih ćelija koristi se za pogon električnih motora koji pokreću vozilo. Kao što je ilustrovano na slici 3, mnoga vozila sa gorivnim ćelijama imaju pogon na prednje točkove sa električnim pogonskim motorom i pogonom koji se nalazi u „motornom prostoru“ postavljenim poprečno preko prednje osovine; Međutim, druge konfiguracije i pogon na zadnje točkove su takođe u opcijama proizvođača FCV: pogon na sve točkove sa električnim motorima na prednjoj i zadnjoj osovini ili sa kompaktnim motorima na svakom točku.

„Položaj gasa“ koristi kontroler pogonskog motora ili više njih za određivanje količine snage koja se šalje na pogonske točkove. Mnoga vozila sa gorivnim ćelijama koriste baterije ili ultra-kondenzatore da dopune izlaz gorivih ćelija. Ova vozila takođe mogu da “vrate” energiju tokom zaustavljanja putem regenerativnog kočenja, čime se pune baterije ili ultrakondenzatori i na taj način povećava efikasnost.

Pogonski motori mogu biti DC ili AC. Ako su pogonski motori naizmenične struje, kontroler pogonskog motora će konvertovati jednosmernu struju iz gorivih ćelija, baterija i ultrakondenzatora u naizmeničnu struju. Suprotno tome, ako vozilo ima regenerativno kočenje, kontroler pogonskog motora će konvertovati naizmeničnu struju proizvedenu u pogonskom motoru nazad u jednosmernu tako da se energija može uskladištiti u baterijama ili ultrakondenzatorima.

EC 79/2009 i 406/2010/EU - odobrenje tipa motornih vozila sa pogonom na vodonik

UREDBA KOMISIJE (EU) br. 406/2010 od 26. aprila 2010. o primeni Uredbe (EZ) br. 79/2009 Evropskog parlamenta i Saveta o homologaciji tipa motornih vozila na vodonik [9] predstavlja sledeću listu standarda:

ISO 188:2007 Rubber, vulcanised or thermoplastic — Accelerated ageing and heat resistance tests.

ISO 306:2004 Plastics — Thermoplastic materials — Determination of Vicat softening temperature (VST).

ISO 527-2:1993/Cor 1:1994 Plastics — Determination of tensile properties — Part 2: Test conditions for moulding and extrusion plastics.

ISO 1431-1:2004/Amd 1:2009 Rubber, vulcanised or thermoplastic — Resistance to ozone cracking — Part 1: Static and dynamic strain testing.

ISO 2768-1:1989 General tolerances — Part 1: Tolerances for linear and angular dimensions without individual tolerance indications.
ISO 2808:2007 Paints and varnishes — Determination of film thickness.
ISO 3864-1:2002 Graphical symbols – Safety colours and safety signs – Part 1: Design principles for safety signs in workplaces and public areas.
ISO 4624:1978 Paints and varnishes — Pull-off test for adhesion.
ISO 6506-1:2005 Metallic materials — Brinell hardness test — Part 1: Test method
ISO 6957:1988 Copper alloys — Ammonia test for stress corrosion resistance.
ISO 7225:2005 Gas cylinders — Precautionary labels.
ISO 7866:1999 Gas cylinders — Refillable seamless aluminium alloy gas cylinders-Design, construction and testing.
ISO 8491:2004 Metallic materials — Tube (in full section) — Bend test.
ISO 9227:2006 Corrosion tests in artificial atmospheres — Salt spray tests ISO 9809-1:1999 Gas cylinders — Refillable seamless steel gas cylinders — Design, construction and testing — Part 1: Quenched and tempered steel cylinders with tensile strength less than 1 100 Mpa.
ISO 9809-2:2000 Gas cylinders — Refillable seamless steel gas cylinders — Design, construction and testing — Part 2: Quenched and tempered steel cylinders with tensile strength greater than or equal to 1 100 Mpa.
ISO 11114-1:1997 Transportable gas cylinders — Compatibility of cylinder and valve materials with gas contents — Part 1: Metallic materials.
ISO 11114-4:2005 Transportable gas cylinders — Compatibility of cylinder and valve materials with gas contents — Part 4: Test methods for selecting metallic materials resistant to hydrogen embrittlement.
ISO/TS 14687-2:2008 Hydrogen fuel — Product specification — Part 2: Proton exchange membrane (PEM) fuel cell applications for road vehicles.
EN 1251-2:2000/AC:2006 Cryogenic vessels — Transportable vacuum insulated vessels of not more than 1 000 litres volume — Part 2: Design, fabrication, inspection and testing.
EN 1252-1:1998/AC:1998 Cryogenic vessels — Materials — Part 1: Toughness requirements for temperatures below – 80 °C.
EN 1797:2001 Cryogenic vessels — Gas/material compatibility.
EN 1964-3:2000 Transportable gas cylinders — Specification for the design and construction of refillable transportable seamless steel gas cylinders of water capacities from 0,5 litre up to and including 150 litres — Part 3: Cylinders made of seamless stainless steel with an Rm value of less than 1 100 Mpa.
EN 10204:2004 Metallic products — Types of inspection documents
EN 12300:1998/A1:2006 Cryogenic vessels — Cleanliness for cryogenic service.
EN 12434:2000/AC:2001 Cryogenic vessels — Cryogenic flexible hoses.
EN 12862:2000 Transportable gas cylinders — Specification for the design and construction of refillable transportable welded aluminium alloy gas cylinders.
EN 13322-2:2003/A1:2006 Transportable gas cylinders — Refillable welded steel gas cylinders — Design and construction — Part 2: Stainless steel.
EN 13648-1:2008 Cryogenic vessels — Safety devices for protection against excessive pressure — Part 1: Safety valves for cryogenic service.
EN 13648-2:2002 Cryogenic vessels — Safety devices for protection against excessive pressure — Part 2: Bursting disc safety devices for cryogenic service.

EN 13648-3:2002 Cryogenic vessels — Safety devices for protection against excessive pressure — Part 3: Determination of required discharge — Capacity and sizing
ASTM B117 - 07a Standard practice for operating salt spray (fog) apparatus.
ASTM D522 - 93a(2008) Standard test methods for mandrel bend test of attached organic coatings.
ASTM D572 - 04 Standard test method for rubber — Deterioration by heat and oxygen.
ASTM D1308 - 02(2007) Standard test method for effect of household chemicals on clear and pigmented organic finishes.
ASTM D2344 / D2344M - 00(2006) Standard test method for short-beam strength of polymer matrix composite materials and their laminates.
ASTM D2794 - 93(2004) Standard test method for resistance of organic coatings to the effects of rapid deformation (impact) ASTM D3170 - 03(2007) Standard test method for chipping resistance of coatings.
ASTM D3359 - 08 Standard test methods for measuring adhesion by tape test.
ASTM D3418 - 08 Test method for transition temperatures and enthalpies of fusion and crystallisation of polymers by differential scanning calorimetry.
ASTM G154 - 06 Standard practice for operating fluorescent light apparatus for UV exposure of nonmetallic materials.
U bitne protokole ispitivanja i testiranja mogu se uvrstiti i:
HPRD1 za uređaje za smanjenje pritiska za kontejnere sa gorivom u vozilima sa kompresovanim vodonikom.
HGV 2 za kontejnere za gorivo u vozilima sa pogonom na kompresovani vodonik
HGV 3.1 za komponente sistema goriva za vozila sa pogonom na kompresovani vodonik.
SAE TIR J2601 za protokole za punjenje goriva za laka površinska vozila sa gasovitim vodonikom koji se bave sistemima skladistenja, njihovom komponentama i protokolima prilikom punjenja rezervoara.

ZAKLJUČAK

Potvrda da vozila ispunjavaju relevantne Zakonske propise i standarde je ključni deo njihovog uključivanja u saobraćaj. Procesi ispitivanja i kontrolisanja za vozila na konvencionalna goriva su odavno uspostavljena i zasnivaju se na sistemu odobrenja tipa. Ako je testirano vozilo usaglašeno, onda su i sva ostala istog tipa takođe sertifikovana kao usaglašena. Da bi vozila sa alternativnim gorivom, kao što su električna vozila (EV) i električna vozila sa gorivnim ćelijama (FCV) dostigla potpuno komercijalni status, takođe moraju da prođu kroz odgovarajuće procese ispitivanja i kontrolisanja. Iako postoji legislativa za vodonična električna vozila, odgovarajući standardi i propisi se još uvek razvijaju.

U ovom radu je dat prikaz aktuelne međunarodne regulative u oblasti vodoničnih gorivnih ćelija za pogon motornih vozila. Potreba za ekološki čistijim i ekonomičnijim vozilima, uslovila je intenzivni rast novih tehnologija u koje spadaju i vozila na vodonične gorivne ćelije.
Republici Srbiji su neophodna veća ulaganja u razvoj novih tehnologija, ali i donošenje odgovarajuće domaće regulative, kako bi ispratili savremene tokove napretka u zemljama oko nas.

LITERATURA

[1] Economic Commission for Europe. 2018. Agreement concernig the establishing of global technical regulations for wheeled vehicles, equipement and parts which can be fitted and/or used on wheeled vehicles, ECE/TRANS/132, Geneva, 25. June 1998.

[2] Economic Commission for Europe. 2013. Proposal for a global technical regulation on hydrogen and fuel cell vehicles, ECE/TRANS/WP.29/2013/41, Geneva, 26. June 2013.

[3] W. R. Grove, Philosophical Magazine and Journal of Science, 14 (1839), pp. 127-130.

[4] Alischalmers fuel cell tractor 15 kW, Photo documentation, National Museum of American Hystory.

[5] S.M.Brkovic, M.P.Marceta Kaninski, P.Z.Lausevic, A.B.Saponjic, A.M.Radulovic, A.A..Rakic, I.A.Pasti, V.M.Nikolic.2020. Non-stoichiometric tungsten-carbide-oxide-supported Pt–Ru anode catalysts for PEM fuel cells – From basic electrochemistry to fuel cell performance, International Journal of Hydrogen Energy 45. pp.13929-13938.

[6] US Department of Energy, Compare Fuel Cell Vehicles, Dostupno na: https://www.fueleconomy.gov/feg/fcv_sbs.shtml [datum pristupa: 16.08.2022.]

[7] ECE-TRANS-WP29-GRB-53-inf10e, UNECE – WP.29 .2011.– Hydrogen Fuel Cell Cehicles - (HFCV), GRPE - SUB-WORKING GROUP ENVIRONMENT (SGE),.

[8] ECE - United Nations. 2016. UN ECE 134 for Hydrogen Fuel Cell Vehicle Safety.

[9] Official Journal of the European Union. 2010. COMMISSION REGULATION (EU) No 406/2010 of 26 April 2010 implementing Regulation (EC) No 79/2009 of the European Parliament and of the Council on type-approval of hydrogen-powered motor vehicles, L 122/1.

[10] Hyewon Yang; Young Jae Han; Jiwon Yu; Sumi Kim; Sugil Lee; Gildong Kimand, and Chulung Lee. 2022. Exploring Future Promising Technologies in Hydrogen Fuel Cell Transportation. Sustainbility 14 (2), 917, pp. 1-19. https://doi.org/10.3390/su14020917

[11] Kovac, A.; Paranos, M. 2021. Hydrogen in energy transition: A review. Int. Journal Hydrogen Energy, 46, pp.10016–10035.

[12] Lan, H.; Ma, Q.; Chang, Z.;Wang, D.; Zheng, T. 2022. Research on the Performance Comparison of Two Fuel Cell Electric Vehicles with Typical Energy Management Strategies. World Electric Vehicle Journal, 13 (89). pp. 1-17. https://doi.org/10.3390/wevj13050089

[13] Qinyang, L.; Teng, T.; Baodi, Z.; Xin, Z.; Qicheng, X. 2021. Optimal control strategy for economy and durability of range extended fuel cell vehicles. Journal of Harbin Institute of Technology 53. pp. 126–133

[14] Gröger, O., Gasteiger, H.A., Suchsland, J.P. 2015. Electromobility: Batteries or fuel cells ?. Journal of the Electrochemical Society.162 (14). pp. A2605-A2622.

HYDROGEN ELECTRIC MOTOR VEHICLES - TESTING AND CONTROL TRENDS

Predrag Popović[1], Živko Stjelja[1], Branimir Miletić[1], Đorđe Vranješ[1], Veljko Stojanović[1], Vladimir Nikolić[1,2*], Milica Marčeta Kaninski[2]

[1]Environ LLC, Center for research and development, 11000 Belgrade, R. of Serbia
[2]Institute of General and Physical Chemistry, Studentski trg 12/V, Belgrade, R. of Serbia

Abstract: Electric vehicle (EV) testing goes way beyond homologation testing for the vehicles and their components.

Hydrogen Fuel Cell Vehicles (FCVs) are similar to EVs, in the aspect that they use an electric motor instead of an internal combustion engine to power the wheels.

The main difference is that EVs run on batteries that must be plugged in to recharge, while FCVs generate their electricity onboard.

This manuscript presents overview of the hydrogen vehicle certification legislation. Inspection and testing of motor vehicle technology today represent a set of a whole series of procedures that are applied in different stages of the vehicle development, production and operation of vehicles, and whose task is to provide objective information about the quality of the vehicle and its assemblies and parts, as well as about the conditions in which the vehicles operate, about workloads, environment, etc.

Although there are adopted technical regulative for hydrogen powered EVs, the appropriate standards and legislation are still evolving.

Key words: *certification, inspection and testing, hydrogen, fuel cells, hydrogen vehicles*

Prijavljen: **01.08.2022.**
Submitted:
Ispravljen: **28.10.2022.**
Revised:
Prihvaćen: **10.12.2022.**
Accepted:

CIP Каталогизација у публикацији
Народна библиотека Србије, Београд
631(059)
ПОЉОПРИВРЕДНА техника : научни часопис =
Agricultural Engineering : Scientific Journal /
одговорни уредник Мићо В. Ољача – Год. 1, бр. 1
(1963)- . Београд; Земун : Институт за пољопривредну
технику, 1963 - Београд. (Штампарија: DUGA MOTIV ,
11030 Београд). - 25 цм
Тромесечно. – Прекид у излажењу од 1987-1997. године
ISSN 0554-5587 = Пољопривредна техника
COBISS.SR-ID 16398594